1969

Computer Simulation of a New Redundancy Reduction Technique

Uldis Birznieks

COMPUTER SIMULATION OF A NEW REDUNDANCY REDUCTION TECHNIQUE

BY

ULDIS BIRZNIEKS

A thesis submitted
in partial fulfillment of the requirements for the
degree Master of Science, Department of
Electrical Engineering, South Dakota
State University

January, 1969

COMPUTER SIMULATION OF A

NEW REDUNDANCY REDUCTION TECHNIQUE

This thesis is approved as a creditable and independent investigation by a candidate for the degree, Master of Science, and is acceptable as meeting the thesis requirements for this degree, but without implying that the conclusions reached by the candidate are necessarily the conclusions of the major department.

Thesis Advisor ✓ Date

Head, Electrical Engineering Department Date

ACKNOWLEDGEMENTS

The author wishes to express his appreciation and gratitude to Dr. D. E. Sander, whose guidance and advice made this investigation possible and to his wife, Patricia, who typed the rough draft and final copy of this thesis.

U. B.

TABLE OF CONTENTS

LIST OF FIGURES AND TABLES

Table

CHAPTER I

INTRODUCTION

The compression of information into smaller and smaller bandwidths has been a constant struggle against an expanding demand. Since the modulation of a carrier necessarily produces sidebands, signals cannot be sent in zero bandwidth. For some time, attempts were made to beat nature, until the natural limits of noise and bandwidth were established. Men like Hartley, Nyquist, and Shannon set a sound scientific base and as a result, rules and limits have been developed. But this struggle continues with ever more sophisticated demands.[6]

As requirements for larger amounts of scientific data arise, methods for utilizing the available means of data transmission efficiently are needed. For many years, communication engineers have discussed the advantages of a simple and reliable means of transmitting, recording, and processing all of the data. Although these engineers contemplated such means, they concentrated on designing for wider bandwidths and more power--the brute-force way to transfer an ever-increasing mass of data in a given period of time. Eventually, realizing that this effort was futile, communication engineers used the knowledge gained from their past efforts and applied it to design a way for

transmitting only the significant data or information. The methods devised are called data compression methods.

Data compression is a technique to reduce the bandwidth needed to transmit a given amount of information in a given time or to reduce the time needed to transmit a given bandwidth signal. Such compression must eliminate redundancies so that only those values which are essential to the faithful reproduction of the input signal (relative to some error criterion) are transmitted. The performance enhancement of a basic data acquisition system by incorporation of data compression can be manifested in a variety of ways, depending, in part, on the manner in which the data compressor is utilized in the system and the performance desired. As indicated in Figure 1, the engineer has the option of incorporating data compression into either the transmitter or the receiver portions of the system. Four basic categories of data handling come under this definition: parameter extraction, adaptive sampling, redundancy reduction, and encoding.[18]

Parameter Extraction

Parameter extraction represents the oldest and most widely used form of data compression. It is a technique that reduces the bandwidth required to transmit a given data sample by extracting a particular characteristic or parameter of the signal. These parameters are then transmitted over the data link. Signal conditioning devices producing reductions in information bandwidth are included in

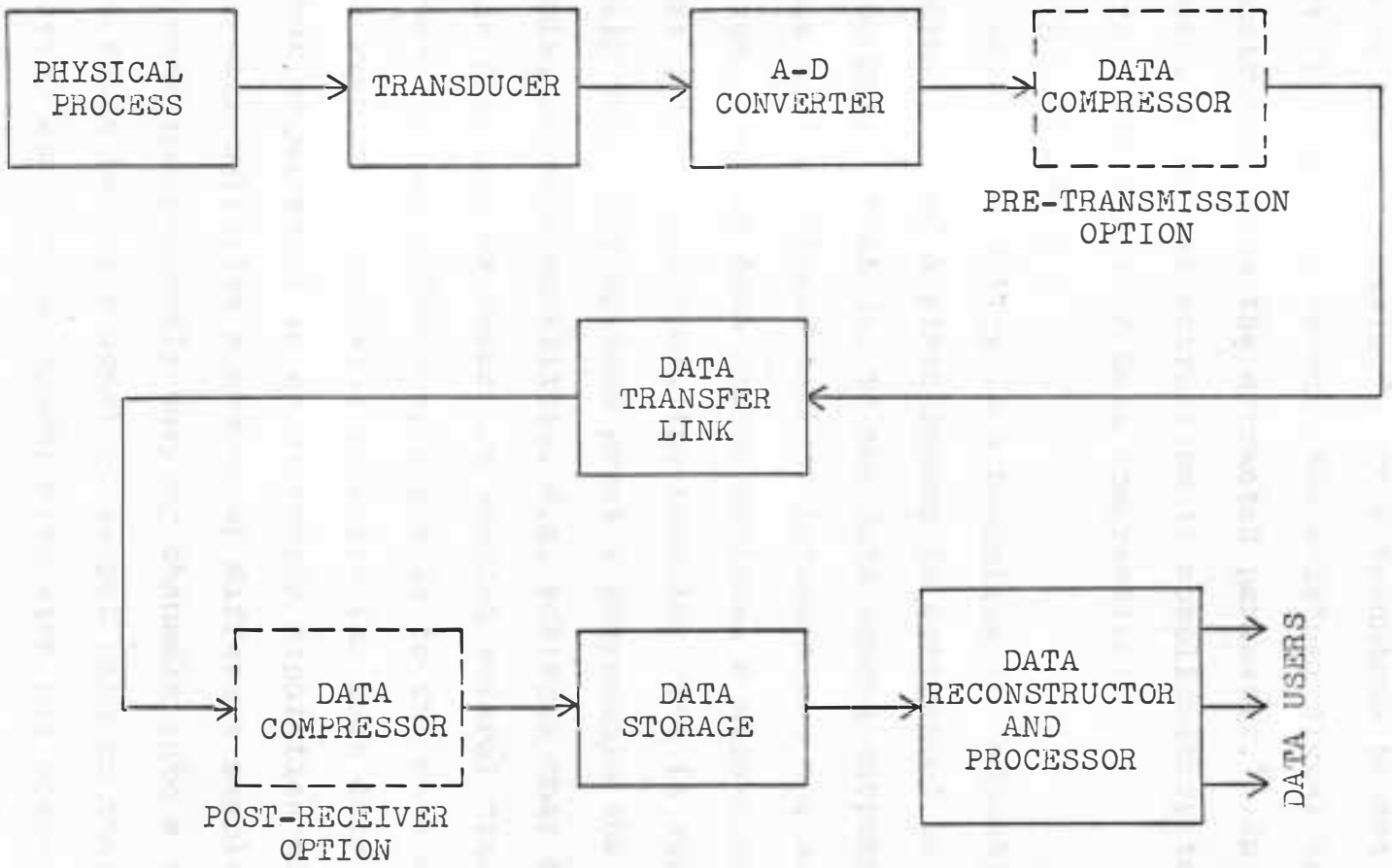

Fig. 1. Basic data acquisition system block diagram showing integration of data compression.

this category. Spectrum analysis, peak detection, and phase comparison are just a few of the techniques that have been used or could be devised. This technique is not an irreversible operation because the original signal cannot be reconstructed from the extracted parameter.[2] In most instances, parameter extraction is complimentary to and enhances other forms of data compression.

Adaptive Sampling

Adaptive sampling is a technique for adjusting the sampling rate of a given sensor to correspond to its information rate. That is, if the data source outputs a vast amount of significant data or information, the sampling rate is high. If the data source produces a slow-changing or almost quiescent output, the sampling rate is very low. Usually telemetry systems greatly oversample the data. For example, on some satellites, d.c. voltages that do not change for days or weeks are sampled several times a second. However, to match the sampling rate to the data activity would require an activity detector for each data channel. Another requirement is an extremely sophisticated system which will multiplex a number of different sample rates from many independently varying channels into a single data pulse train having a constant output rate so that the receiving station can synchronize with the transmitted pulse train and thereby recover the data. While in principle

such a system makes the most effective use of bandwidth and keeps the sampling rates at a minimum, it is extremely difficult to implement.

Redundancy Reduction

Redundancy reduction is a technique for eliminating data samples that can be implied by examination of preceding or succeeding samples or by comparison with arbitrary reference patterns. The basic difference between adaptive sampling and redundancy reduction is that in adaptive sampling the sampling rate of the original data waveform is varied, while in redundancy reduction the waveform is initially sampled at a constant rate and nonessential samples are eliminated later. Thus, as in adaptive sampling, an output is provided only when the data change exceeds the predetermined tolerance. Many practical mechanizations of this technique have been developed and some of them will be discussed in Chapter II.

Shannon defined redundancy as "that fraction of a message or datum which is unnecessary and hence repetitive in the sense that if it were missing the message would still be essentially complete, or at least could be completed."[9] Redundancy exists whenever the sampling rate for the input exceeds the frequency required to describe the input function within the accuracy requirements set for the reconstructed waveform. The choice of reference patterns used to detect

redundancy is virtually unlimited. Polynomials, exponentials, and sine waves are good examples of reference patterns by which real data can often be approximated. The process of redundancy reduction can be achieved by means of "prediction" from a priori knowledge of previous samples, or by a posteriori "interpolation" from future samples. Unlike parameter extraction, both adaptive sampling and redundancy reduction are designed such that the original source or input waveform can be reconstructed within bounds of an error criterion set by the user.

Encoding

Encoding is a technique for transforming a given message into a corresponding sequence of code words. Generally, to achieve the desired coding it is desirable to know the source statistics. If the statistics are stationary and are known a priori, a nonadaptive encoding procedure can be specified. In many cases, however, the statistics are not well-known to the experimentor, or the statistics of the source may be nonstationary, which is usually the case for natural processes. Under these conditions a nonadaptive encoding procedure can result in a bandwidth expansion instead of a reduction. To overcome this problem, adaptive encoding techniques can be devised whereby the code assignments are based upon the most recent statistics measured by the encoder itself. In general, encoding, like adaptive sampling and

redundancy reduction, can reproduce the input waveform within certain error bounds.[18]

The purpose of the investigation reported here is to analyze, by computer simulation, a redundancy reduction technique which was proposed by Sander in (25). A function of time is sampled and a redundancy reduction technique is applied that determines the sampling instants by holding constant or fixing the sampled amplitude changes from one non-redundant sampling instant to the next. This redundancy reduction technique reduces the number of samples needed to reproduce the function from sampled data within acceptable accuracy limits, thereby decreasing memory requirements in computers and data storage systems. The technique will be advantageous for large volume data storage, function modeling, sampled data control systems, and bioengineering problems dealing with both measurement and simulation.[25]

Chapter II of this dissertation contains a review of previous redundancy reduction techniques including a discussion of delta modulation which is similar in many respects to the method analyzed. Chapter III explains the operation of this new redundancy reduction technique along with its function in an adaptive data reduction system. The redundancy reduction technique is investigated using both a sine wave and biased random input waveforms. Two quantizers are investigated using the zero-order and first-order

reconstruction techniques. Chapter IV has a discussion of the results of the computer simulation while Chapter V has the conclusions that were obtained from the results. The basic parameters used for comparison and evaluation of the technique are:

(a) Compression Ratio

(b) Average Mean-Square Error

(c) Signal to Noise Ratio

(d) Variance of the Error.

These parameters are obtained for various sampling rates and quantization step sizes, two quantization techniques, two reconstruction techniques, and for both a sine wave and a uniformily distributed random waveform.

CHAPTER II

LITERATURE REVIEW OF REDUNDANCY REDUCTION TECHNIQUES

A. Sampling Theorem

Before any subject of data compression in general or redundancy reduction in particular can be investigated in depth, a thorough knowledge and understanding of the basis for this entire process must be clearly understood. This basis is the sampling theorem.

The sampling theorem is probably one of the most misunderstood and misquoted theories in use. In general, if sampling is used in a given system, the following question may be asked: What are the limitations on the rate of sampling? Obviously there is no upper limit on the sampling rate. In fact, when the sampling rate approaches infinity (if this were physically possible), the continuous case is approached. As far as the lower limit is concerned, every engineer associated with data compression has his own idea as to how many samples per cycle are needed to recover the original data. A restricted but widely used form of the theorem states:

> If a signal that is a magnitude-time function is sampled instantaneously at regular intervals and at a rate of twice the highest significant signal frequency, then the samples contain all the information of the original signal.[5]

Another widely used version states:

> If the r.m.s. spectrum $|G(f)|$ of the time function g(t), is identically zero at all frequencies above W cycles per second, then g(t) is uniquely determined by giving its ordinates at a series of points spaced 1/2W seconds apart, the series extending throughout the time domain.[9]

What the theorem basically states is that in order to reconstruct the values of an unknown magnitude-time function for all significant times from a knowledge of discrete instantaneous samples, the spacing of the sampling ordinates has to be less than half the period of the highest significant frequency component of the original wave. The discrete instantaneous samples do not even have to be equally spaced as stated by this version of the sampling theorem:

> If a signal is a magnitude-time function, and if time is divided into equal parts forming subintervals such that each subdivision comprises an interval T seconds long where T is less than half the period of the highest significant frequency component of the signal; and if one instantaneous sample is taken from each subinterval in any manner; then a knowledge of the instantaneous magnitude of each sample plus a knowledge of the instant within each subinterval at which the sample is taken contains all of the information of the original signal.[5]

Strictly speaking, a band-limited signal does not exist physically since filters cannot be built that are capable of cutting off perfectly above a frequency, W = 1/T, where W is the highest significant frequency mentioned in the quoted theorems and T is it's period. All physical signals do contain components of a large frequency range. In general,

because the amplitudes of the higher frequency components are greatly diminished, a band-limited signal is assumed. Therefore, because of this assumption, the exact reproduction of a continuous signal from the sampled signal is impossible, even if the sampling theorem is satisfied.[19] If the power content of the frequencies greater than the highest significant frequency, $W = 1/T$, is small, the theorem "nearly" holds. A compensation for the "nearly" would be to sample at a rate higher than that dictated by the sampling theorem.

B. Polynomial Predictors

Many techniques for redundancy reduction are possible; however, at present those most effective and widely used are the polynomial predictors and interpolators. Other mathematical forms such as sine wave and exponentials, are more complex and generally not as efficient as the polynomials for most data compression applications. Because there is a greater likeness between the polynomials and most real data, only the polynomial methods of redundancy reduction will be discussed.

A predictor is an algorithm that estimates the value of each new data sample based on past performance of the data. If the new value falls within the tolerance range about the estimated new value, it is rejected as redundant, since it is

known that the data value can be reconstructed within the specified tolerance.

Polynomial predictors are based on a finite difference technique which permits an nth-order polynomial to be fitted to (n + 1) data points. The polynomial is extrapolated one unit at a time, which produces a predicted data point. A polynomial of the type

$$y(t) = a_0 + a_1 t^2 + \ldots + a_n t^n \qquad (2\text{-}1)$$

may be fitted to the data points by means of a difference equation,

$$Y_t = y_{t-1} + \Delta y_{t-1} + \Delta^2 y_{t-1} + \ldots \Delta^n y_{t-1} \qquad (2\text{-}2)$$

where

Y_t = predicted value at time t

y_{t-1} = data sample value at one sample period prior to t

$$\Delta y_t = y_t - y_{t-1}$$

$$\Delta^2 y_{t-1} = \Delta y_{t-1} - \Delta y_{t-2}$$

$$\vdots$$

$$\Delta^n y_{t-1} = \Delta^{n-1} y_{t-1} - \Delta^{n-1} y_{t-2}$$

The simplest case of Eq. (2-2), the zero-order predictor, is the one which reduces the right hand side of that equation to only one term. In this case n = 0, and Eq. (2-2) becomes:

$$Y_t = y_{t-1} \qquad (2\text{-}3)$$

In interpreting this equation, y_{t-1} must be defined as the actual sample value only if that value is transmitted, and as the value which is predicted if no transmission occurred. The new predicted value thus becomes the last transmitted value.

There are basically three versions of the zero-order predictors given in the literature. One version, the fixed aperture, uses apertures of width 2K on the amplitude scale as shown by the dotted lines in Figure 2. A sample is transmitted only if it falls outside the aperture belonging to the last transmitted sample.

The floating-aperture version of the zero-order predictor always positions an aperture of width 2K symmetrically about the last transmitted data point. If each new data point lies within the aperture placed about the last transmitted data point, the new data point is not transmitted. If the new data point lies outside the aperture, then that point is transmitted, the 2K aperture is placed about it, and the process is repeated. Thus, the aperture is in effect "floating" with the last transmitted sample.[2] Medlin gives simple implementations for both the fixed-aperture and floating-aperture versions of the zero-order predictor.[22]

The zero-order offset predictor is a modification of the floating-aperture zero-order predictor, which attempts to take advantage of knowledge of the data trend established at the time of the last transmitted sample. As before, the predicted value remains constant as long as a sample is not transmitted. However, in this case the floating-aperture is offset from the previously transmitted value by a fixed, pre-determined amount. The sign of the offset is determined by noting the sign of the most recent out-of-tolerance deviation of the data. The offset would be in the positive direction if the deviation showed a positive trend and vice versa. The process is illustrated in Fig. 4.[2]

If in Eq. (2-2), n = 1, then the result is a first-order predictor of the form:

$$Y_t = y_{t-1} + \Delta y_{t-1} \qquad (2\text{-}4)$$

or

$$Y_t = 2y_{t-1} - y_{t-2} \qquad (2\text{-}5)$$

The first-order predictor of Andrews (4) and Gardenhire's (11) two-point projection method are the same operation under two different names. The prediction is made that y_t will equal the last sample value, plus the same change as the last value changed from the one before it. Graphically, the prediction would be made by extending a straight line drawn between the two latest samples, and placing Y_t on this line, as shown in Fig. 5. The same

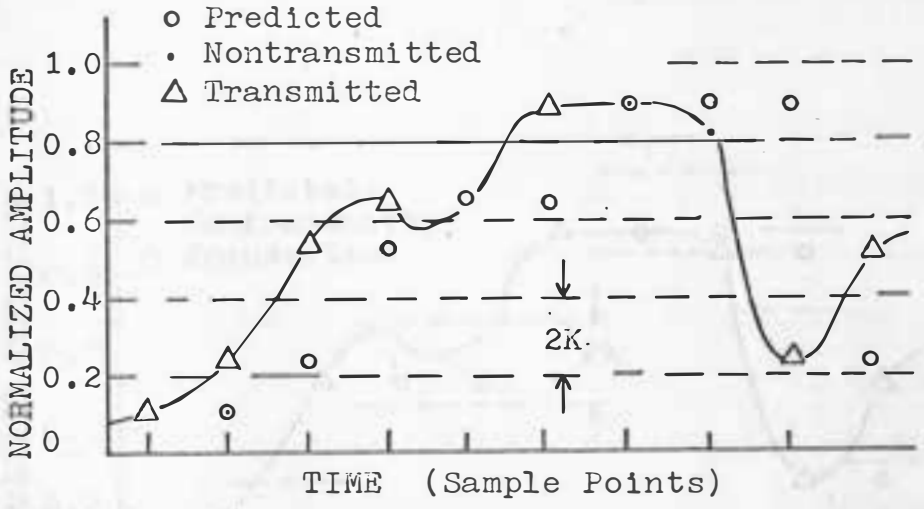

Fig. 2. Data sampling and selection; zero-order, fixed-aperture predictor.[22]

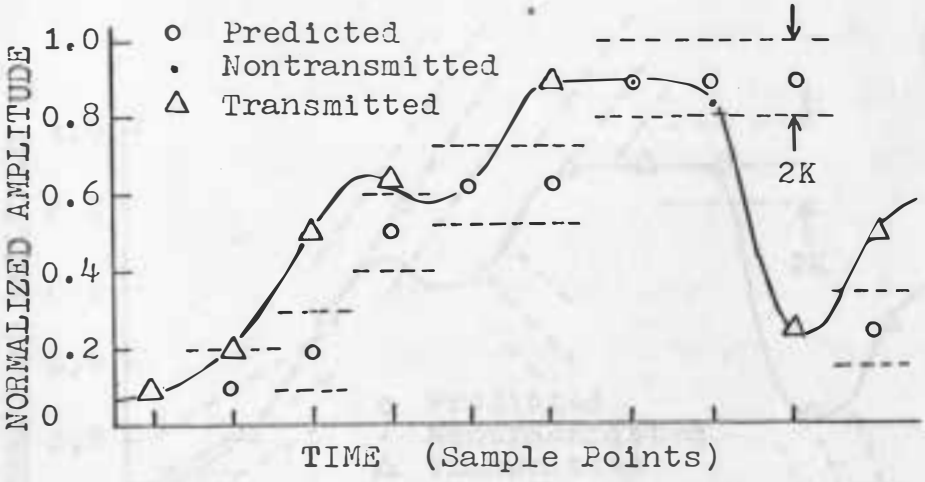

Fig. 3. Data sampling and selection; zero-order, floating-aperture predictor.[22]

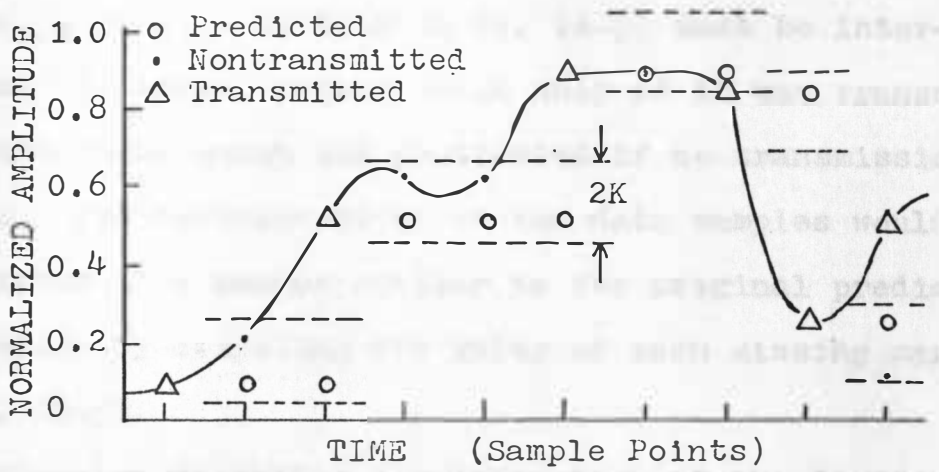

Fig. 4. Data sampling and selection: zero-order offset predictor.[22]

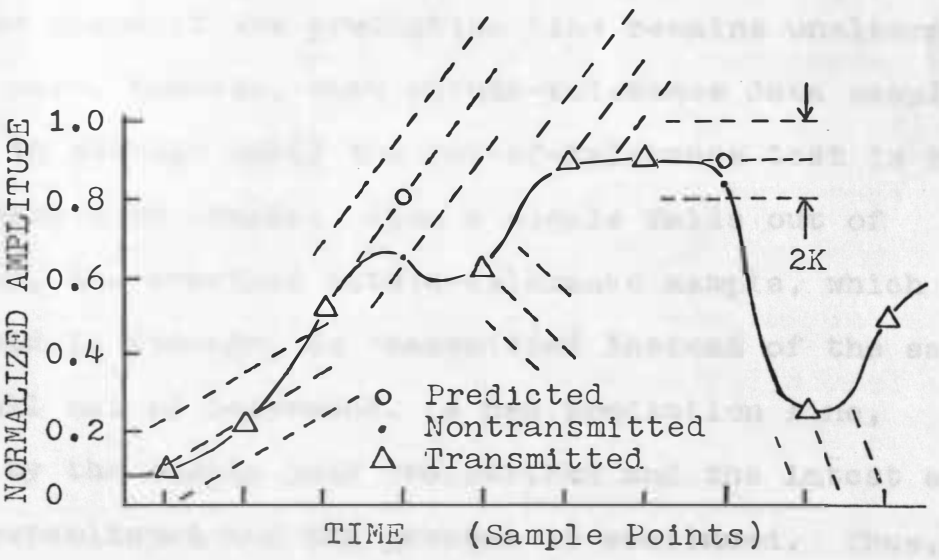

Fig. 5. Data sampling and selection: first order predictor.[11]

interpretation must be given to Eq. (2-5) as in the case of the zero-order predictors for Eq. (2-3). That is, to avoid uncontrollable errors in the reconstructed data samples, either y_{t-1} or y_{t-2} or both in Eq. (2-5) must be interpreted as the actual sample value only if it was transmitted, and as the value which was predicated if no transmission occurred. The reconstruction of the data samples would be accomplished in a manner similar to the original prediction process by computing the value of each missing sample from Eq. (2-5).

Gardenhire describes a modification of the first-order predictor and calls it the fan method. As with the previous method, as long as the data samples remain within tolerance, the slope of the prediction line remains unaltered. In this case, however, each within-tolerance data sample is held in storage until the out-of-tolerance test is made on the next data sample. When a sample falls out of tolerance, the previous within-tolerance sample, which was being held in storage, is transmitted instead of the sample which fell out of tolerance. A new prediction line, defined by the sample just transmitted and the latest sample, is now established and the process is continued. Thus, whenever an out-of-tolerance sample follows a within-tolerance sample, the prediction line will be defined by two actual data points, rather than one actual and one

predicted data sample as with the first-order predictor. The cost of this improvement is the necessity for storage in the compressor of one additional data sample.[11]

The polynomial prediction philosophy can be extended to include higher orders of polynomial redundancy reduction. Although higher-order polynomial predictors will, at times, provide a greater compression efficiency on very active data, usually the price paid for the added complexity is not worth the effort.

C. Interpolators

In order for predictors to be effective, the characteristics of the data must remain relatively constant from one time interval to the next. If the data is varying in a continuous but random manner or if it is intersperced with high-frequency components, the efficiency of the predictor will generally be low for reasonable system accuracy. On such data, a greater number of redundant samples could have been eliminated if both past and future data samples had been used. This process of after-the-fact polynomial curve fitting is termed interpolation.

The simplest interpolator is the zero-order polynomial interpolator. It is similar to the zero-order predictor in that a horizontal line is used to represent the largest set of consecutive data samples within a prescribed peak-error tolerance. The primary difference is that the transmitted

sample for the interpolator is determined at the end of the redundant set as compared with the first sample for the predictor. Furthermore, the transmitted sample Y_t used for the interpolator is computed as the average between the most positive sample y_u and the most negative sample y_l in the set. All samples in the set are within the prescribed peak-error tolerance from the transmitted sample.[18]

The first-order interpolator with two degrees of freedom draws a straight line between the present sample and the last transmitted sample and determines whether all intermediate data points are within a preset tolerance limit of any interpolated value which is on the straight line. This is accomplished by first drawing a line between the transmitted point and the second sampled data value after the transmitted point. If the first point after the transmitted value is within a tolerance K of the interpolated value, then a straight line is drawn between the transmitted point and the third point after the transmitted point. The interpolated value of the first and second points are now checked to see if they are within a tolerance of the actual values. If at the Kth sample value after the last transmitted sample, a line is drawn, and if any of the actual values differ from the interpolated values by a quantity greater than the tolerance, then the (K -1)th sample is transmitted and the process is repeated.[2]

The polynomial predictors and interpolators just discussed are the basic redundancy reduction algorithms. Figure 6 shows the essential components required to implement any of these redundancy reduction algorithms. The reference memory stores the data values, tolerance limits, algorithm selection (if needed), plus any additional information required to enable the comparator to determine if each new data value is significant or redundant. If the new value is redundant, the reference information is returned to the reference memory and the next data value is examined. However, if a new value is significant, the reference information is updated and returned to the reference memory. At the same time the significant data value is inserted into the buffer memory and stored until it can be read out. The buffer is required in most systems to permit the acceptance of significant data points at an irregular rate and submit the data to a data link at a constant rate.[18]

D. Comparison of Basic Redundancy Reduction Techniques

If a comprehensive summary is to be made of all the results obtained by the various contributors in this literature review, the summary would be as varied as the results. The major obstacles to such a summary are the wide variety of input signals and different criteria used

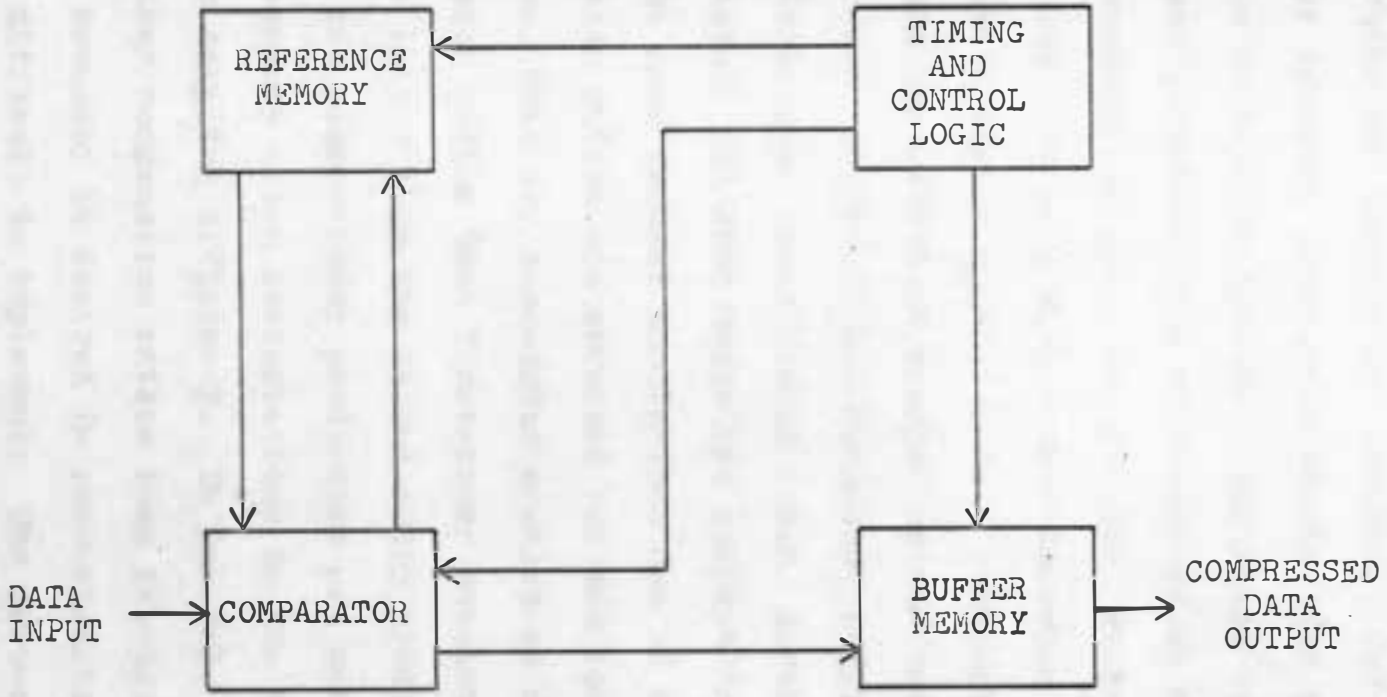

Fig. 6. Simplified block diagram of a redundancy reduction type data compressor.

to determine the conclusions reached. The inputs used for actual or computer simulation studies for these redundancy reduction techniques include: satellite telemetry data, television pictures, time responses of an Nth-order system, electrocardiograph data, and finally, statistically describable inputs such as a first-order Gaussian Markov process. Evaluation criteria used include: compression ratio, bandwidth, and non-redundant samples versus maximum mean-square error; r.m.s. error and non-redundant samples versus sampling ratio; peak error versus r.m.s. error, signal to noise ratios, and even human eye evaluation.

But some general conclusions can be drawn. The best compression ratios are obtained for the lower order processes, that is, zero-order predictors have better compression ratios than first-order predictors which in turn are better than the second-order predictors. This is because the higher-order predictors are more sensitive to high-frequency noise perturbations in the data, resulting in lower sampling efficiency. In general, interpolators have better compression ratios than predictors. Also, if greater accuracy is desired in reconstruction, the process is more difficult to implement. The zero-order predictors are the simplest to implement, but need high sampling rates to obtain a given desired accuracy. The first-order predictor is fairly simple to implement but is more sensitive

to noise than the zero-order predictor. The fan method or the modified first-order predictor has very good accuracy but is hard to implement. The first-order interpolator with two degrees of freedom has good performance, especially for large apertures and is near the median on an implementation scale.[2, 11, 22] From observations made in this literature review, it can be said that the choice of a basic redundancy reduction scheme is definitely a function of the input data, but there is usually a trade-off between complexity and actual data reduction. These basic redundancy reduction techniques submit amplitude information to the data transfer link. Next we shall investigate a method which submits time information to the data transfer link, which is similar to the new redundancy reduction technique under investigation.

E. Delta Modulation

Delta modulation ($\triangle$M) is basically a pulse modulation system with pulses produced at the sending end in equal intervals, even though they are not all transmitted. The criteria for transmitting pulses is decided in the following manner. An "echelon curve" formed from the pulses is compared with the modulating signal. A decision is made when a new step is formed on the echelon curve. If the value of the modulating signal is greater than the echelon curve,

a positive step is added to that curve. If the modulating signal is smaller than the echelon curve, then a negative step is added to that curve. Thus the echelon curve is the quantized form which approximates the modulating signal. The formation of a positive step is arranged to dictate the transmission of a pulse, while the formation of a negative step results in a gap in transmission at that moment in time. A series of pulses as shown in Fig. 8 is transmitted through the data transfer link.

At the receiving end of the data transfer link the step-shaped approximating signal is built up again from the series of pulses received and converted into a continuous signal by smoothing filters to give a reproduction of the original signal. Clearly, if transmission channel interference does not mutilate the pulses beyond recognition or displace them in time, then this interference is eliminated at the reconstruction end.[26] At each sample time the transmitted signal is simply a correction which, when added to the decoded signal at the previous time sample, gives an approximation of the modulating signal at the current sample time. This, in effect, can be called a differential feedback pulse-code modulated system.

The basic single integration ΔM system is shown in Fig. 9. The adder and delay element in the feedback loop around the quantizer form an accumulator. The transfer

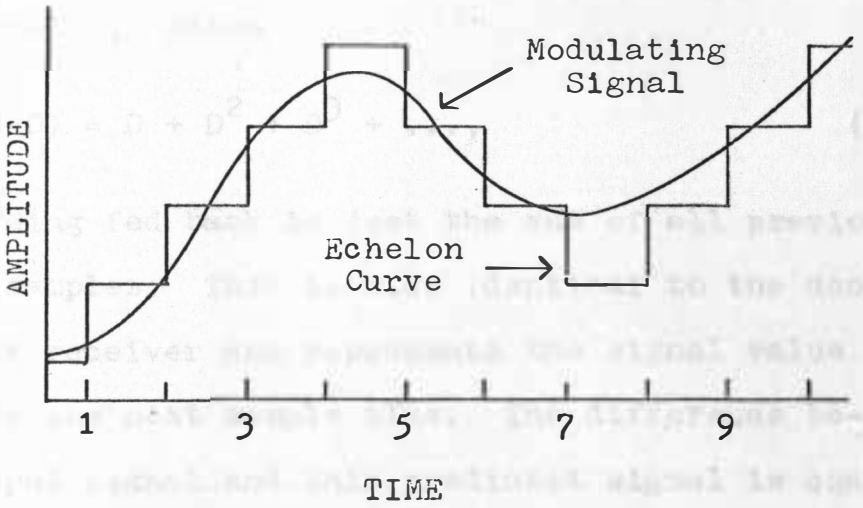

Fig. 7. Basic idea for delta modulation. When the approximating signal is less than the modulating signal, the step goes up. When the approximating signal is greater, the step goes down.[23]

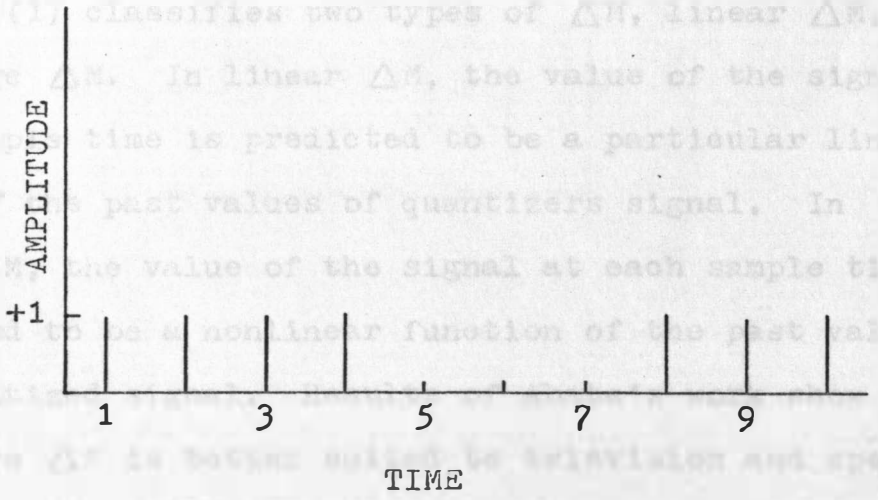

Fig. 8. Output of ΔM transmitter. If the step goes up in Fig. 7, a pulse is emitted while no pulse is emitted if the step goes down.

function of the feedback loop is $D/(1-D)$ where D is the unit delay operator e^{-sT} and represents a delay of one sample interval T. Since

$$D/(1-D) = D + D^2 + D^3 + \ldots, \qquad (2\text{-}6)$$

the signal being fed back is just the sum of all previously transmitted samples. This is also identical to the decoder signal at the receiver and represents the signal value predicted for the next sample time. The difference between the input signal and this predicted signal is quantized and transmitted through a discrete channel. Usually the quantizer has only two levels, $\pm K$, where K is called the step size. Thus the coded output before filtering, Y(t), can assume values $\pm iK$, where i can be any positive integer.[23]

Abate (1) classifies two types of ΔM, linear ΔM, and adaptive ΔM. In linear ΔM, the value of the signal at each sample time is predicted to be a particular linear function of the past values of quantizers signal. In adaptive ΔM, the value of the signal at each sample time is predicted to be a nonlinear function of the past values of the quantized signal. Results of Abate's work show the adaptive ΔM is better suited to television and speech signals than linear ΔM and that the signal-to-noise ratio performance of adaptive ΔM is the same as that for linear ΔM.[1]

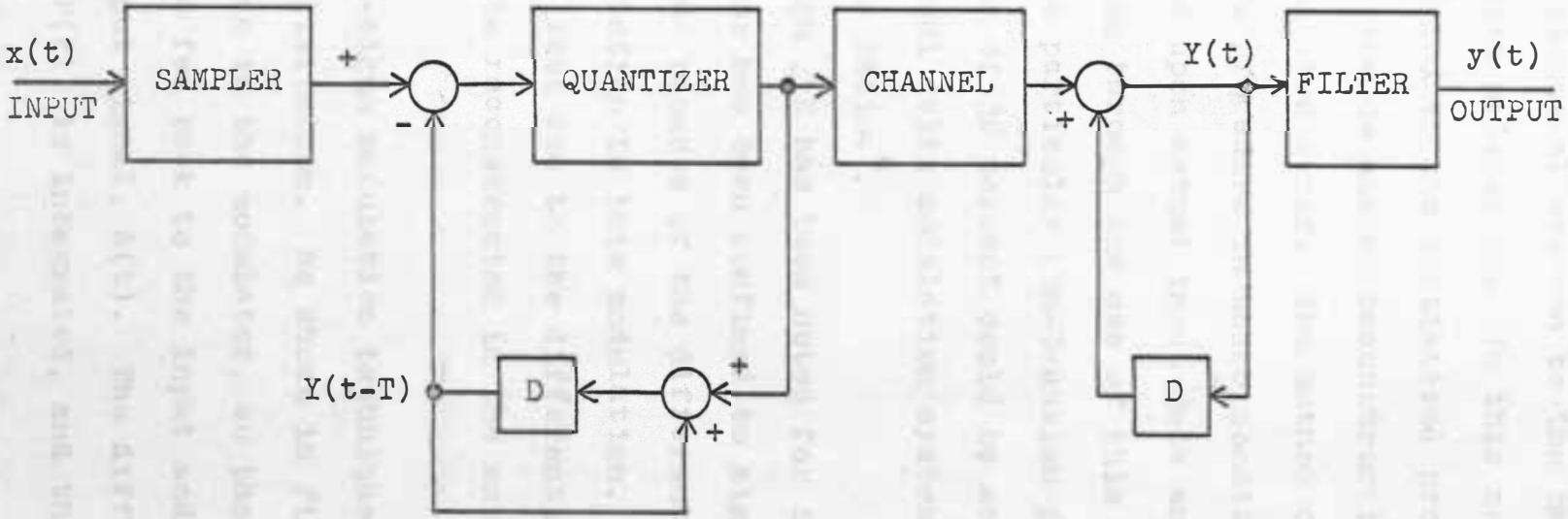

Fig. 9. Basic binary delta modulation system.[23]

Another slight alteration to the basic ΔM method is statistical delta modulation. In this method the system design is tailored to the statistical properties of the input data to provide analog reconstruction values with a minimum mean-squared error. The method of system design is an iterative procedure in which conditional means are evaluated based upon actual input data and system components are chosen through the use of this data. Comparisons show that for a particular non-Gaussian process, sampling rate reductions of 38 percent could be achieved relative to a conventional delta modulation system at the same signal-to-noise ratio.[4]

Even though ΔM has been noted for its circuit simplicity, its use has been confined to signals not having a d.c. component because of the differentiation and inherent integration in this modulation. Any d.c. components would be lost due to the differentiation in encoding and would not be reconstructed in the subsequent decoding integration.

The delta-sigma modulation technique was designed to overcome this limitation. As shown in Fig. 10, integration takes place in the modulator, so that the output pulse, P(t), is fed back to the input and subtracted from the sampled input signal, S(t). The difference signal, $D(t) = S(t) - P(t)$, is integrated, and the integrated

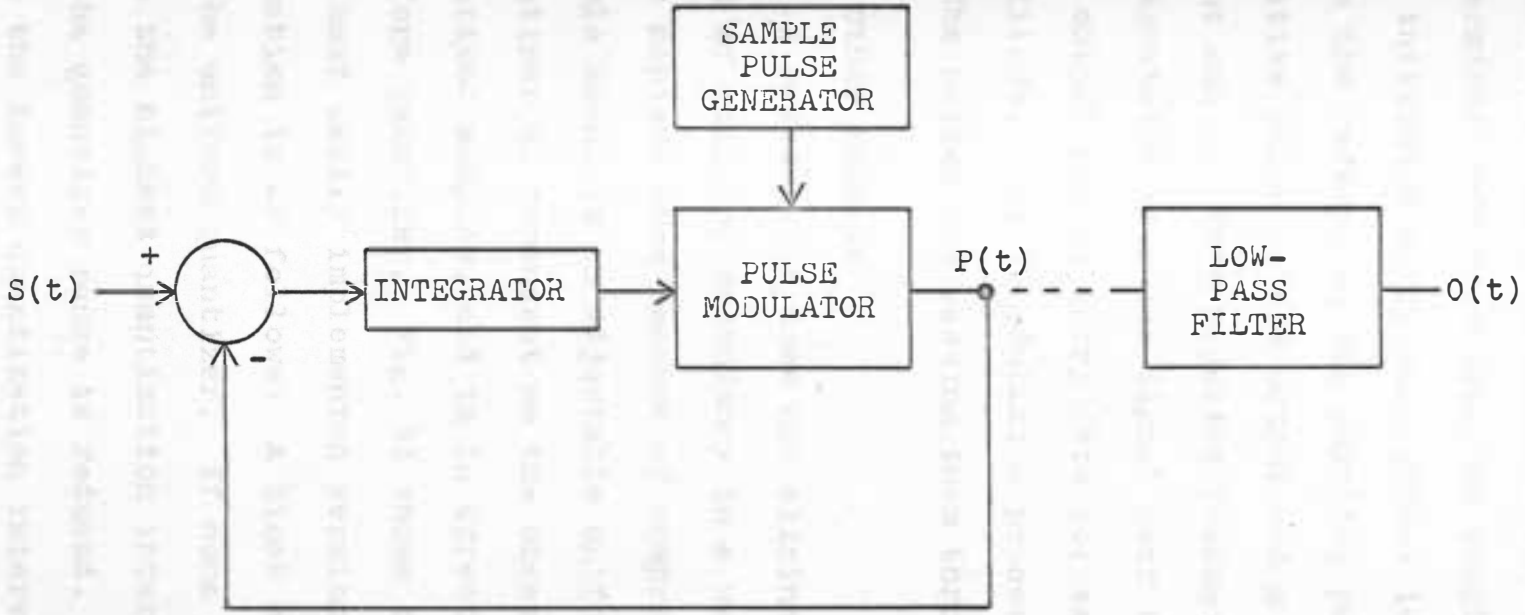

Fig. 10. Simplified block diagram of the delta-sigma modulator.[16]

difference signal is compared in amplitude with a predetermined reference from the sample pulse generator. If the integrated difference signal is positive and larger than the reference, the sampling pulse generator feeds a positive pulse to the output and a negative pulse to the input adder. This negative feedback always keeps the integrated difference signal near the reference. Thus, the output pulses carry data corresponding to the input amplitude. The demodulation process requires only reshaping of the pulses and passing them through a low-pass filter.[16]

F. Other Methods

A system that does not eliminate all or even a major part of existing redundancy in a waveform, but one that does achieve some measure of compression by relatively simple means is an adjustable uniform quantizer. This quantizer is dependent on the observation of blocks of quantized samples, and is in effect a variable-range uniform quantizer. Fig. 11 shows the simplest, though not the most easily implemented version of this system. The operation is as follows: A block of n samples is processed by the uniform quantizer. If none of the samples fall into the highest quantization interval, the upper limit (K) of the quantizer range is reduced. If no samples fall into the lowest quantization interval, the lower limit

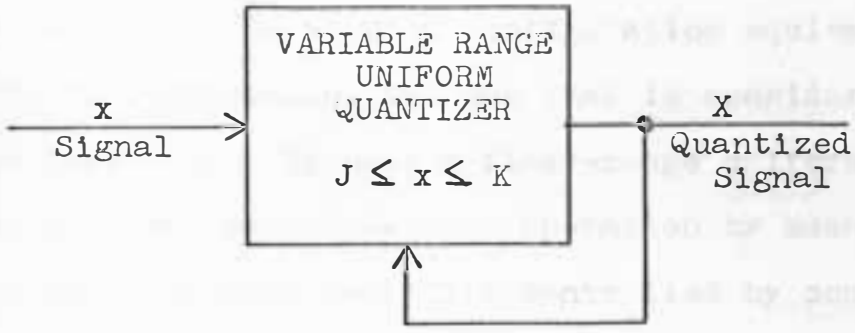

Fig. 11. Block diagram of the adaptive uniform quantizer-hard implementation case.[14]

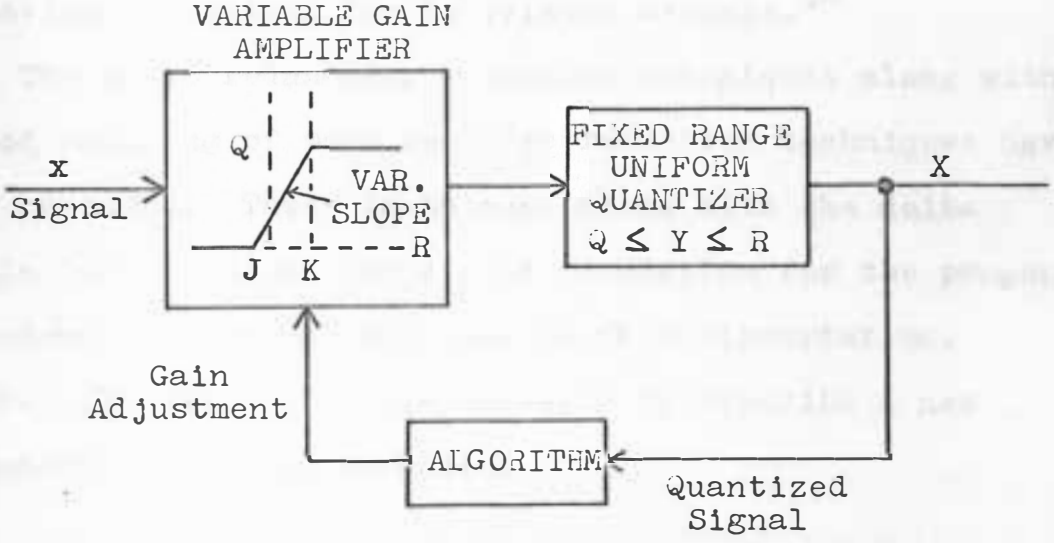

Fig. 12. Block diagram of the adaptive uniform quantizer - easy implementation case.[14]

(J) of the quantizer range is raised. If samples do fall into the end intervals, the range is expanded by an amount depending on the number of samples falling into each end interval. Fig. 12 shows a configuration equivalent to Fig. 11 in performance, but one that is considerably easier to implement. It uses a fixed-range uniform quantizer and achieves variable-range operation by means of a preceding variable-gain amplifier controlled by counters recording the number of samples falling into the extreme quantization intervals. Comparisons made of quantizer's with fixed saturation levels show the variable-range quantizer has definite advantages over its counterpart in achieving reductions for television signals.[14]

The basic redundancy reduction techniques along with a good sampling of more specific reduction techniques have been reviewed. These techniques along with the delta modulation technique lay a good foundation for the proposed redundancy reduction technique in this dissertation. Chapter III will use these concepts to describe a new redundancy reduction technique.

CHAPTER III

A NEW REDUNDANCY REDUCTION TECHNIQUE

If the redundancy reduction techniques discussed in Chapter II are classified according to the output data, there would be two classifications: the delta modulation techniques which transmit time difference information and the other techniques which transmit time and amplitude information. If the reduction efficiency of similar techniques are such that an equal number of samples are transmitted and stored as two different types of output data, the delta modulation class is much better as far as bandwidth and storage requirements are concerned, since only one type of data has to be transmitted and stored instead of two. But the delta modulation technique has been confined to signals not having a d.c. component because of the differentiation and subsequent integration in the modulation. Delta-sigma modulation alleviates this problem by having the integration take place in the modulator so that the d.c. component is not lost, but the implementation problem is greater than for delta modulation. Thus, there is a need for a redundancy reduction technique that utilizes data in the form

$$t = Q(Y) \tag{3-1}$$

instead of in the usual form,

$$y = g(t) \qquad (3\text{-}2)$$

and yet is easy to implement.

A redundancy reduction technique with the above-mentioned characteristics would have many and varied uses and applications. In digital computer applications it would reduce the number of samples or function values to be stored in function modeling situations, data storage, or other related problems. It could be especially advantageous for function modeling in a rapid access memory when large computer programs are being used and memory space is needed.

Presently there are many computer programs which manipulate and solve systems of equations of large dimensions. These programs use stored information for processing data to produce a desired output. The new redundancy reduction technique to be discussed reduces the number of data points needed to reproduce the stored functions within a desired accuracy limit and stores only the time information, thereby increasing the memory space available for program instructions and other additional data.

This technique is also advantageous for data storage and processing in biomedical research. An application would be in recording and processing of electrocardiograms.

The electrocardiogram (ECG) waveform is characterized by a portion of rapidly changing magnitude followed by a period of relative inactivity. The rapidly changing portion of the waveform relays the most information to a physician while the inactive portion relays very little information unless abnormal activity is present in this portion. If abnormal activity does occur in the inactive region, the new redundancy reduction technique will preserve the waveform since it can be designed to be sensitive to any significant amplitude changes. Therefore, using this technique, many unnecessary data points can be omitted and more memory space is made available for additional data, yet all meaningful data is preserved.[25]

A. Theory of Operation

The data compressor of the new redundancy reduction technique is shown in Fig. 13. The signal, f(t), is first fed through a sample and hold circuit which samples at a uniform, predetermined rate. This rate is fast enough to satisfy the Sampling Theorem. Figure 14 shows the input to the sample and hold unit, while Fig. 15 shows its output. The signal is then passed to a combination analog-to-digital (A-D) converter and quantizer. This unit not only converts the analog signal to digital form, but it also quantizes the digital signal so the amplitude values of the sample points can only take on a set of discrete values that are the

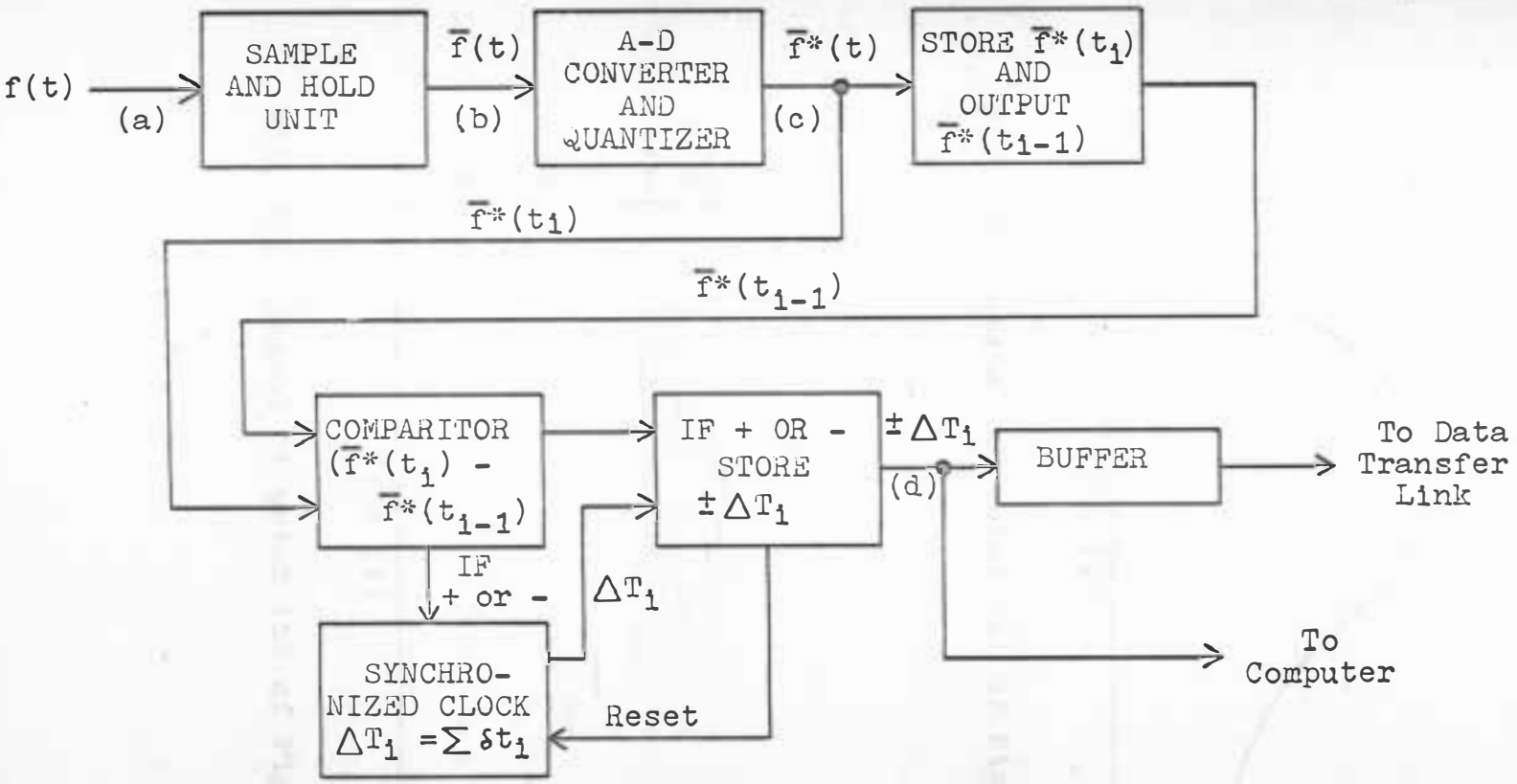

Fig. 13. Block diagram of data compressor for the redundancy reduction technique.

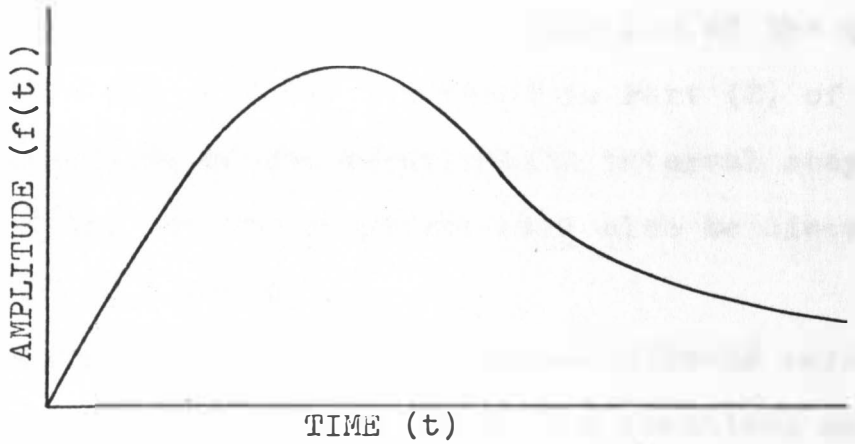

Fig. 14. Signal at point (a) of Fig. 13.

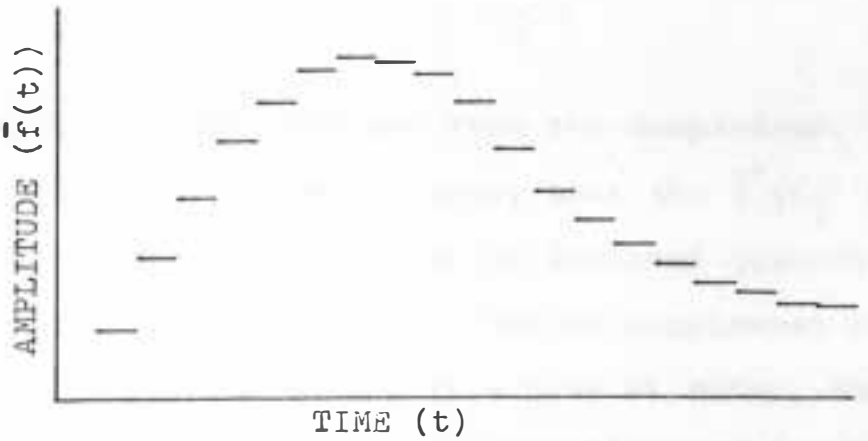

Fig. 15. Signal at point (b) of Fig. 13.

quantization levels. The output of this unit is shown in Fig. 16. Which quantization level or value the digital output of the quantizer assumes is a function of the quantizer and this will be fully discussed in Part (C) of this chapter. The choice of the quantization interval step size or quantum, R(M), for the quantizer will also be discussed in Part (C) of this chapter.

The comparitor takes the quantized-amplitude value of the present sample and compares it to the quantized amplitude value of the previous sample which was in storage. The comparison is actually a subtraction of $\bar{f}^*(t_i) - \bar{f}^*(t_{i-1})$. If this comparison is plus or minus, the value of the time difference of the two samples,

$$\Delta T_i = t_i - t_j \qquad \begin{matrix} 1 \leq i \leq N \\ j < i \end{matrix} \qquad (3\text{-}3)$$

is stored with the sign obtained from the comparison. That is, if the comparitor outputs a zero, then the $\bar{f}^*(t_i)$ and $\bar{f}^*(t_{i-1})$ are in the same quantization interval (quantized to the same value) and thus $\bar{f}^*(t_i)$ can be considered redundant. If the comparitor output is a plus or minus, then the last sample is in a higher or lower quantization level than the previous sample and is significant. If this is the case, the sign of the comparison is attached to the time difference of the two samples. The time difference, ΔT_i, is obtained by using a clock that is synchronized with the

sample rate on the sample and hold unit. Starting with the last compared sample value that was plus or minus, the clock evaluates the time until another pulse from the comparitor indicates a change in quantization levels for the $\bar{f}^*(t_i)$. The clock then outputs a time interval to the storage unit and is automatically set back to zero for the next time interval value $\pm\Delta T_i$ to be stored. The stored time difference values along with the corresponding non-redundant sample amplitude values at point (d) of Fig. 13 are shown in Fig. 17. The values, $\pm\Delta T_i$, are output by the "if" block at irregular intervals depending on the shape of the waveform, the step size, and the uniform sample rate. The buffer stores this time information and outputs it at a uniform rate to the data transfer link. The $\pm\Delta T_i$ values are also sent directly to a computer, which does not need the information at a uniform rate for further processing or reconstruction.

The reconstruction of the signal is achieved as shown in Fig. 18. The $\pm\Delta T_i$ information travels from the data transfer link to an adder. The adder has two parts: one for the addition of the time portion of $\pm\Delta T_i$ and one for the addition of the amplitude portion. Thus the value of time, t, at some sample point, t_k, will be:

$$t_k = \sum_{i=1}^{k} \Delta T_k \qquad (3\text{-}4)$$

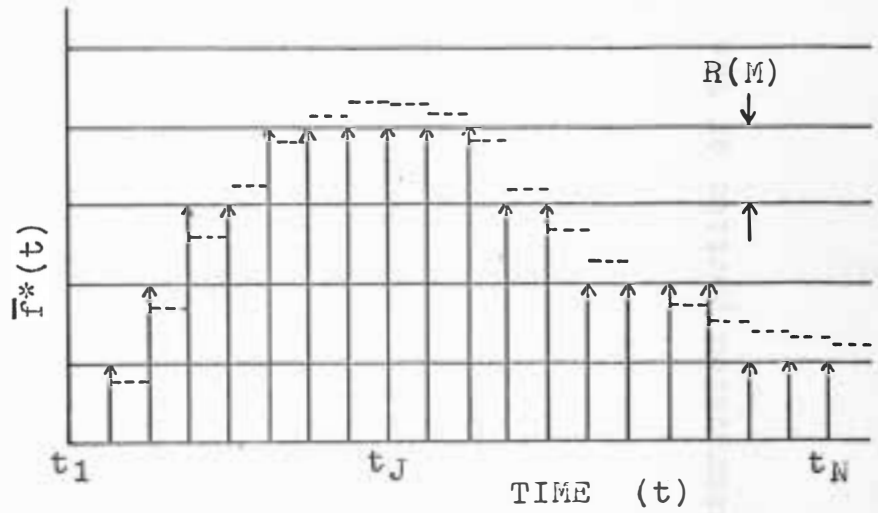

Fig. 16. Signal at point (c) of Fig. 13.

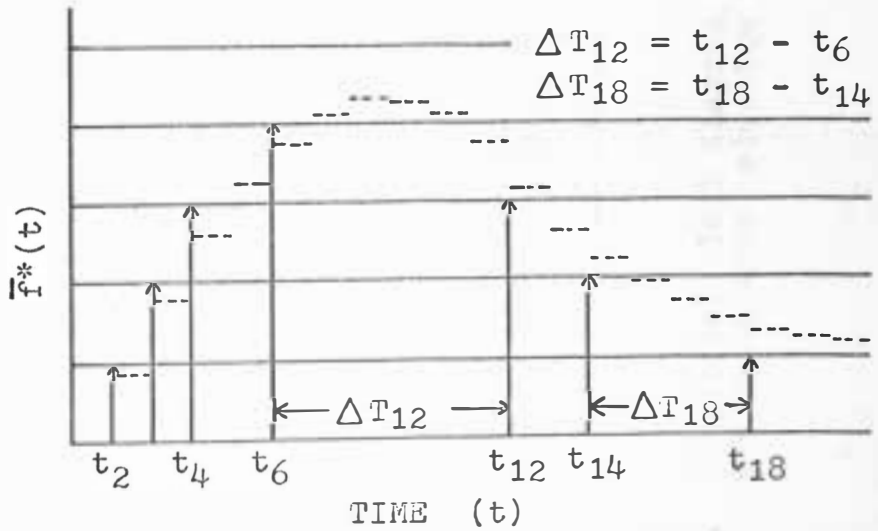

Fig. 17. At point (d) of Fig. 13, the ΔT_i difference values are stored in the buffer. They correspond to the non-redundant sample amplitude values shown.

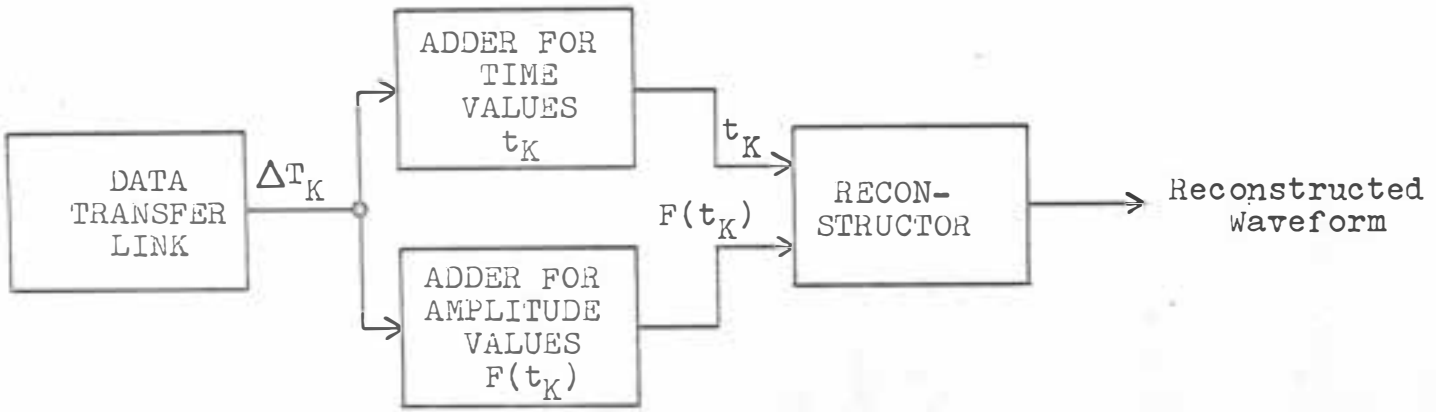

Fig. 18. Simplified block diagram of the reconstruction portion of the new redundancy reduction technique.

The amplitude value of the quantized signal at the point in time, t_k, will be:

$$F(t_k) = R(M) * \sum_{i=1}^{k} (\text{sign of } \Delta T_k) * 1.0 \qquad (3\text{-}5)$$

where:

R(M) = step size or quantization interval size

plus sign = 1.0

minus sign = -1.0.

Using the two pieces of information, t_k and $F(t_k)$, the reconstructor, using a particular reconstruction scheme, reconstructs the input signal. Reconstruction techniques will be discussed in Part (C) of this chapter.

B. The New Redundancy Reduction Technique in an Adaptive Data Reduction Scheme

The redundancy reduction technique under investigation in this dissertation may be used as an independent unit for data compression, or it may be used as only a portion of a larger data compression unit. One such application would be for a proposed adaptive data reduction scheme.

Many analog signals associated with biological telemetry measurements, such as the ECG, electroencephalogram (EEG), nerve action potentials, blood pressure, respiration, and chemical concentration levels are composed of portions of high frequency and high amplitude variations as well as

portions of relatively low frequency, low amplitude variations as shown in Fig. 19. This adaptive data reduction scheme would reduce transmission, storage, and mathematical manipulation requirements on a wide bandwidth signal which has piecewise portions of relatively low frequency data and is subject to large shifts in average value which can drive the signal out of an A-D converter's operating range. The block diagram in Fig. 20 shows essential parts of the scheme.

The analog signal, f(t), is fed to one input of an adder which adds a bias voltage, V_A, to f(t). Then $(f(t) + V_A)$ is fed to the sample and hold unit of the data compressor. The voltage, V_A, is adjusted by the central processing unit (CPU) to maintain variations of f(t) within the range of the A-D converter. The sample and hold unit has a variable sample rate corresponding to a variable time between samples, δt_i, which is adjusted by the CPU. After the signal is sent through the data compressor and processed as described in Part (A) of this chapter, the output data of the data compressor, $\pm\Delta T_i$, is sent to a storage element in a computer, or, if further transmission is necessary over radio or wire links, to a buffer. If the data is scanned and/or used in calculations for functions such as ensemble average or autocorrelation, the sampling criterion block of the CPU unit could adjust the

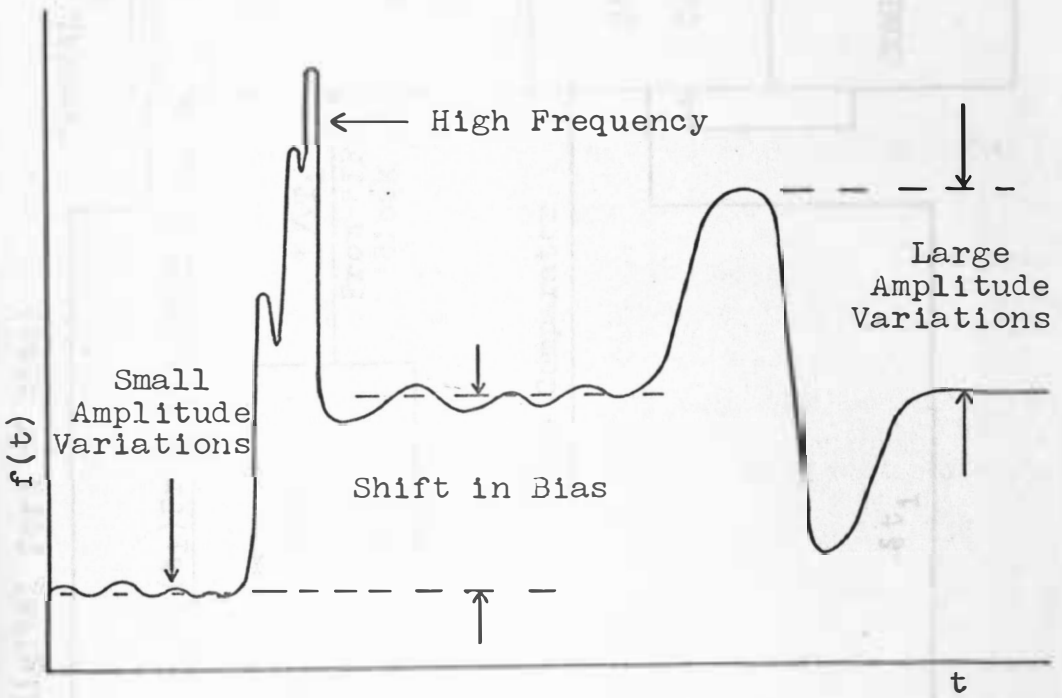

Fig. 19. Possible signal variations in biological telemetry measurements.

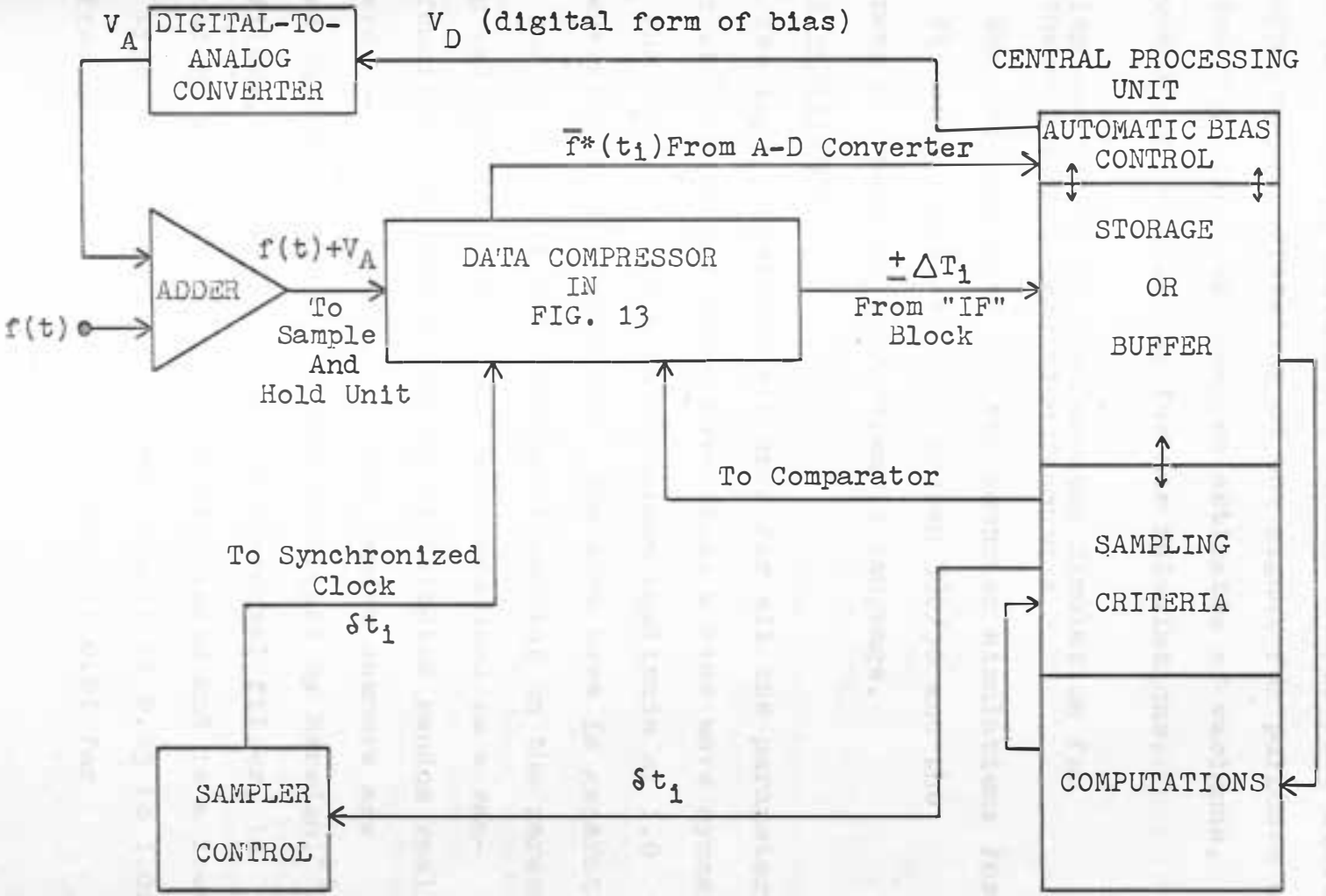

Fig. 20. Simplified block diagram of an adaptive data reduction scheme.[24]

sample rate and the quantization step size of the quantizer to maintain maximum and minimum sample rate limits, perform low-pass filtering of the signal for purposes of eliminating noise, or based on estimates of variance, improve incoming data for further calculations.

C. Implementation of the Computer Simulation for the Redundancy Reduction Technique

The computer used for the computer simulations for this dissertation is the IBM System 360/30 and the programs are written in Fortran IV language.

Input Waveforms

Two input waveforms are used for all the parameters under study. One of these waveforms, a sine wave symmetric with the abscissa and with a maximum amplitude of 1.0 is generated in the computer. The sine wave is generated from one cycle to thirty cycles, depending on the parameter being calculated. The second waveform used is a random function that has uniformly distributed random real numbers between 0 and 1.0. These random numbers are passed through a digital filter developed by Marsden.[21] The filter, generally called a transversal filter, is defined by a set of weighting coefficients and is a low-pass type filter. The filter has a gain of 0.95 to 1.00 for frequencies below 10Hz and a gain of 0.01 for

frequencies above 20Hz.[21] Computer runs using two sets of data, one of 500 samples and another of 1000 samples, are made to insure uniformity of the input data and convergence of the parameters calculated. Since this entire process is simulated on the computer, the same random waveform is used for all the parameter studies so that results for the second set of data are consistent with the first set.

Sample Rate and Quantization Interval Size

Two preliminary questions to be answered are: what should be the range of the quantization step size, R(M), and what should be the range of the constant sample rate associated with the sample and hold unit? Since the values for optimum results for both quantities are desired, as wide a range as is feasible should be used. Thus the quantization step size, R(M), is varied from 0.01 to 0.5 for an input signal normalized to have a maximum amplitude of unity so that the results of the simulation are not restricted by the signal input amplitudes. The independent variable, M, is the number of quantization levels in the positive half plane. Twice that number gives the total number of quantization levels (both positive and negative planes). Therefore there is a maximum of 100 quantization levels and a minimum of 2 quantization levels in the positive half plane. This gives a maximum of 200 quantization levels and a minimum of 4 quantization levels in the entire plane.

Henceforth, when referring to the number of quantization levels, the number used will be only for those in the positive half plane with the understanding that an equal number exist for the negative half plane. When parameters such as mean square error, variances, etc., are obtained, these parameters are calculated for 35 different quantization levels. The number of quantization levels, M, is varied from 2 to 20 by 1's and from 25 to 100 by 2's.

The sample rate for the sine wave input is varied from 11 samples/cycle to 121 samples/cycle. This is equivalent to a degrees/sample interval, I, from 36 to 3. The degrees/sample intervals used were for I from 3 to 12 by 3's and I from 18 to 36 by 6's.

Quantizers

Two quantizers are used in this investigation to determine which is better for the data and parameters studied. Characteristics of the two quantizers are shown in Figs. 21 and 22. The quantizer shown in Fig. 21 will henceforth be called Quantizer No. 1 with R(M) defined as the quantizer step size. The characteristic in Fig. 21 is such that for an input, f(t), where

$$0 \leq f(t) \leq R(M) \tag{3-6}$$

the output, F(t), is equal to R(M)/2. In general, if the

input, f(t), satisfies the following,

$$(K-1)*R(M) \leq f(t) < K*R(M) \tag{3-7}$$

then the output, F(t), is

$$F(t) = \frac{(2K-1)}{2}*R(M), \tag{3-8}$$

where K = 0, ± 1, ± 2, ... Since the inputs are normalized to unity maximum excursions, the following inequality holds,

$$|K*R(M)| \leq 1.0 \tag{3-9}$$

The quantizer in Fig. 22 will be called Quantizer No. 2. Its characteristic is such that for an input, f(t),

$$0 \leq f(t) < \frac{R(M)}{2} \tag{3-10}$$

the output, F(t), is zero, but for an input, f(t), which satisfies the following condition;

$$\frac{R(M)}{2} \leq f(t) < R(M) \tag{3-11}$$

the output, F(t) is equal to R(M). In general for an input, f(t),

$$\frac{2K-1}{2}*R(M) \leq f(t) \leq \frac{2K+1}{2}*R(M) \tag{3-12}$$

the output, F(t), is

$$F(t) = K*R(M) \tag{3-13}$$

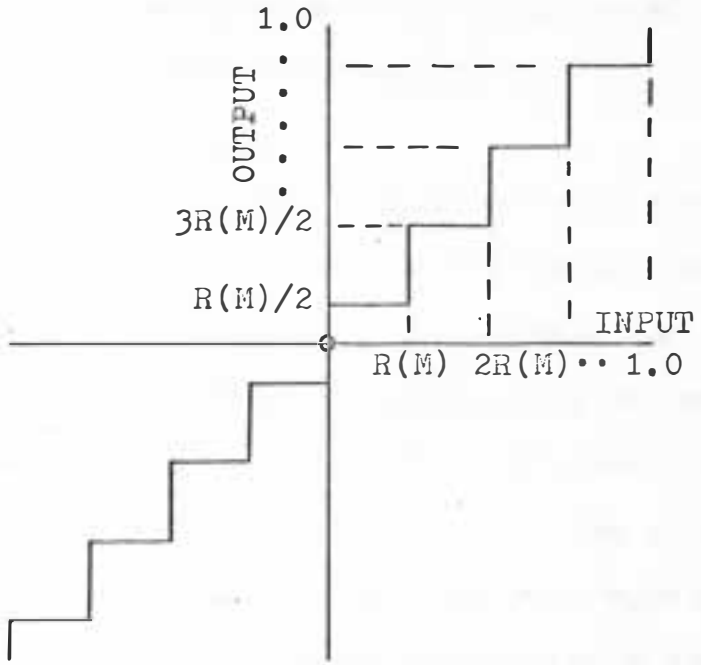

Fig. 21. Quantizer Characteristic for Quantizer No. 1.

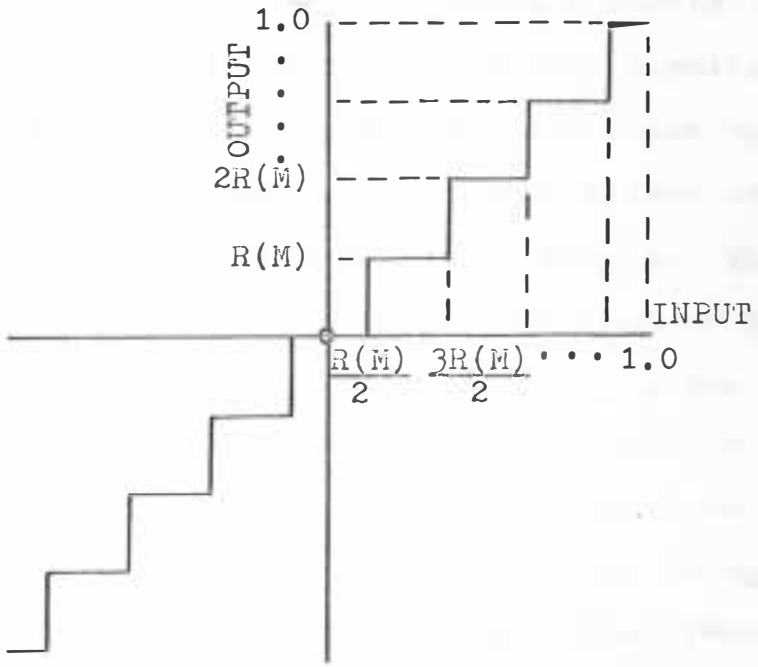

Fig. 22. Quantizer Characteristic for Quantizer No. 2.

for all K. Both quantizer outputs saturate at ± 1.0 for inputs of magnitude greater than unity.

Reconstruction Techniques

The two reconstruction techniques used for reconstruction of the input signals are the zero-order reconstruction and a modified first-order reconstruction. The information from the two adders preceeding the reconstructor in Fig. 18 gives the time and amplitude of each significant sample as shown previously in Fig. 17. The zero-order reconstruction method is realized by construction of a horizontal line from each significant sample to the next significant sample as shown in Fig. 23.

For the first-order reconstructor, a straight line is drawn between the amplitude values of each significant sample. The modified first-order reconstructor has the straight line drawn on the half-interval points of the quantization level of each significant sample. That is, if the present sample quantized has an amplitude of A_k, and it is more positive than the previous one, A_{k-1}, the reconstruction point for the present sample is $A_k - (R(M)/2)$. If the present quantized amplitude, A_k, is more negative than the previous one, A_{k-1}, the reconstruction point is $A_k + (R(M)/2)$. The reasoning behind the modified first-order reconstruction method and its use will be discussed in Chapter IV.

The method is shown in Fig. 24 along with the basic first-order reconstruction.

D. Causes of Noise and Error in the Redundancy Reduction System

Time Jitter Error

There are, generally speaking, two kinds of errors introduced by any data compression system: errors in amplitude and errors in timing. If x(t) is a continuous parameter signal which is being sampled at discrete multiples of the period T, then the samples

$$x_n = x(nT) \tag{3-14}$$

provide a discrete-parameter process. For errors in timing, the sampling epochs are subject to "jitter" so that the samples received do not correspond to the time, t = nT, but to t = nT + λ_n where λ_n represents the error of jitter and the corresponding received samples become[3]

$$y(nT + \lambda_n) = x(nT) \tag{3-15}$$

The time jitter error introduced by the data transmission medium can be eliminated if it is sufficiently small with respect to the sampling rate of the sample and hold unit. This is because the basic sample rate of the sample and hold unit is known and it is the time information, not the amplitude information, that is transmitted through

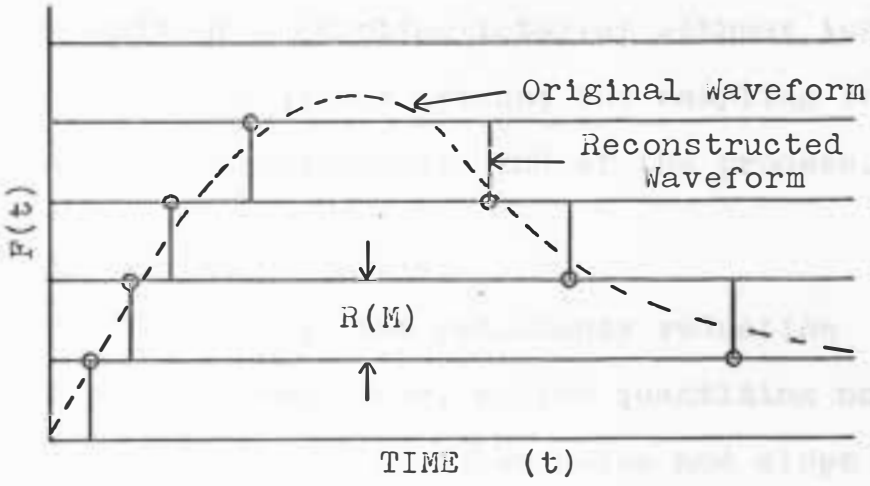

Fig. 23. Zero-order reconstruction of data supplied to the reconstructor by the adder. Data supplied is as shown in Fig. 17. Quantizer No. 2 was used in the A-D converter and quantizer.

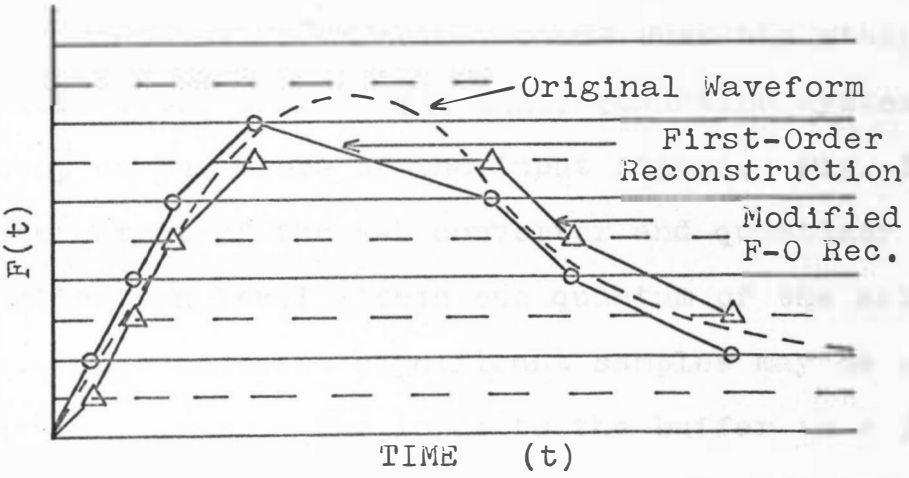

Fig. 24. First-order and modified first-order reconstruction of data supplied by the adder. Data supplied is as shown in Fig. 17. Quantizer No. 2 was used in the A-D converter and quantizer.

the data transfer link. The time information could be in error up to one-half of a sampling interval without introducing error due to time jitter because the sampling rate is also known at the reconstruction end of the process.

Granular and Slope Overload Noise

The principal errors in the redundancy reduction technique are errors in amplitude, called quantizing noise, of which there are two types, granular noise and slope overload noise. Granular noise is similar to the quantizing noise of pulse code modulation. It is caused by the fact that quantizer output samples can assume only discrete values which for this technique are multiples of the step size, R(M).[23] Slope overload noise occurs when the steepest reproducible slope of the redundancy reduction system is not as steep as the slope of the input signal. Fig. 13 shows that the output of the A-D converter and quantizer is set to a quantization level within one quantum of the actual input signal. Thus adjacent significant samples may be any number of quantums apart. The input to the buffer is $+\Delta T_i$ or $-\Delta T_i$. From this point on, the adjacent significant samples are interpreted as being only one quantum apart, either the next one higher or lower. This process, in the transmission of only the $\pm\Delta T_i$, introduces the possibility

for slope overload noise. The maximum slope producible between adjacent significant samples is

$$S_m = \frac{R(M)}{I} \tag{3-16}$$

where

S_m = maximum slope

$R(M)$ = one quantum

I = basic sampling interval.

Thus, in order for slope overload not to occur in the reconstruction process, the following condition must be satisfied:

$$\frac{R(M)}{I} = S_m \geq |f'(t)| \tag{3-17}$$

where

$|f'(t)|$ = magnitude of the input signal derivative with respect to time.

In the example illustrated in Fig. 25 the noise n(t), which is defined as

$$n(t) = f(t) - F(t) \tag{3-18}$$

where

$f(t)$ = input signal

$F(t)$ = reconstruction signal

is granular before time t_0. At time t_0 the slope of the input f(t) exceeds that which the data compression system

is capable of reconstructing. The period of slope overload in the case shown is from t_0 to t_1 and the slope overload noise during this period is approximately,

$$n(t) = f(t) - (F(t_0)+(t-t_0)*S_m), \quad t_0 \leq t \leq t_1 \qquad (3\text{-}19)$$

where $S_m = R(M)/I$ is the maximum slope the data compressor is capable of reproducing. The quantizing noise is not independent of the signal. Granular noise is determined by the instantaneous amplitude of the input signal and slope overload noise is determined by the slope of the input signal. For very large step sizes or quantums almost all of the noise is granular. As the step size is decreased the reconstructed signal loses its ability to rise and fall rapidly and slope overload noise becomes dominant.[23] This is true for any one sampling rate. If the sampling rate is varied as is done in this dissertation, the slope overload noise is dependent on both step size and sampling rate as shown in Eq. (3-16).

If the input signal is a sine wave such that

$$f(t) = A \sin(\omega t) \qquad (3\text{-}20)$$

then the slope at any time t is given by:

$$\frac{df(t)}{dt} = A\omega \cos(\omega t) \qquad (3\text{-}21)$$

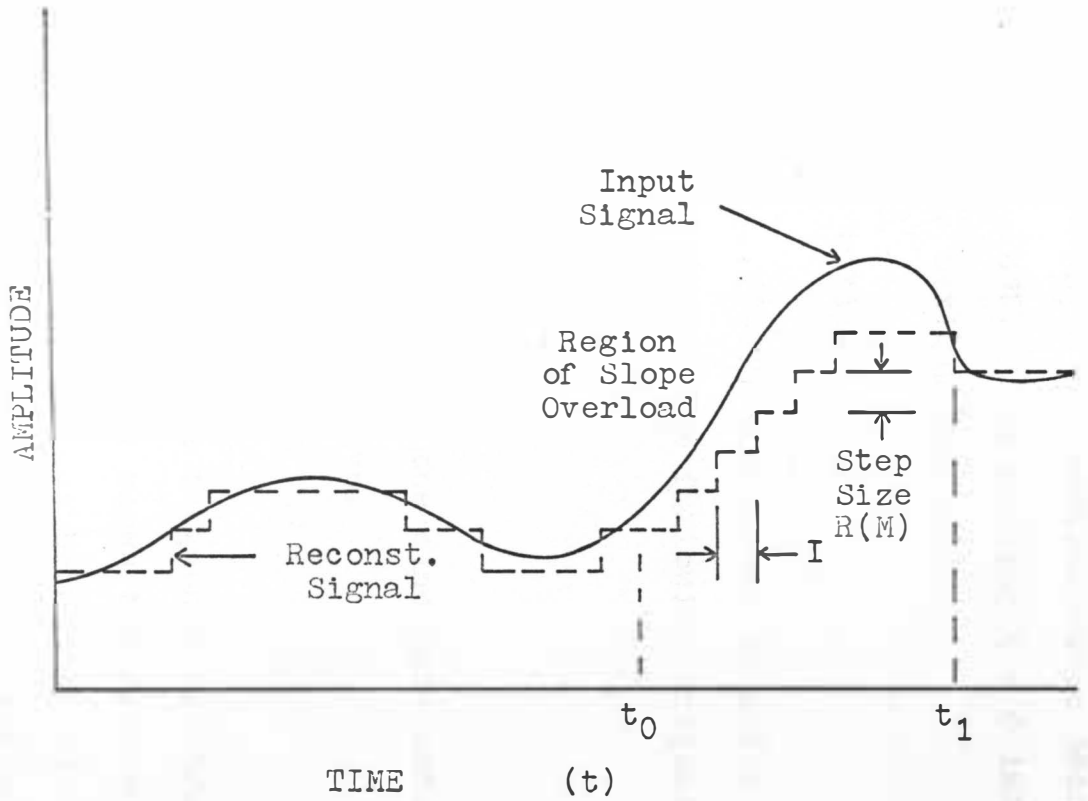

Fig. 25. Input signal and corresponding reconstructed signal of the redundancy reduction system, showing regions of granular noise ($0 \leq t \leq t_0$) and slope overload noise ($t_0 \leq t \leq t_1$).

In order to determine the maximum slope of the sine wave, a second derivative is taken and set equal to zero:

$$\frac{d^2f(t)}{dt^2} = -A\omega \sin(\omega t) = 0 \qquad (3\text{-}22)$$

Therefore the time at which the maximum slope occurs is $t = 0, 2\pi, 4\pi, \ldots 2n\pi$. Thus putting $t = 0$ into Eq. (3-21) yields the maximum slope.

$$\frac{df(t)}{dt} = A\omega = \text{maximum slope.} \qquad (3\text{-}23)$$

For the sine wave, Eq. (3-17) shows that in order for slope overload not to occur, the following inequality must hold;

$$\frac{R(M)}{I} > A\omega \qquad (3\text{-}24)$$

where A is maximum amplitude of the sine wave and ω is angular frequency of the sine wave.

Aliasing

Figure 26(A) shows an ideal frequency spectrum with a bandwidth of F Hz. Figure 26(B) shows the frequency spectrum of ideal data after it has been sampled. Images of the original data appear at multiples of the sampling frequency. In actual practice, however, data looks more like that in Figure 26(C). If F is chosen to be the 3 db point on the curve, one can see that a considerable amount

of energy exists above F. This energy will produce large errors if the sampling rate is only 2F, as seen in Fig. 26(D). The amount of overlap, as seen on these two curves, is what is known as foldover or aliasing error. Figure 27 shows the result of aliasing error if the sampling frequency is less than the minimum described by the sampling theorem. In actual practice the sampling rate is usually chosen 5 to 10 times higher than required by the sampling theorem so that the amount of error due to the overlap is less than the allowed error. If the skirts of the frequency spectrum contain a large part of the noise associated with the signal, placing a pre-sampling filter on the analog input before the sample and hold process could reduce the aliasing error. The cut-off characteristic of the filter is arranged so the frequencies above F are reduced before the sampling process is performed.[13]

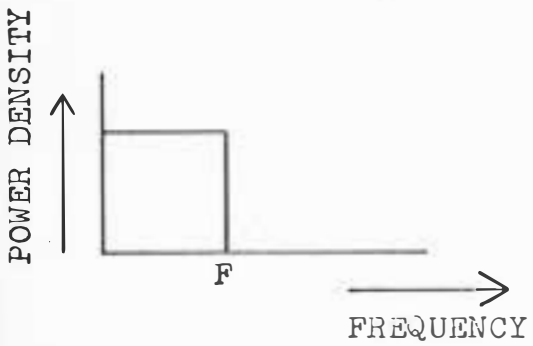

A. Frequency spectrum of ideal data.

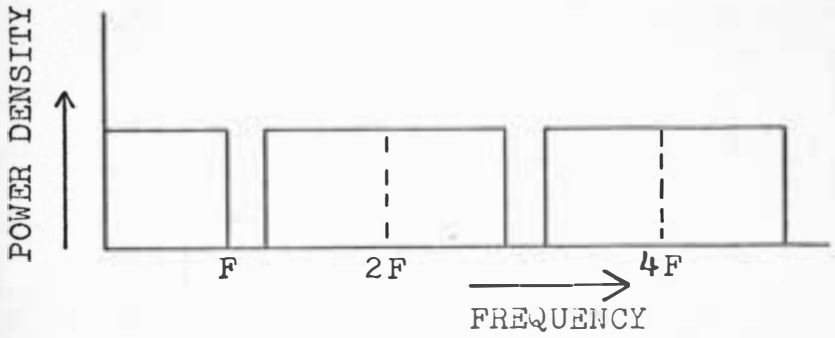

B. Frequency spectrum of ideal sampled data.

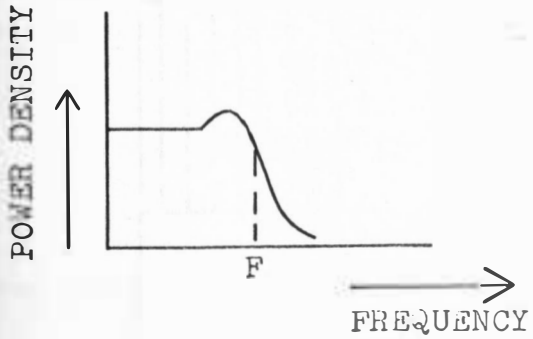

C. Actual data showing F at 3 db cutoff point.

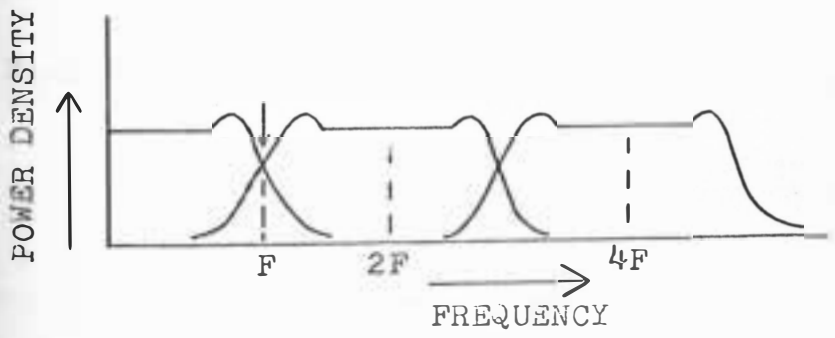

D. Frequency spectrum of actual sampled data.

Fig. 26. Frequency of ideal and actual data.[13]

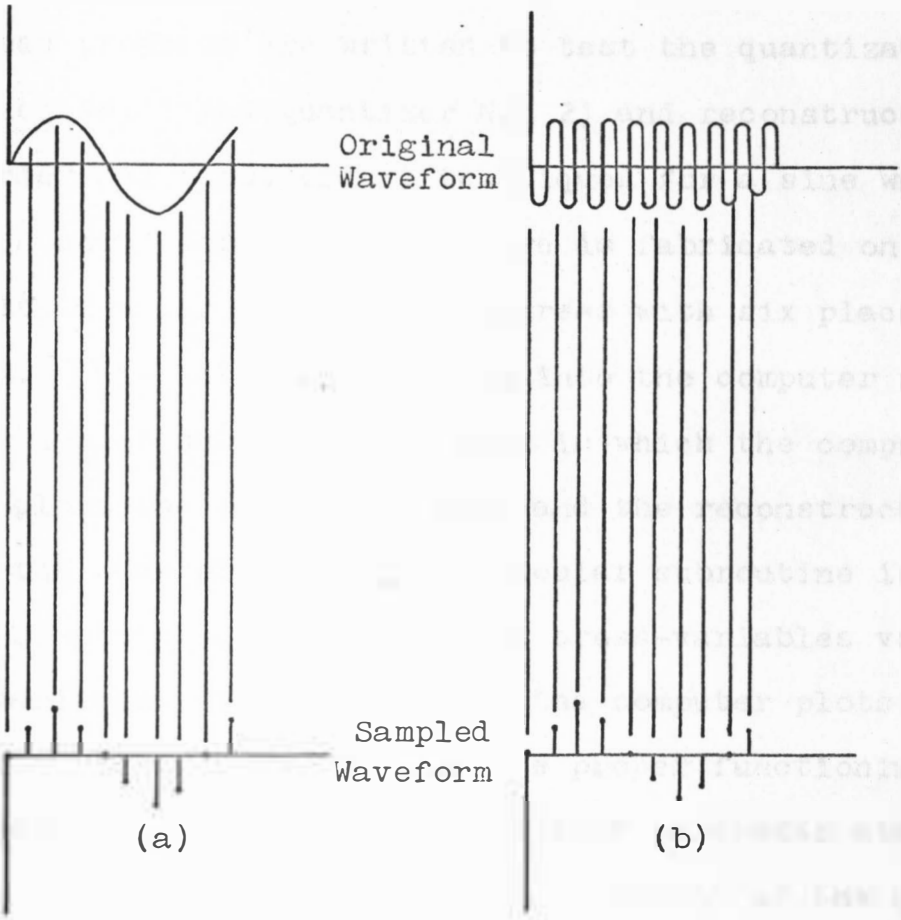

Fig. 27. Waveform (a) has a sampling frequency 8 times the waveform frequency. Waveform (b) has a frequency 8/7 of the waveform frequency, with the sampling frequency below the minimum set by the Sampling Theorem. The result is the very apparent aliasing problem.[13]

CHAPTER IV

EXPERIMENTAL DATA AND DISCUSSION OF RESULTS

A. Plot Routines

These programs are written to test the quantization (Quantizer No. 1 and Quantizer No. 2) and reconstruction (zero-order and first-order) techniques for a sine wave input. A unity amplitude sine wave is fabricated on cards with a value every three degrees with six place accuracy. This data deck is read into the computer when needed. A plot subroutine is used in which the computer printer plots the input sine wave and the reconstructed wave on the same plot. This particular subroutine is capable of plotting nine different cross-variables versus a base variable. The function of the computer plots are two-fold: first, as a check on the proper functioning of the redundancy reduction system so that parameter studies could be made, and also for "eye evaluation" of the quantizing and reconstruction techniques. The plots shown in this section are obtained using the information from the computer print-out plots.

Figure 28 shows the results for Quantizer No. 1 with zero-order reconstruction. The two cases shown are the extreme cases of quantum size ranging from $R(M) = 0.5$ in Fig. 28(A) to $R(M) = 0.01$ in Fig. 28(B). The error in

reconstruction for R(M) = 0.5 is almost all due to granular noise because of the courseness of the quantum size. The R(M) = 0.01 case has severe slope overload error due to the fact that the quantum size is too fine. This greatly decreases the slope that the reconstruction process can follow. For quantum sizes of R(M) = 0.05 to R(M) = 0.0833, the reconstructor produces a near facsimile of the input signal. All quantum sizes smaller than this range produce very evident slope overload noise while all quantum sizes larger produce reconstructed signals that have granular noise. Because of the Quantizer No. 1 characteristic, the peaks of the sine wave always have some degree of attenuation, even before slope overload becomes dominant.

Figure 29 shows the same two plots for Quantizer No. 2 with zero-order reconstruction. The reconstructed signals for both R(M) = 0.5 and R(M) = 0.01 have the same types of noise for each particular quantum size as Quantizer No. 1. The range of near facsimile reproduction by "eye evaluation" is from R(M) = 0.05 to R(M) = 0.1. The same trends follow as in the last case for either side of the range. At this point, with no statistical analysis, Quantizer No. 2 appears to give a better reproduction of the input sine wave for zero-order reconstruction.

Figure 30 shows the first-order reconstruction of a sine wave using Quantizer No. 1. A phase lag of the

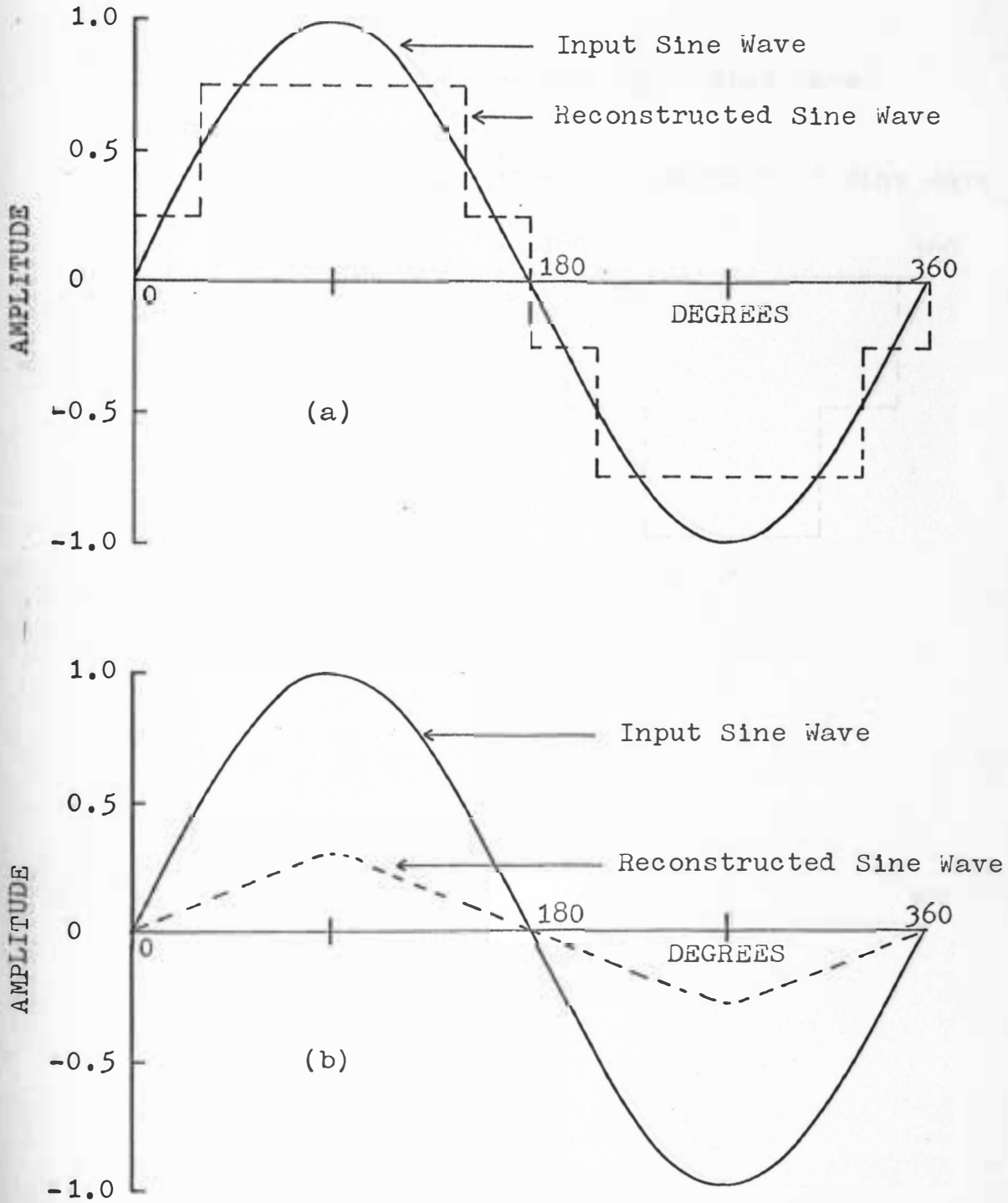

Fig. 28. Input and reconstructed sine wave for Quantizer No. 1 and with zero-order reconstruction. (a) R(M) = 0.5 (b) R(M) = 0.01.

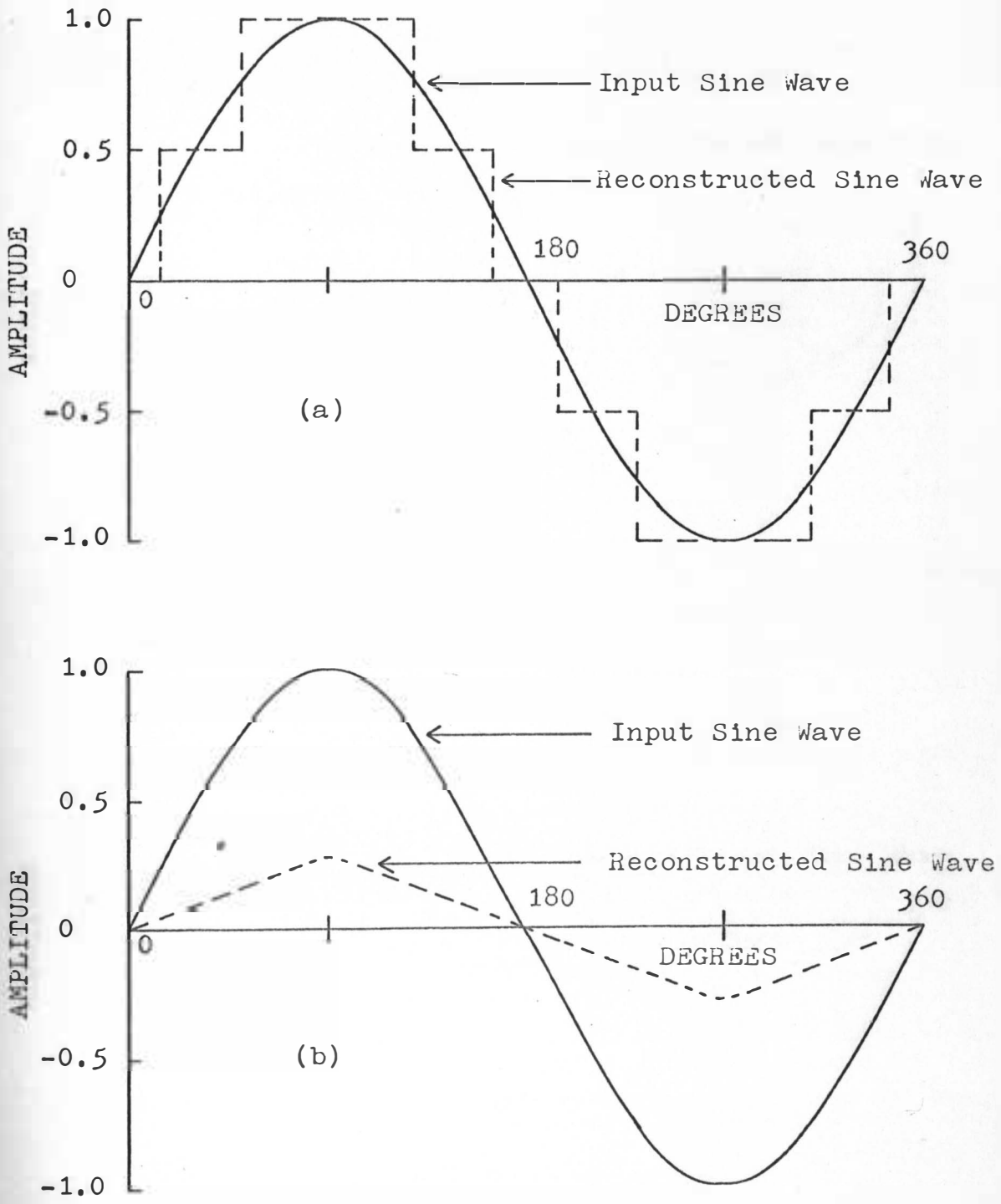

Fig. 29. Input and reconstructed sine wave for Quantizer No. 2 with zero-order reconstruction. (a) R(M) = 0.5 (b) R(M) = 0.01.

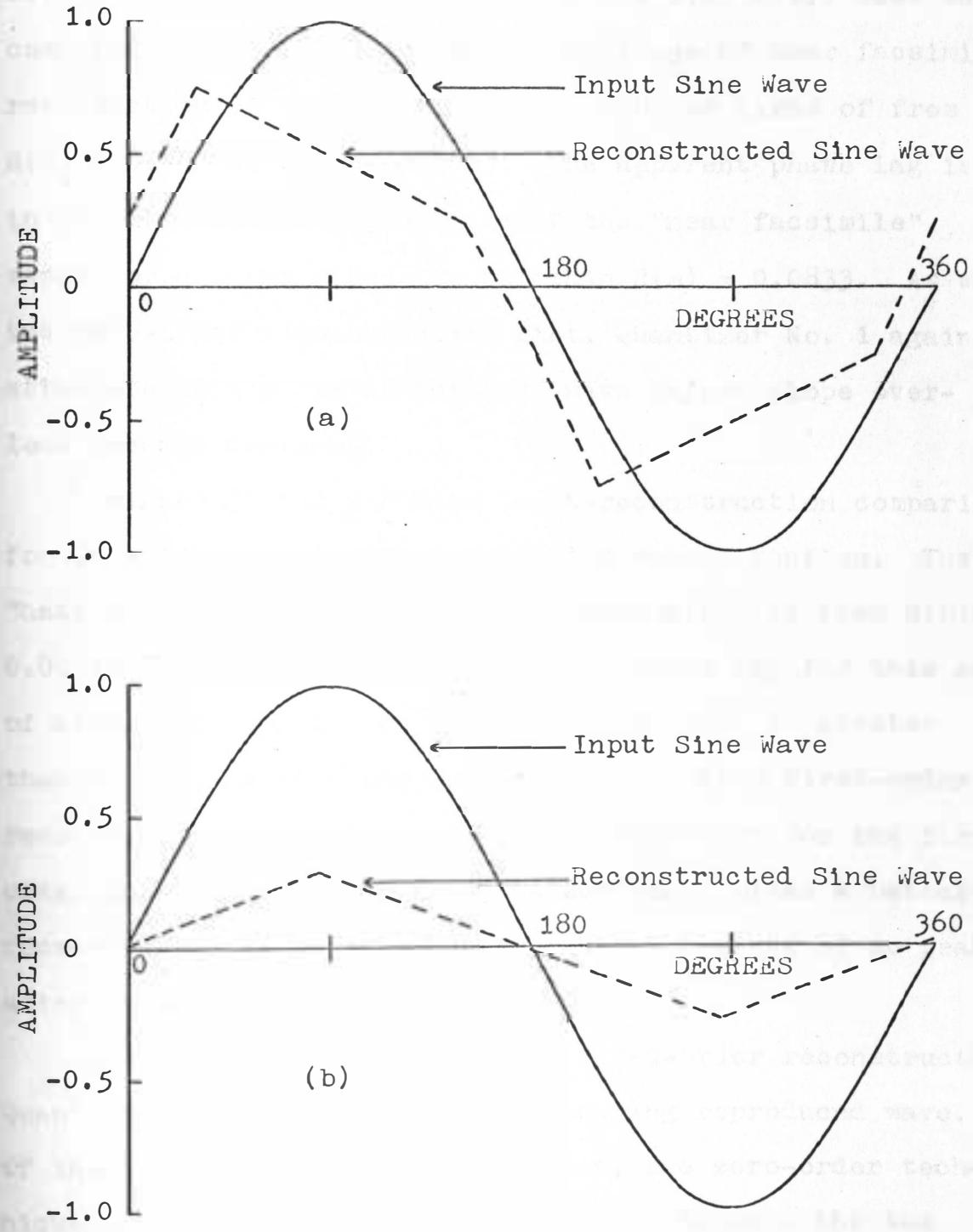

Fig. 30. Input and reconstructed sine wave for Quantizer No. 1 with first-order reconstruction (a) R(M) = 0.5 (b) R(M) = 0.01.

reconstructed wave is evidenced in the R(M) = 0.5 case when compared with previous graphs. The range of near facsimile reproduction of the input is for quantizer sizes of from R(M) = 0.055 to R(M) = 0.0833. The apparent phase lag is in evidence on the higher side of the "near facsimile" range for quantum sizes greater than R(M) = 0.0833. As with the zero-order reconstruction plot, Quantizer No. 1 again attenuates the peaks of the sine wave before slope overload becomes dominant.

Figure 31 has the same input-reconstruction comparison for Quantizer No. 2 with first-order reconstruction. The "near facsimile" range for the quantum sizes is from R(M) = 0.05 to R(M) = 0.0833. The apparent phase lag for this set of conditions appears on the plot where R(M) is greater than 0.0833, as with the Quantizer No. 1 with first-order reconstruction conditions. Visual comparison for the first-order reconstruction shows Quantizer No. 2 gives a better reconstructed wave than Quantizer No. 1 because of no peak attenuation.

Thus for both zero-order and first-order reconstruction, Quantizer No. 2 gives a better appearing reproduced wave. Of the two reconstruction techniques, the zero-order technique appears better in each comparison between the two reconstruction techniques for the same quantizer.

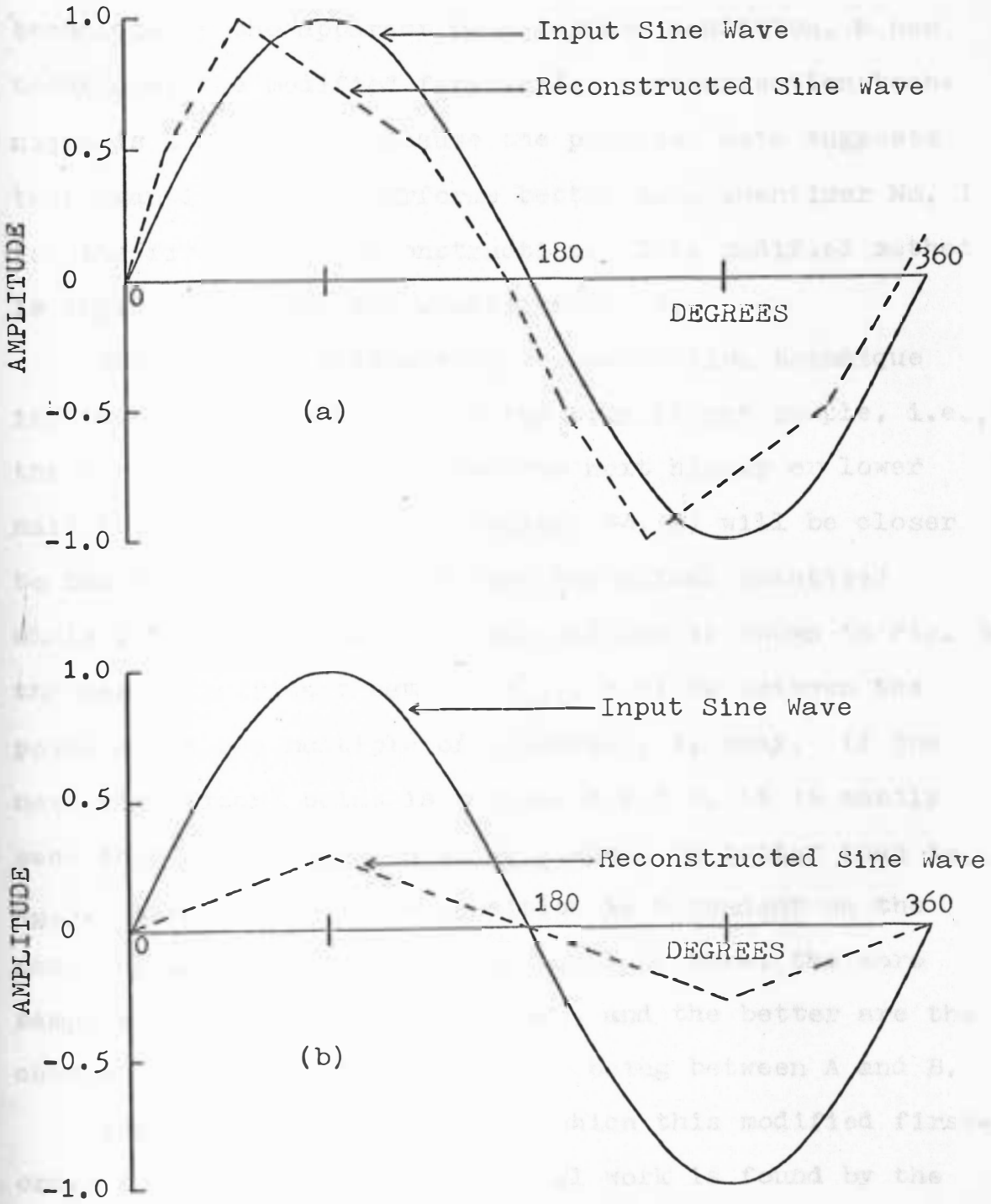

Fig. 31. Input and reconstructed sine wave for Quantizer No. 2 with first-order reconstruction. (a) R(M) = 0.5 (b) R(M) = 0.01.

In an attempt to rid the first-order reconstruction technique of the apparent out-of-phase condition, a new technique, the modified first-order reconstruction technique is considered, because the previous data suggests that Quantizer No. 2 performs better than Quantizer No. 1 for the first order reconstruction. This modified method is implemented only for Quantizer No. 2.

The modified first-order reconstruction technique implies the supposition that the significant sample, i.e., the first sample that crosses the next higher or lower half interval point (for Quantizer No. 2) will be closer to the half interval point than the actual quantized whole interval point. This supposition is shown in Fig. 32; the next significant sample, P_{n+1}, must be between the point A and B a multiple of intervals, I, away. If the next significant point is between A and B, it is easily seen that a quantization to H_{R+1} would be better than to Q_{N+2}. Naturally, this supposition is dependent on the sampling rate. The higher the sampling rate, the more samples are taken of the waveform, and the better are the chances of the significant sample being between A and B.

The slowest sample rate at which this modified first-order (M.F.O.) reconstruction will work is found by the following method. The maximum slope at which the M.F.O. will work is where the two adjacent samples are both

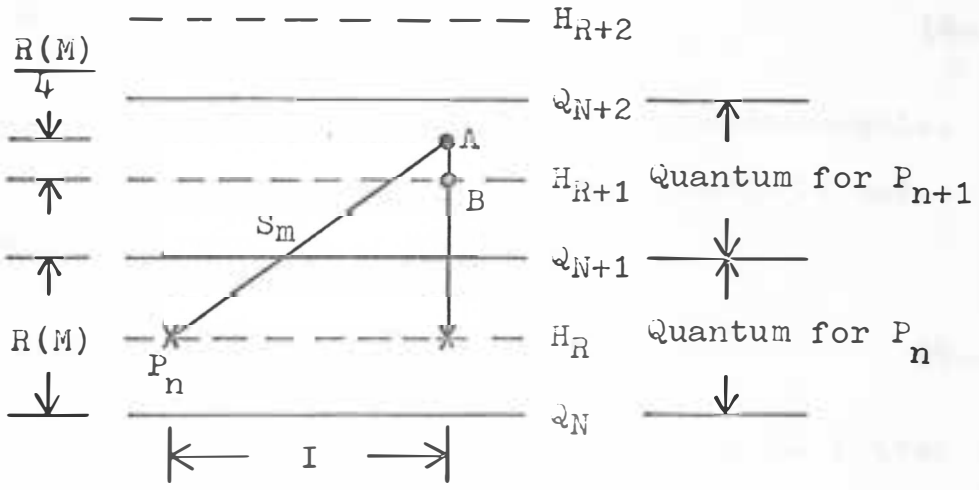

Fig. 32. Quantization levels used for the modified first-order reconstruction technique development.

significant samples. Thus the maximum slope for this condition is

$$S_m = \frac{A-H_R}{I} = \frac{(5/4)*R(M)}{I} \qquad (4-1)$$

If the slope of the input is S_i then for the M.F.O. reconstruction to be better than the basic first-order reconstruction, the condition

$$\frac{5R(M)}{4I} > S_i \qquad (4-2)$$

must be met. For the sine wave, I is in degrees/sample. Since the sampling rate, S.R., is in samples/cycle and 1 cycle = 360 degrees, then obviously

$$S.R. > \frac{1440\ S_i}{5R(M)} \qquad (4-3)$$

Thus in order for the M.F.O. reconstruction to be better than the basic first-order reconstruction at a sample point with slope S_i, the condition in Eq. (4-3) has to be met. Figure 33 shows the input and reconstructed sine wave for the Quantizer No. 2 with M.F.O. reconstruction for R(M) = 0.5 and R(M) = 0.01. A comparison of Fig. 33(A) with the basic first-order reconstruction in Fig. 31(A) shows the vast improvements made by the M.F.O. reconstruction method. Except for the peak attenuation, the "near facsimile" range for this reconstruction for Quantizer No. 2 is from R(M) = 0.05 to R(M) = 0.5. Weaknesses of

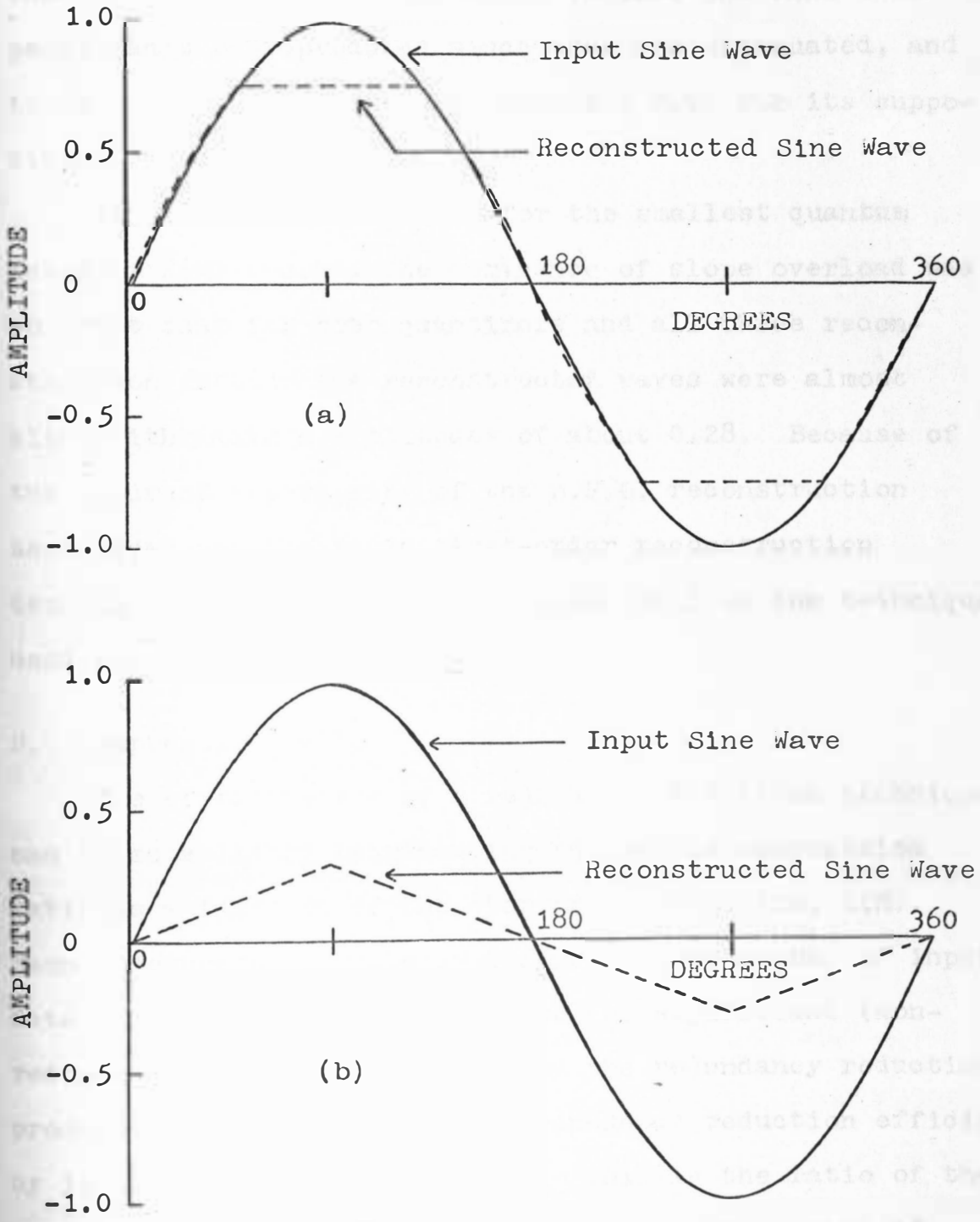

Fig. 33. Input and reconstructed sine wave for Quantizer No. 2 with modified first-order reconstruction. (a) R(M) = 0.5 (b) R(M) = 0.01.

the M.F.O. reconstruction method include the fact that peaks can't be reproduced since they are attenuated, and the method depends on a high sampling rate for its supposition to hold true.

It should be noted that for the smallest quantum level of R(M) = 0.01, the dominance of slope overload was so great that for both quantizers and all three reconstruction methods the reconstructed waves were almost alike with maximum amplitudes of about 0.28. Because of the apparent superiority of the M.F.O. reconstruction technique over the basic first-order reconstruction technique, the M.F.O. reconstruction will be the technique used for the parameter studies.

B. Compression Ratio

The effectiveness of a redundancy reduction technique can be established by measuring the sample compression ratio as a function of the step or quantum size, R(M). Sample compression ratio is defined as the number of input data samples divided by the number of significant (non-redundant) data samples output by the redundancy reduction process. A second measure of redundancy reduction efficiency is the bit compression ratio. This is the ratio of the number of bits presented at the input to the number of bits output by the redundancy reduction process. This

ratio includes all penalties for identification, timing, and sychronization. Although the bit compression ratio would be a more meaningful parameter, its value cannot be specified in general terms, since other system variables such as accuracy requirements, coding, and buffer requirements can influence this value.[15, 18] Therefore the performance criterion presented in this section is the sample compression ratio.

Figures 34 and 35 give the sample compression ratios for 120 and 60, 30 and 10 samples/cycle respectively for a sine wave input. For all four sample rates, Quantizer No. 1 has a better compression ratio as the step sizes increase. Generally, below R(M) = 0.07, the compression ratios for the two quantizers are about the same. Because of the quantizer characteristics, Quantizer No. 2 has one more quantization level between the saturation levels $\pm$1.0. Thus, since the sine wave moves between $\pm$1.0, it would be expected that Quantizer No. 1 had a better compression ratio. As the number of quantization levels increase, the fractional quotient of the numbers of quantization levels for the two quantizers becomes less and so should the difference in the compression ratios of the two quantizers. It should be noted that the general shape for all four sample rates is about the same. That is, for very small step sizes, where almost all of the input samples are significant, the

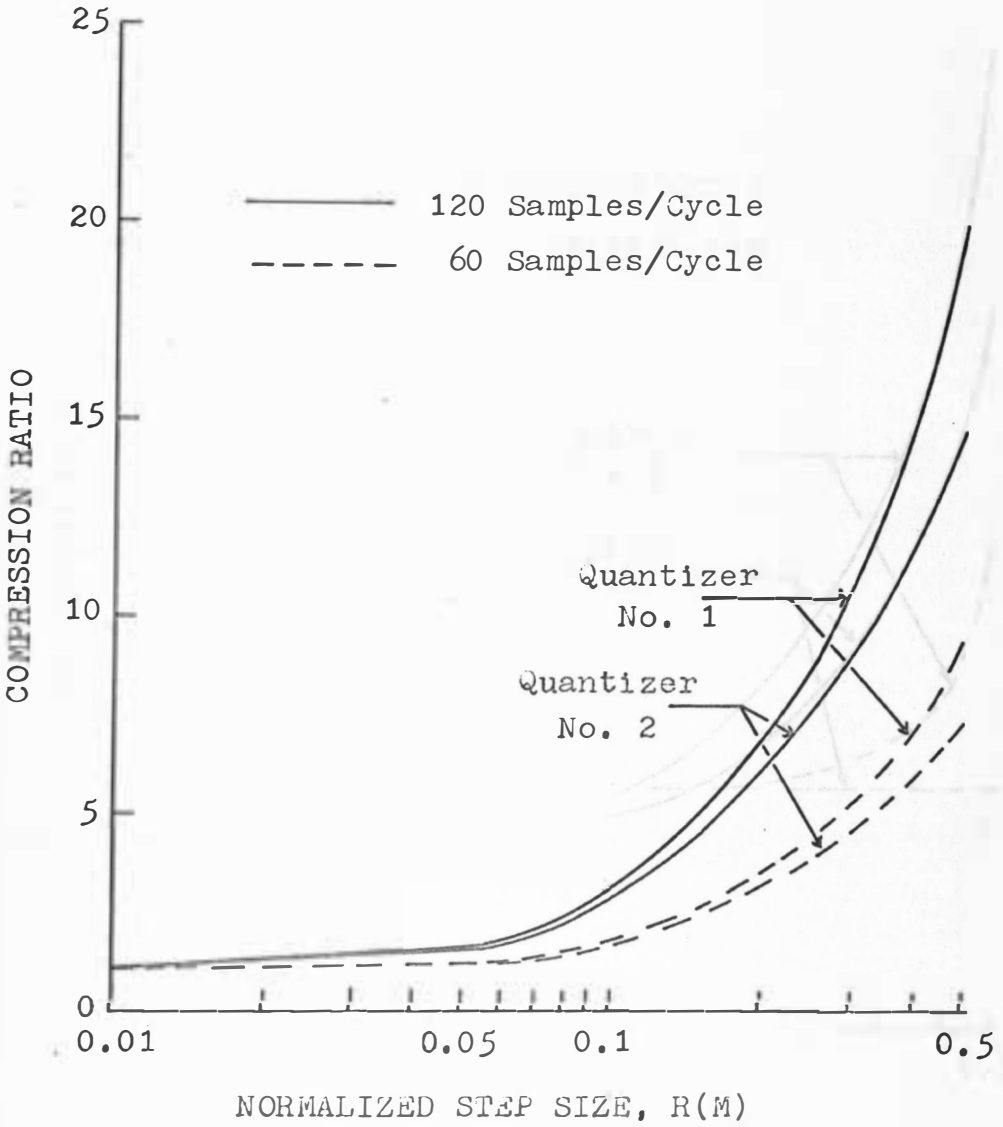

Fig. 34. Compression ratio versus normalized step size for sample rates of 120 samples/cycle and 60 samples/cycle of a sine wave input.

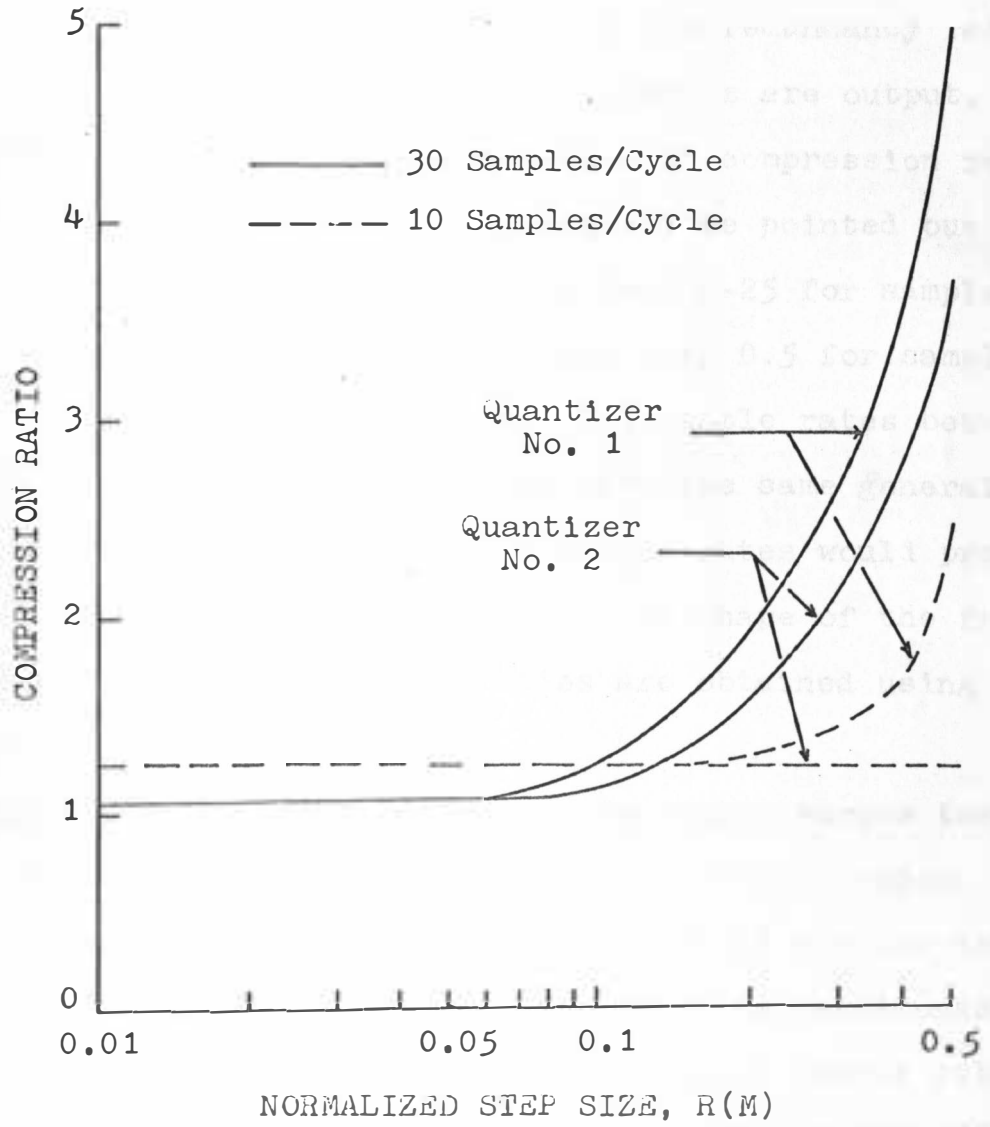

Fig. 35. Compression ratio versus normalized step size for sample rates of 30 samples/cycle and 10 samples/cycle of a sine wave input.

compression ratio is just a little greater than one. As the step size decreases, fewer and fewer input samples are significant and the compression ratio increases to the largest quantum size, R(M) = 0.5. As the sample rate decreases, fewer samples are input to the redundancy reduction process, and fewer significant samples are output. Both quantizers clearly show this reduction in compression ratio as the sample rate decreases. It should be pointed out that the compression ratio range is from 0-25 for sample rates of 120 and 60 samples/cycle and only 0.5 for sample rates of 30 and 10 samples/cycle. All sample rates between those four presented in the graphs have the same general shapes and a single plot with all sample rates would produce a smooth family of curves in the general shape of the four presented. These compression ratios are obtained using 10 cycles of a sine wave.

Figure 36 is a plot of compression ratio versus the normalized step size for a 1000 sample filtered random waveform. The general shape of the curves is similar to those for the sine wave inputs. The relative magnitudes are similar to those for the 60 samples/cycle sample rate for the sine wave input. The compression ratios for 500 samples were, on the average, within 4.1% for Quantizer No. 1 and within 5.1% for Quantizer No. 2 of those for 1000 samples, proving the convergence of the compression ratio

values to their significant values for the random input. Figure 36 differs from the sine wave input results in that Quantizer No. 2 has a better compression ratio than Quantizer No. 1. This is entirely due to the input waveform. The random waveform before filtering is uniformly distributed between 0 - 1.0. Filtering this waveform smooths the data. Thus the majority of the points are near the center of the range. Quantizer No. 2 has one more quantization level between the values 0 and 1.0, but two of these levels are the extremities of the range 0 and 1.0 where inputs of 0 to R(M)/2 are quantized to 0 and inputs of 1-R(M)/2 to 1.0 are quantized to 1.0. Thus, where the majority of input points lie, Quantizer No. 1 has one more quantization level. As the quantum size becomes larger, the fractional ratio of the number of quantization levels for the two quantizers becomes greater and the difference in compression ratios becomes more evident with the fewer quantization levels for Quantizer No. 2 giving it the greater compression ratio.

C. Average Mean-Square Error

To remove any ambiguity, the average mean-square error as used in this dissertation is found in the following manner. The absolute difference between the input signal and the reconstructed signal is found at every point

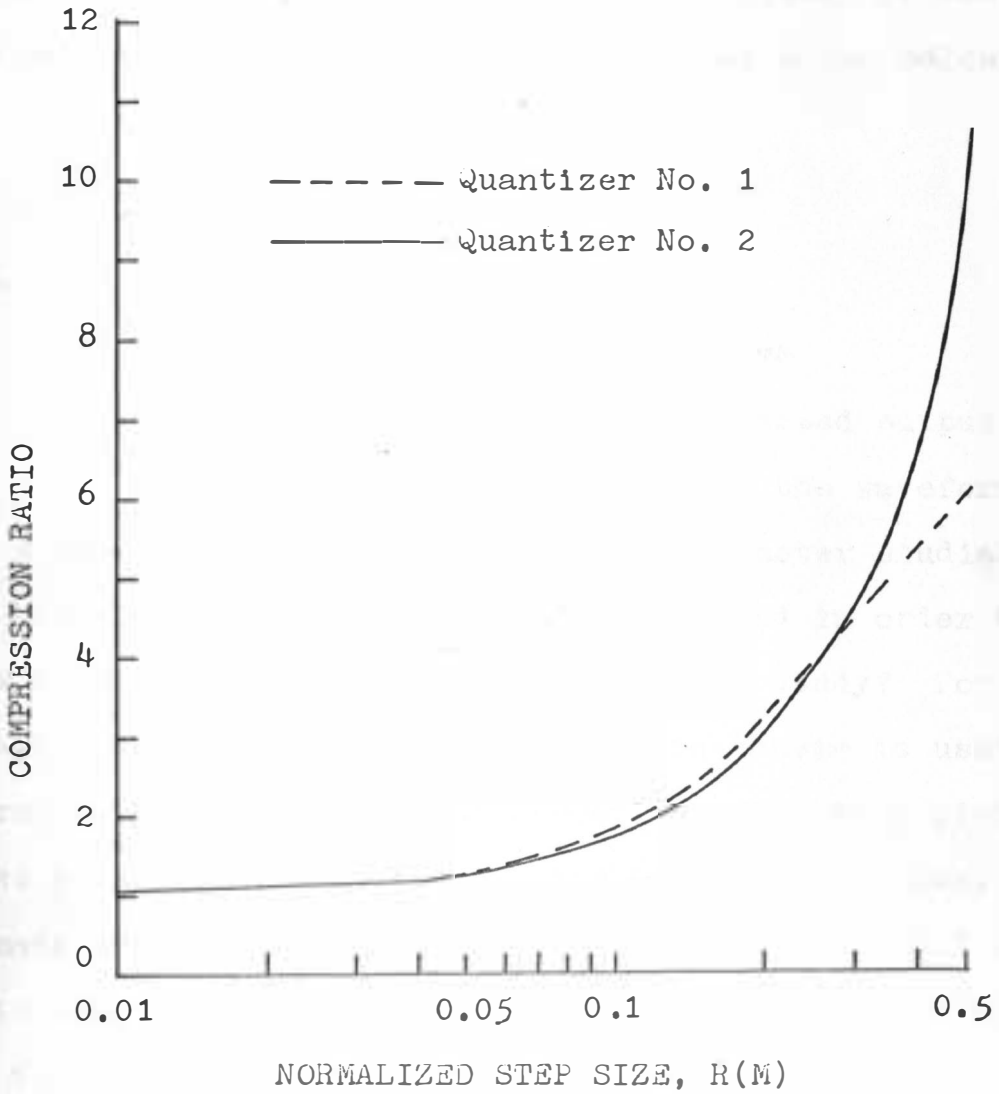

Fig. 36. Compression ratio versus normalized step size for a 1000 sample filtered random waveform.

generated by the basic sampler and these differences are squared. The squared differences are summed for the entire waveform and divided by the total number of samples to obtain the average mean-square error as shown below:

$$\overline{M.S.E.} = \frac{\sum_{i=1}^{N} (f(t)_i - F(t)_i)^2}{N} \qquad (4-4)$$

where

$f(t)_i$ = ith sample of the input wave

$F(t)_i$ = ith sample of the reconstructed output wave

N = total number of samples in the waveform.

A common question for all of the parameter studies is: how much of the input should be sampled in order to get a true picture of the parameters under study? For the average mean-square error, a convergence scheme is used to determine the length of input needed to get a true picture of the parameters. For the average mean-square error, checks are made every five cycles for R(M) = 0.01, 0.02, 0.1 and 0.5 to determine if the average mean-square error deviates from the previous multiple-of-five-cycle (5, 10, 15, ... cycles) data by not more than 0.01. All four R(M)'s must deviate less than 0.01 at the multiple-of-five cycle points in order for the computations to stop. The fewest cycles that the average mean-square error is calculated for is ten cycles. The upper bound for the cyclical checks is thirty cycles.

Figures 37 and 38 show the average mean-square error ($\overline{M.S.E.}$) versus the normalized step size for sample rates of 120, 60, 30, and 10 samples/cycle (s/c) for a sine wave input. This relationship is found for Quantizer No. 1 and No. 2 with zero-order reconstruction and for Quantizer No. 2 with the modified first-order reconstruction. The 120 s/c and 60 s/c groups which have three curves (Qnt. No. 1 - Z.O., Qnt. No. 2 - Z.O., Qnt. No. 2 - M.F.O.) are shown in Fig. 37, and the 30 s/c and 10 s/c groups with the same three curves are shown in Fig. 38. For very small step sizes the error is relatively large and due to dominant slope overload error. The curves then drop to a minimum point where both slope overload noise and granular noise are at a minimum, with the higher sample rates giving a sharper but lower drop. For example, the minimum point for Quantizer No. 1 for 120 s/c is 0.0003 while for 10 s/c it is only 0.085. The $\overline{M.S.E.}$ increases sharply again as granular noise becomes dominant after the minimum points. As the sample rate decreases, the ability of the sampler to transfer to the redundancy reduction processor accurate signal values decreases, and the $\overline{M.S.E.}$ increases. As the sample rate decreases, the point of minimum $\overline{M.S.E.}$ moves to the right or to the larger step sizes. This indicates that slope overload is dominant for larger step sizes as the sample rate decreases. It is easily justified by looking

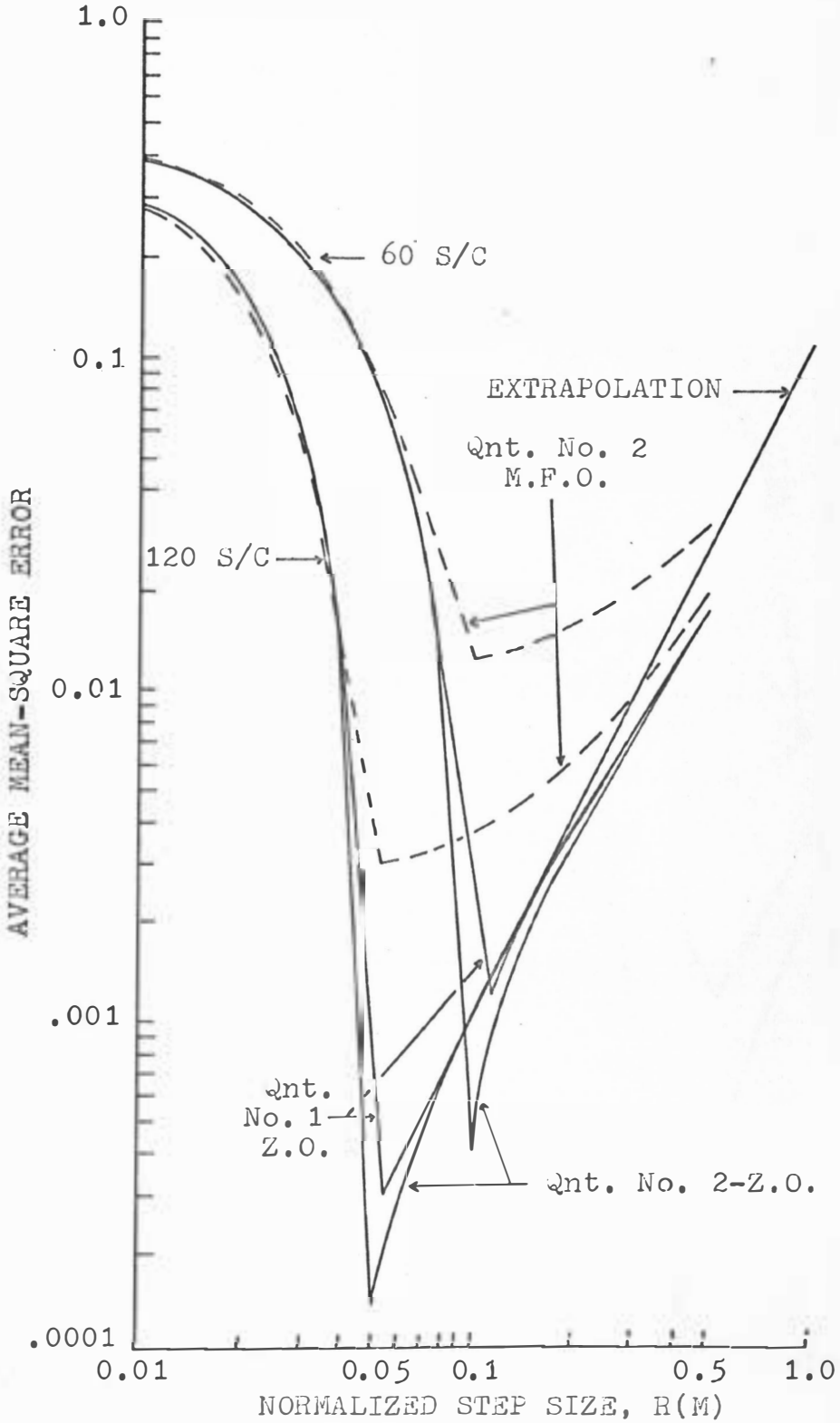

Fig. 37. $\overline{\text{M.S.E.}}$ versus normalized step size for sample rates of 120 and 60 S/C for a sine wave.

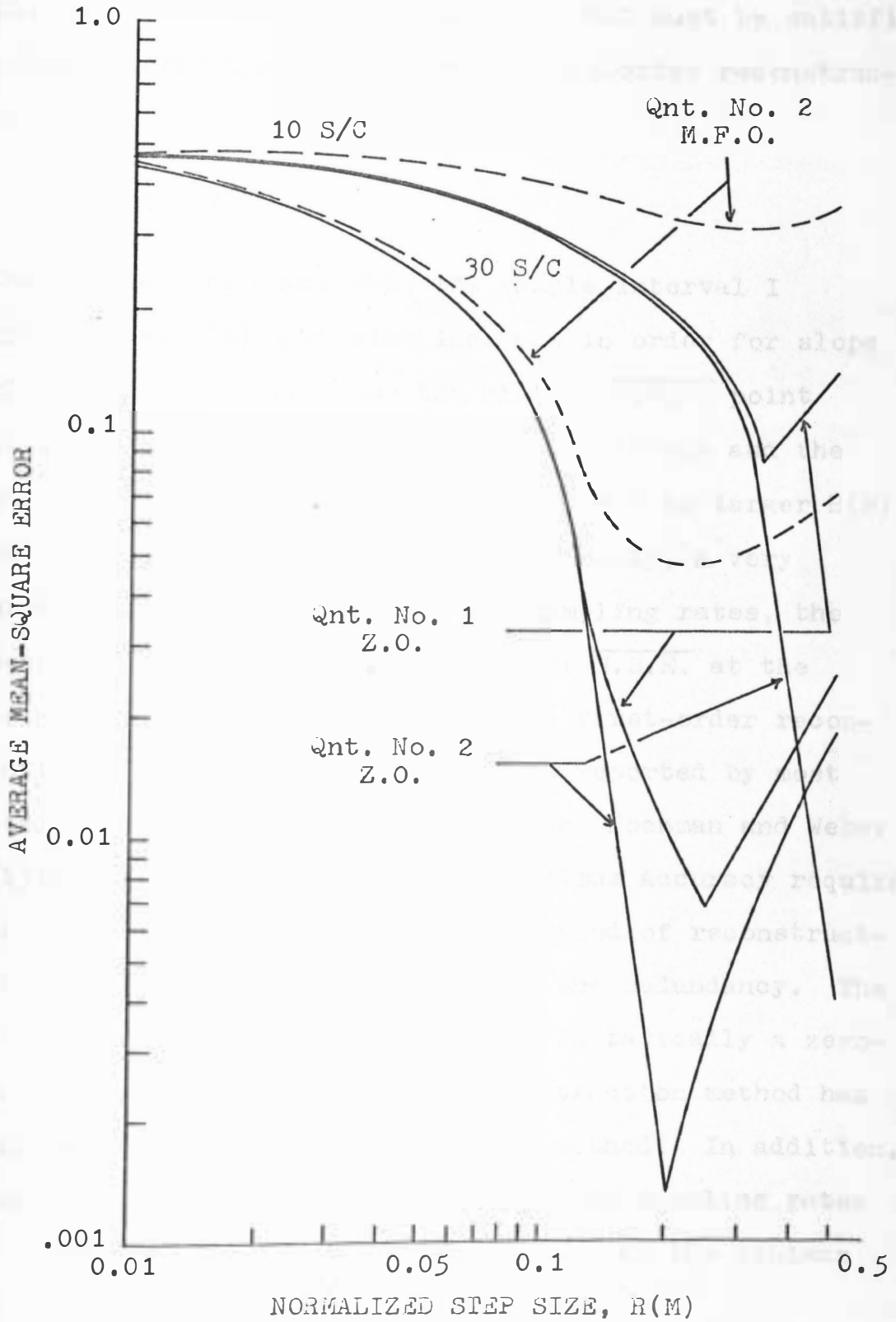

Fig. 38. $\overline{\text{M.S.E.}}$ versus normalized step size for sample rates of 10 and 30 S/C for a sine wave.

at Eq. (3-16), which is the condition that must be satisfied for slope overload not to occur for zero-order reconstruction;

$$\frac{R(M)}{I} > A\omega$$

As the sample rate decreases, the sample interval I increases, and R(M) must also increase in order for slope overload not to occur. Thus the minimum $\overline{M.S.E.}$ point which marks the end of slope overload dominance and the beginning of granular noise dominance moves to larger R(M) sizes as the sample rate decreases. Finally, a very important fact is that for all four sampling rates, the zero-order reconstruction has a smaller $\overline{M.S.E.}$ at the minimum $\overline{M.S.E.}$ point than the modified first-order reconstruction. This substantiates what is reported by most authors including Gardenhire in (12) and Hochman and Weber in (15). They report that to meet maximum accuracy requirements, one must always use the same method of reconstructing the data as was used for removing the redundancy. The method used here to remove redundancy is basically a zero-order method, so the zero-order reconstruction method has a smaller $\overline{M.S.E.}$ than the first-order method. In addition, the zero-order reconstruction for all four sampling rates with Quantizer No. 2 has a smaller $\overline{M.S.E.}$ at the minimum $\overline{M.S.E.}$ point than Quantizer No. 1.

For each sample rate, where slope overload is dominant, all three curves (Qnt. No. 1 - Z.O., Qnt. No. 2 - Z.O., and Qnt. No. 2 - M.F.O.) are close together indicating that the slope overload error dominates all three methods equally. The minimum $\overline{\text{M.S.E.}}$ point, or its general area, was used as the point of comparison because this is the region to implement the process for optimum reproduction accuracy.

The number of cycles for each sample rate family was as follows: 10 cycles for 120 samples/cycle, 15 cycles for 60 samples/cycle and 30 samples/cycle, and 20-30 cycles for 10 samples/cycle. Table I gives the $\overline{\text{M.S.E.}}$ for two sample rates for a sine wave input of both one cycle and ten cycles for Quantizer No. 1 and No. 2 with zero-order reconstruction for various quantum or step sizes. The data shows that for the short sampling epoch of one cycle, the $\overline{\text{M.S.E.}}$ has stabilized very quickly.

Figure 39 shows a family of curves for Quantizer No. 2 and zero-order reconstruction for various sample rates. The previous graphs compared quantizers and reconstruction methods for a sampling rate while this graph compares sampling rates for a quantizer and reconstruction technique. This clearly shows that the minimum $\overline{\text{M.S.E.}}$ point becomes less as the sampling rate increases, and it moves to the left as the sampling rate increases. The family of curves for Quantizer No. 1 with zero-order reconstruction and

TABLE I

SAMPLE RATE (S/C)	STEP SIZE R(M)	$\overline{\text{M.S.E.}}$ QNT. NO. 1 Z.O. 10 Cy.	$\overline{\text{M.S.E.}}$ QNT. NO. 1 Z.O. 1 Cy.	$\overline{\text{M.S.E.}}$ QNT. NO. 2 Z.O. 10 Cy.	$\overline{\text{M.S.E.}}$ QNT. NO. 2 Z.O. 1 Cy.
120	0.0100	0.2874	0.2853	0.2879	0.2858
120	0.0200	0.1390	0.1380	0.1402	0.1391
120	0.0500	0.0013	0.0013	0.0001	0.0001
120	0.0769	0.0005	0.0005	0.0004	0.0004
120	0.1000	0.0010	0.0010	0.0008	0.0008
120	0.1250	0.0015	0.0015	0.0011	0.0012
120	0.1667	0.0027	0.0027	0.0021	0.0021
120	0.2000	0.0039	0.0039	0.0031	0.0031
120	0.3333	0.0113	0.0114	0.0081	0.0082
120	0.5000	0.0264	0.0267	0.0173	0.0177
30	0.0100	0.4397	0.4270	0.4397	0.4270
30	0.0200	0.3849	0.3738	0.3848	0.3737
30	0.0500	0.2520	0.2447	0.2424	0.2354
30	0.0769	0.1548	0.1503	0.1432	0.1390
30	0.1000	0.0912	0.0887	0.0887	0.0862
30	0.1250	0.0430	0.0419	0.0391	0.0380
30	0.1667	0.0151	0.0149	0.0204	0.0198
30	0.2000	0.0261	0.0256	0.0014	0.0013
30	0.3333	0.0109	0.0110	0.0071	0.0069
30	0.5000	0.0265	0.0267	0.0185	0.0184

Comparison of 1 cycle and 10 cycle average mean-square error data of a sine wave using sample rates of 120 and 30 S/C, Quantizer No. 1 and No. 2, and zero-order reconstruction for various step sizes, R(M).

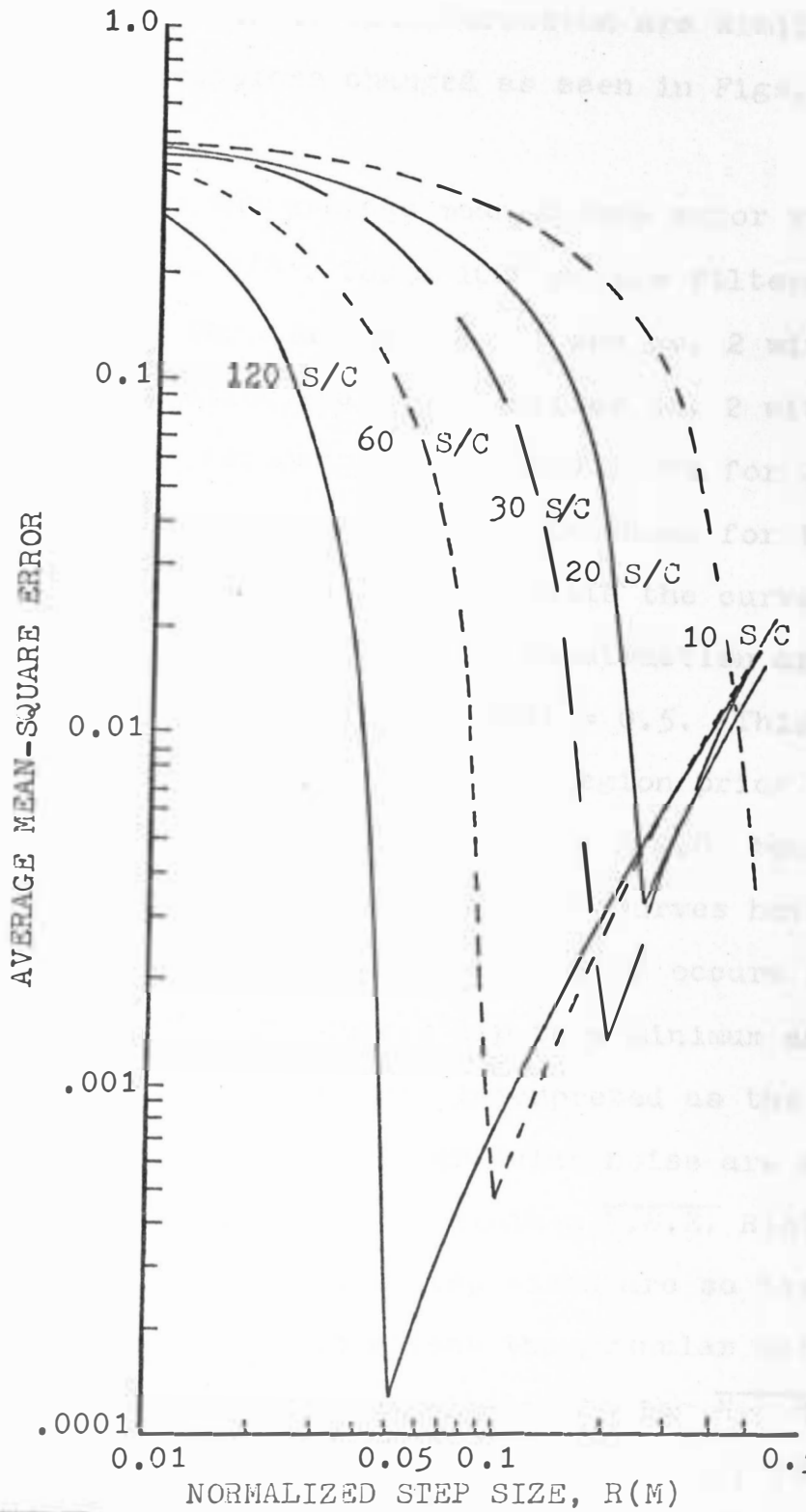

Fig. 39. $\overline{\text{M.S.E.}}$ versus R(M) for various sample rates for Qnt. No. 2 with Z.O. reconstruction for a sine wave.

Quantizer No. 2 with M.F.O. reconstruction are similar with the relative positions changed as seen in Figs. 37 and 38.

Figure 40 shows the average mean-square error versus normalized step size, R(M), for a 1000 sample filtered random input signal for Quantizer No. 1 and No. 2 with zero-order reconstruction and for Quantizer No. 2 with modified first-order reconstruction. The curve for Quantizer No. 2 with M.F.O. reconstruction is shown for the entire range of R(M) from 0.01 to 0.5 while the curves for Quantizer No. 1 and No. 2 with a Z.O. construction are shown only from their last peaks to R(M) = 0.5. This is because these curves are similar in the region prior to the last peaks to the Quantizer No. 2 with M.F.O. reconstruction, that is, random. But all three curves have the same characteristic from the last peak, which occurs for R(M) greater than 0.1. The curves dip to a minimum and then rise again. The minimums are interpreted as the step size where the slope overload and granular noise are at a minimum. For R(M) larger than the minimum $\overline{\text{M.S.E.}}$ R(M) size, granular noise is dominant. The step sizes are so large that the random input does not affect the granular noise characteristic and the curves are similar to the $\overline{\text{M.S.E.}}$ curves for a sine wave input. As explained in Part (B), Quantizer No. 1 has one more quantization level in the

range where most of the random values fall, and the $\overline{M.S.E.}$ for Quantizer No. 1 with zero-order reconstruction is the least at the minimum $\overline{M.S.E.}$ points, as shown in Fig. 40. Slope overload noise dominates the signal for the smaller step sizes. But, since the signal is random, the slope overload is also random in nature because the amount of slope overload or the absence of it will not depend on the input signal and the R(M) size as for the sine wave, but will be random. That is, a large amount of slope overload at one sample may be eliminated at the next sample if the random signal changes rapidly. Thus the amount of slope overload is not dependent on the size of R(M), but rather the random input signal.

D. Mathematical Analysis of Mean-Square Error

Verification of Computer Results for Quantizer No. 1, Zero-Order Reconstruction, 120 Samples/Cycle

This particular analysis determines mathematically the mean-square error for Quantizer No. 1 with one quantization interval in the upper and lower half planes. Figure 41 shows the input and the output of Quantizer No. 1 for this case. Because of the sine wave symmetry with the origin, the mean-square error for the half cycle from 0 to π is the same as that for the whole cycle and for

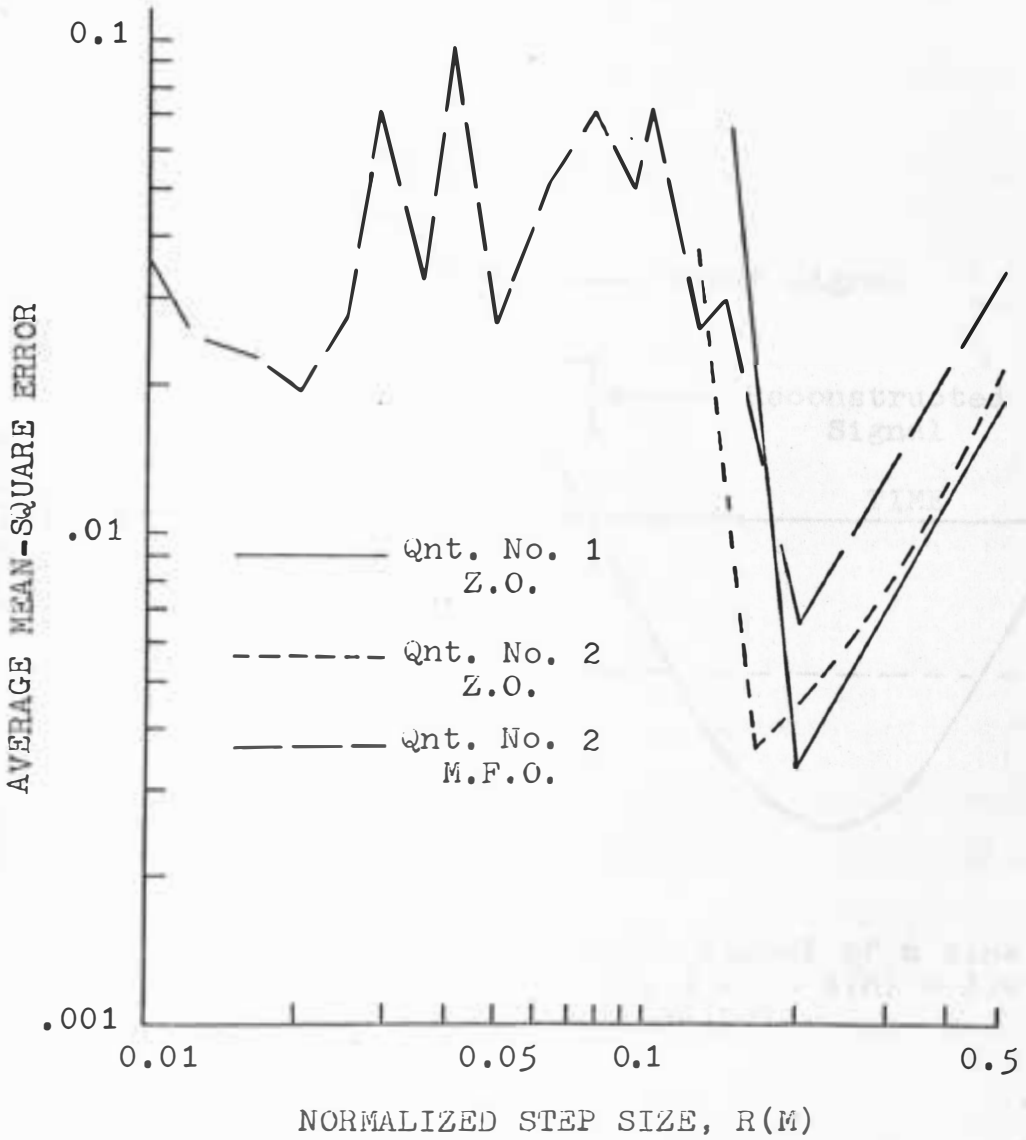

Fig. 40. Average mean-square error versus normalized step size for a 1000 sample filtered random waveform.

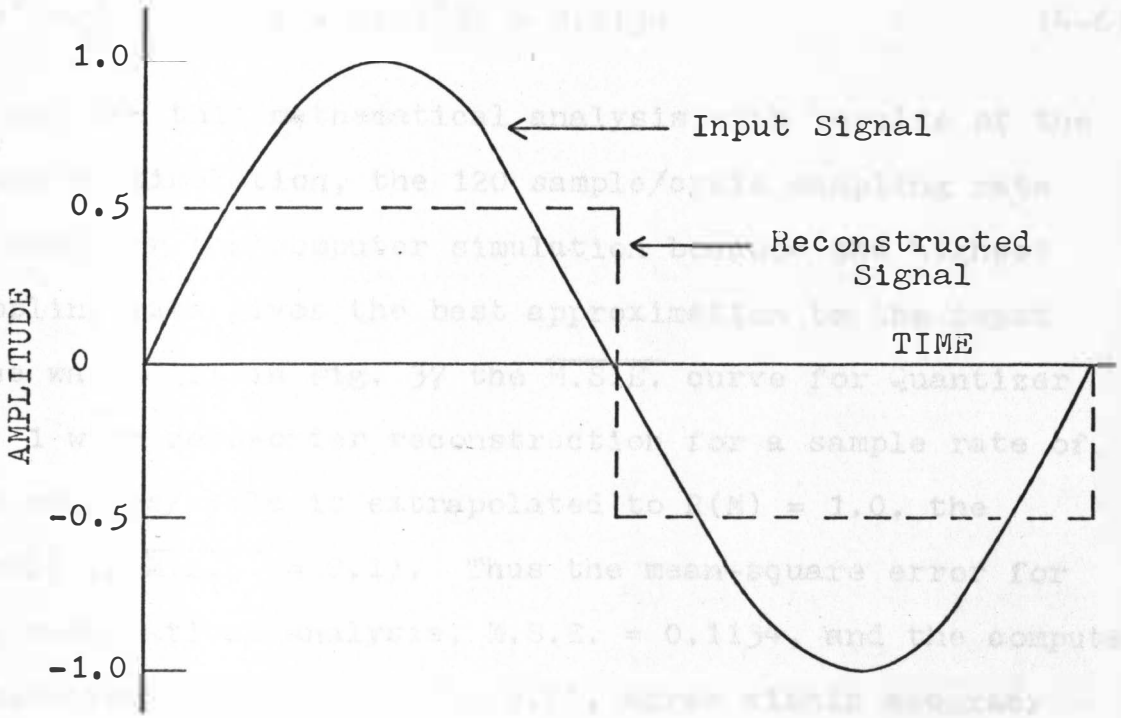

Fig. 41. Input and reconstructed signal of a sine wave for Quantizer No. 1 with R(M) = 1.0 for the mathematical analysis.

any number of cycles desired. The mean-square error, $\overline{e^2}$, is defined as:

$$\overline{e^2} = \frac{1}{T} \int_0^T (\text{input signal} - \text{reconstructed signal})^2 dx \qquad (4\text{-}5)$$

where T is the interval for which $\overline{e^2}$ is taken. Therefore,

$$\overline{e^2} = \frac{1}{\pi} \int_0^{\pi} (\sin x - 0.5)^2 dx = 0.1134 \qquad (4\text{-}6)$$

To compare this mathematical analysis with results of the computer simulation, the 120 sample/cycle sampling rate is used for the computer simulation because the highest sampling rate gives the best approximation to the input sine wave. If in Fig. 37 the $\overline{M.S.E.}$ curve for Quantizer No. 1 with zero-order reconstruction for a sample rate of 120 samples/cycle is extrapolated to R(M) = 1.0, the result is $\overline{M.S.E.}$ = 0.11. Thus the mean-square error for the mathematical analysis, M.S.E. = 0.1134, and the computer simulation result, $\overline{M.S.E.}$ = 0.11, agree within accuracy limits of the calculations.

Analysis of Mean-Square Error Where Slope-Overload Occurs

A mathematical analysis of mean-square error is possible for two cases of slope overload. The first case is when slope overload occurs for the entire input waveform and the other is when slope overload occurs for only a portion of a period of the input waveform. An assumption which is applicable to both cases is shown in Fig. 43.

That is, the zero-order reconstruction produces a staircase waveform that is approximated by a straight line of slope K. For $t_1 \leq t \leq t_2$, the staircase contributes an error more positive than the straight line. For $t_2 \leq t \leq t_3$, the staircase contributes an error more negative than the straight line. If the straight line is symmetric about the staircase, the errors should average, making this a fairly accurate approximation.

CASE I

For Case I, slope overload occurs for nearly the entire input waveform, f(t). In Fig. 42, this is equivalent to;

$$\frac{df(t)}{dt} > K, \text{ for } 0 \leq t \leq \frac{\pi}{2}, \tag{4-7}$$

and $\Theta = \pi/2$ where K = maximum slope of the reconstructed output wave. In this case the output is a series of line segments of slope $\pm K$ for the entire waveform, so for a sine wave input,

$$\begin{aligned} f(t) &= \sin \omega t \\ F(t) &= Kt \\ e(t) &\cong \sin \omega t - Kt \end{aligned} \tag{4-8}$$

where, e(t) is the approximate error between the input and output waveforms.

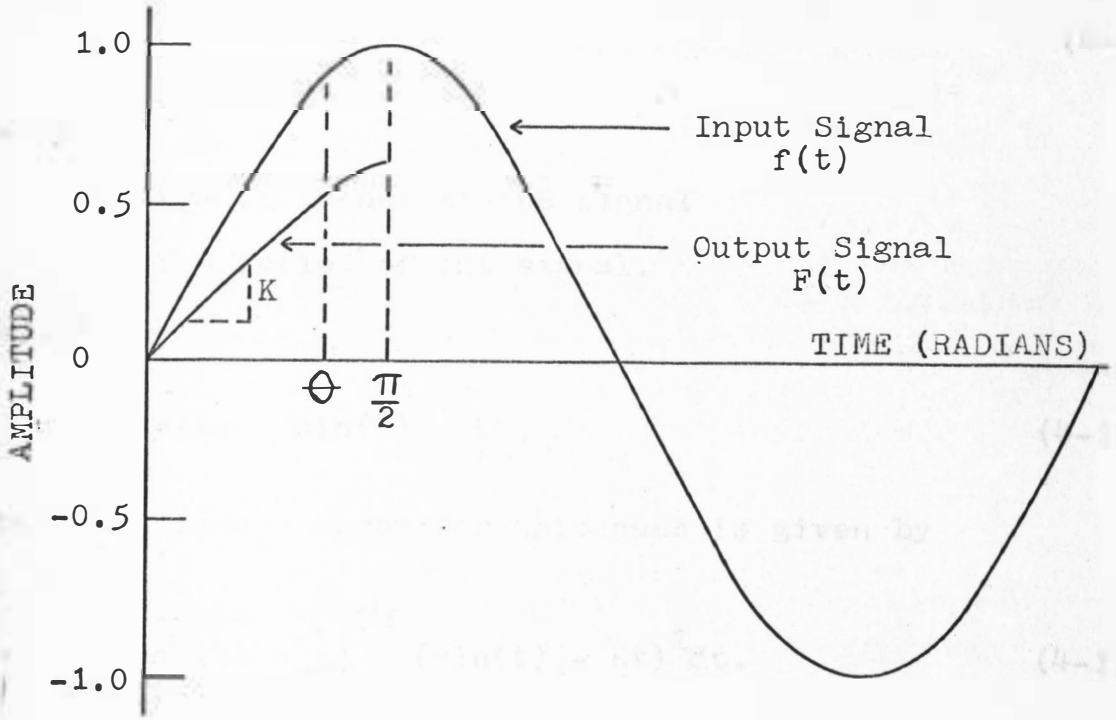

Fig. 42. Mathematical analysis of M.S.E. for $0 \leq t \leq \theta$, slope overload causes output to be attenuated. For $\theta \leq t \leq \pi/2$ there is no slope overload since $df(t)/dt \leq K$, but output is the input minus a bias error.

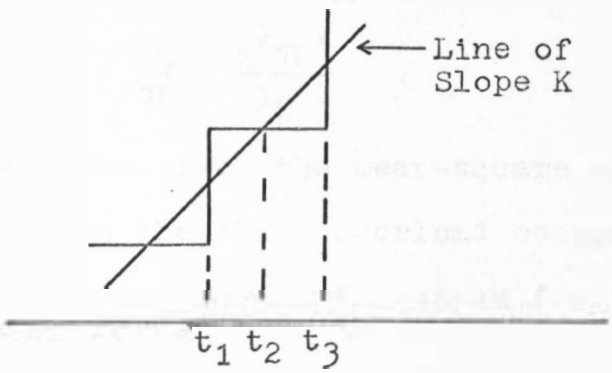

Fig. 43. Straight-line approximation of the zero-order reconstructed signal for the mathematical analysis of M.S.E.

Since $\omega = 2\pi f$ and $T = 1/f$, and assuming $\omega = 1$, then

$$T = 2\pi \tag{4-9}$$

Where

f = frequency of the signal

T = period of the signal.

So, if

$$e(t) = \sin(t) - Kt, \tag{4-10}$$

the mean-square error for this case is given by

$$\overline{e^2(t)} = \frac{1}{\pi}\int_{-\pi/2}^{\pi/2} (\sin(t) - Kt)^2 dt, \tag{4-11}$$

but, since the integrand is symmetric with the origin,

$$\overline{e^2(t)} = \frac{2}{\pi}\int_{0}^{\pi/2} (\sin(t) - Kt)^2 dt \tag{4-12}$$

and integrating and evaluating,

$$\overline{e^2(t)} = \frac{1}{2} - \frac{4K}{\pi} + \frac{K^2\pi^2}{12} \tag{4-13}$$

Equation (4-13) thus gives the mean-square error due to slope overload when the slope overload occurs for nearly the entire sine wave input of frequency $f = 1/2\pi$.

CASE II

This case concerns slope overload occuring for only part of the input signal after which the reconstruction process can follow the input. In Fig. 42 this may be interpreted as:

$$\text{if, } 0 \leq t \leq \theta, \text{ then } \frac{df(t)}{dt} > K \text{ and slope overload occurs}$$
$$\text{if, } \theta \leq t \leq \pi/2, \text{ then } \frac{df(t)}{dt} \leq K \text{ and no slope overload occurs.} \quad (4\text{-}14)$$

If the input is a unit amplitude sine wave,

$$f(t) = \sin(t) \quad (4\text{-}15)$$

Then differentiating Eq. (4-15) gives the slope of the input

$$\frac{df(t)}{dt} = \cos(t) \quad (4\text{-}16)$$

At the point $t = \theta$, the slope overload is at its transition point or

$$\frac{df(t)}{dt} = K = \cos t \quad (4\text{-}17)$$

Therefore, the point θ, which is the slope overload transition point, is

$$\theta = \cos^{-1}(K) \quad (4\text{-}18)$$

For $\theta \leq t \leq \pi/2$, the input curve can be followed by

the redundancy reduction process and no slope overload occurs. At $t = \theta$,

$$f(\theta) = \sin(\cos^{-1}K) \tag{4-19}$$

and

$$F(\theta) = K\theta = K*(\cos^{-1}K) \tag{4-20}$$

Thus the bias error, A, at the point $t = \theta$, is

$$A = f(\theta) - F(\theta) = \sin(\cos^{-1}K) - K*(\cos^{-1}K) \tag{4-21}$$

so

$$A = \sin\theta - K*\theta \tag{4-22}$$

Here the $\overline{e^2(t)}$ is divided into two parts, one where slope overload occurs and the other where it doesn't. In general,

$$\overline{e^2(t)} = \frac{2}{\pi}\left[\int_0^{\theta}(f(t)-F(t))^2dt + \int_{\theta}^{\pi/2}(f(t)-F(t))^2dt\right] \tag{4-23}$$

or for the specified input,

$$\overline{e^2(t)} = \frac{2}{\pi}\left[\int_0^{\theta}(\sin(t)-Kt)^2dt + \int_{\theta}^{\pi/2}[\sin(t)-(\sin(t)-A)]^2dt\right] \tag{4-24}$$

Integrating, substituting in the limits, and remembering that $\cos(\cos^{-1}K) = K$, we obtain

$$\overline{e^2(t)} = \frac{4\theta K^2}{\pi} + \frac{2K^2\theta^3}{3\pi} - \frac{5K\sin\theta}{\pi} + \frac{\theta}{\pi} + A^2 - \frac{2A^2\theta}{\pi} \tag{4-25}$$

where

$$\theta = \cos^{-1} K$$

$$A = \sin(\cos^{-1} K) - K \cos^{-1} K.$$

This gives the mean-square error for the case where slope overload occurs for only a part of a cycle of the input.

For both Case I and Case II, the $\overline{e^2(t)}$ contains terms involving K, which is the maximum slope that the quantizing process can follow as discussed in Chapter III. Thus, according to Eq. (3-16),

$$K = \frac{R(M)}{I} \tag{4-26}$$

where

R(M) = step size in units of amplitude

I = basic sampling interval time in seconds.

Since $T = 2\pi$ and if there are S samples/cycle, then

$$I = \frac{2\pi}{S} \tag{4-27}$$

so

$$K = \frac{S*R(M)}{2\pi} \tag{4-28}$$

In Eq. (3-24) the maximum slope of the sine wave was given as $A\omega$. Since in the case discussed here, A = 1, and $\omega = 1$, then the maximum slope of the sine wave input is one. If the maximum slope the reconstructor can follow is

greater than the slope of the input wave, no slope overload occurs. For the unit amplitude sine wave, if $K < 1$ slope overload will occur.

The mathematical analysis of mean-square error due to slope overload versus normalized step size of a sine wave input for sample rates of 120, 60, 30, and 10 samples/cycle is shown in Fig. 44. The curves are shown only where slope overload errors occur since the approximation holds only for that portion of the curve. Since the slope overload analysis curves begin at the origin, the results of Quantizer No. 2 should be closer to the mathematical analysis since Quantizer No. 2 has its output for the sine wave start at the origin as opposed to Quantizer No. 1 which starts at the half interval. Comparison of Fig. 44 with the family of curves for Quantizer No. 2 in Fig. 39 shows that the mathematical results correspond very closely to the computer simulation results. For the very small step sizes where the error is almost exclusively due to slope overload, Case I is naturally the best. While for the lower portions of the M.S.E. curves, Case II is better because slope overload does not affect the entire waveform. For the entire range of M.S.E. versus step size where slope overload occurs, the Case II for partial slope overload (PSOA) is the better of the two approximations. In Fig. 44, at $R(M) = 0.01$, the greatest difference between the computer

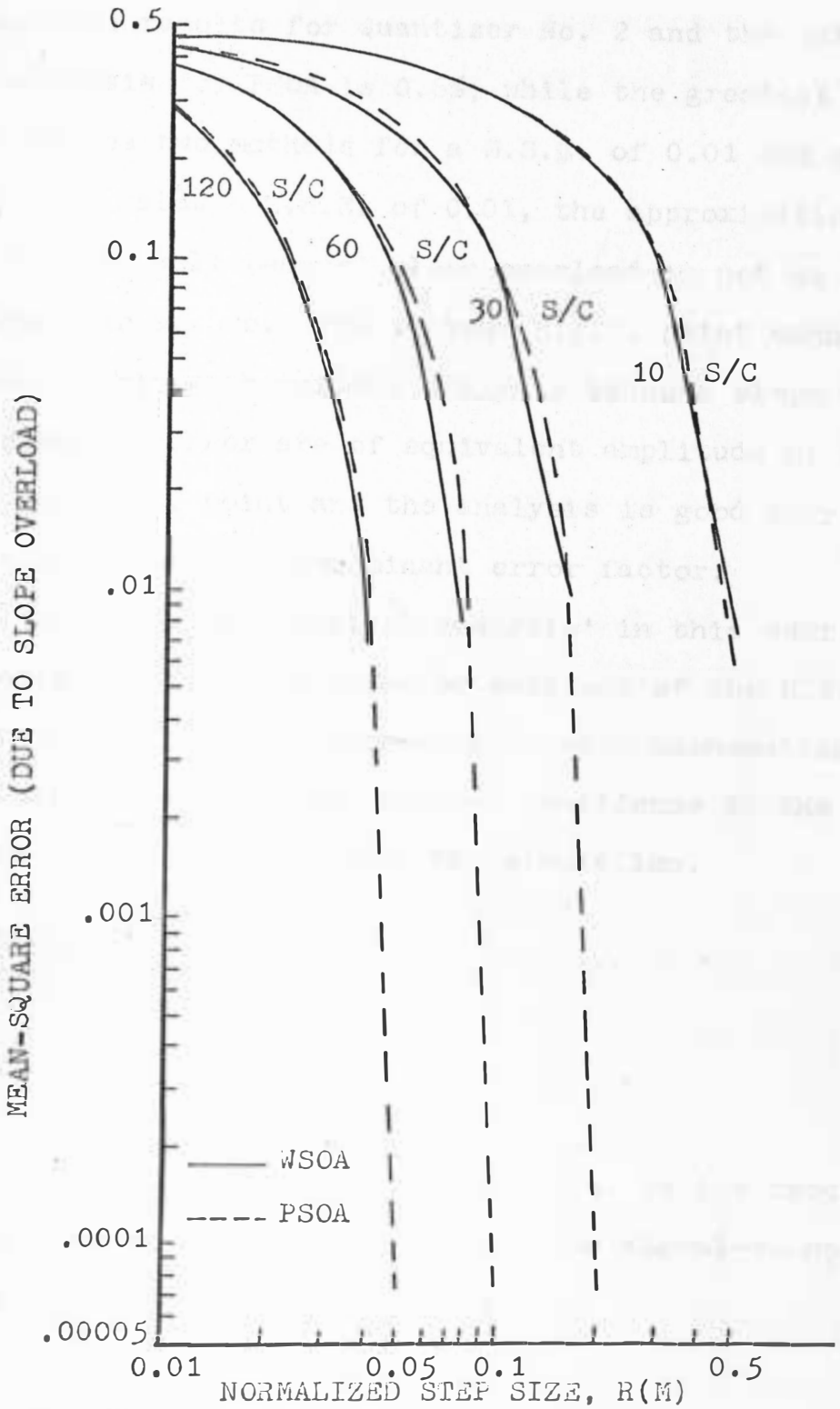

Fig. 44. Mathematical analysis of M.S.E. versus normalized step size of a sine wave for various sample rates. The whole slope overload approximation is WSOA and the partial slope overload approximation is PSOA.

simulation results for Quantizer No. 2 and the mathematical analysis for PSOA is 0.6%, while the greatest difference in the two methods for a M.S.E. of 0.01 and greater is 3.7%. Below a M.S.E. of 0.01, the approximations do not hold as well because slope overload is not as dominant as granular errors. The minimum M.S.E. point cannot be found by this mathematical analysis because slope overload and granular error are of equivalent amplitude at the minimum M.S.E. point and the analysis is good only where slope overload is the dominant error factor.

While the mathematical analysis' in this section are only for specific cases or portions of the M.S.E. versus step size curves, the agreement between mathematical and simulation results gives further confidence in the $\overline{\text{M.S.E.}}$ versus step size curves for the simulation.

E. Signal-to-Noise Ratio

Noise can be defined as

$$n(t) = f(t) - F(t) \tag{4-29}$$

where f(t) is the input signal and F(t) is the reconstructed output signal. Generally the signal-to-noise ratio (S/N) is defined as

$$\frac{S}{N} = 10 \log_{10}\left[\frac{F(t)^2}{n(t)^2}\right] \tag{4-30}$$

where S/N is in db. Because the inputs used in the research are sampled, a slightly different S/N ratio must be used. In our case,

$$\frac{S}{N} = 10 \log_{10}\left[\frac{\sum_{i=1}^{N} (F(t)_i)^2}{N} \Big/ \frac{\sum_{i=1}^{N} (n(t)_i)^2}{N} \right] \quad (4\text{-}31)$$

shere S/N in db is an average S/N ratio. That is, the summation of all the sampled-squared outputs are divided by N, the total number of samples taken. The same is done for the sampled-squared noise which is then divided into the output term, and the $\log_{10}$ is taken and multiplied by 10 to obtain the average S/N ratio ($\overline{S/N}$). The $\overline{S/N}$ is the average S/N for each sampled point of the input signal. Figures 45 and 46 show $\overline{S/N}$ in db versus normalized step size for sample rates of 120, 60, 30, and 10 samples/cycle of the input sine wave. The plots show two general asymptotes. Step sizes smaller than the maximum $\overline{S/N}$ step size have dominant slope overload noise. At the maximum $\overline{S/N}$, slope overload and granular noise are at a minimum. For step sizes larger than the maximum $\overline{S/N}$ step size, granular noise is dominant. The maximum $\overline{S/N}$ ratios occur for the highest sample rate of 120 samples/cycle and the maximum $\overline{S/N}$ decreases as the sample rate decreases. The maximum $\overline{S/N}$ shifts to larger step sizes as the sampling rate decreases and the zero-order reconstruction produces

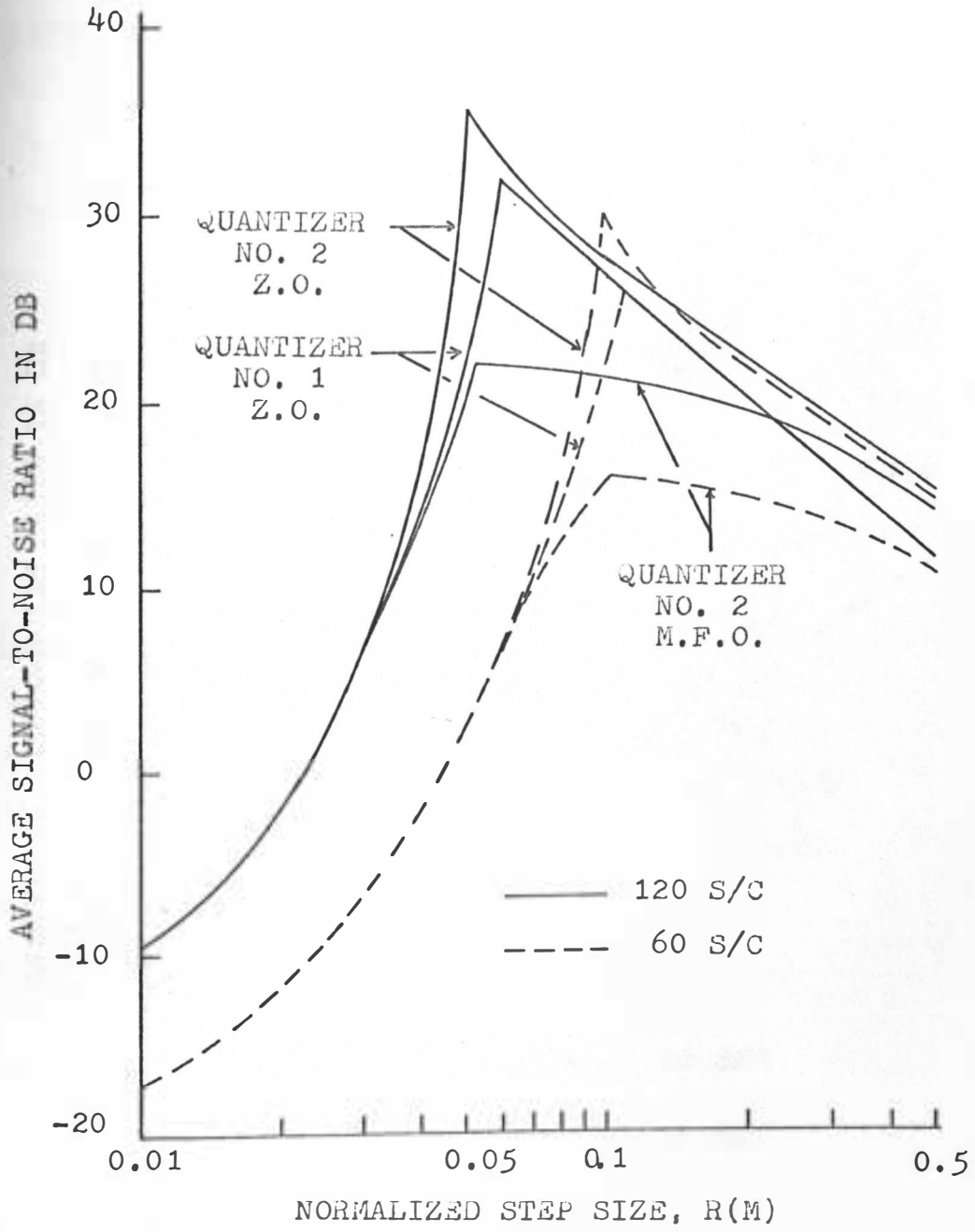

Fig. 45. Average signal-to-noise ratio in db versus normalized step size for a sine wave with sample rates of 120 and 60 S/C.

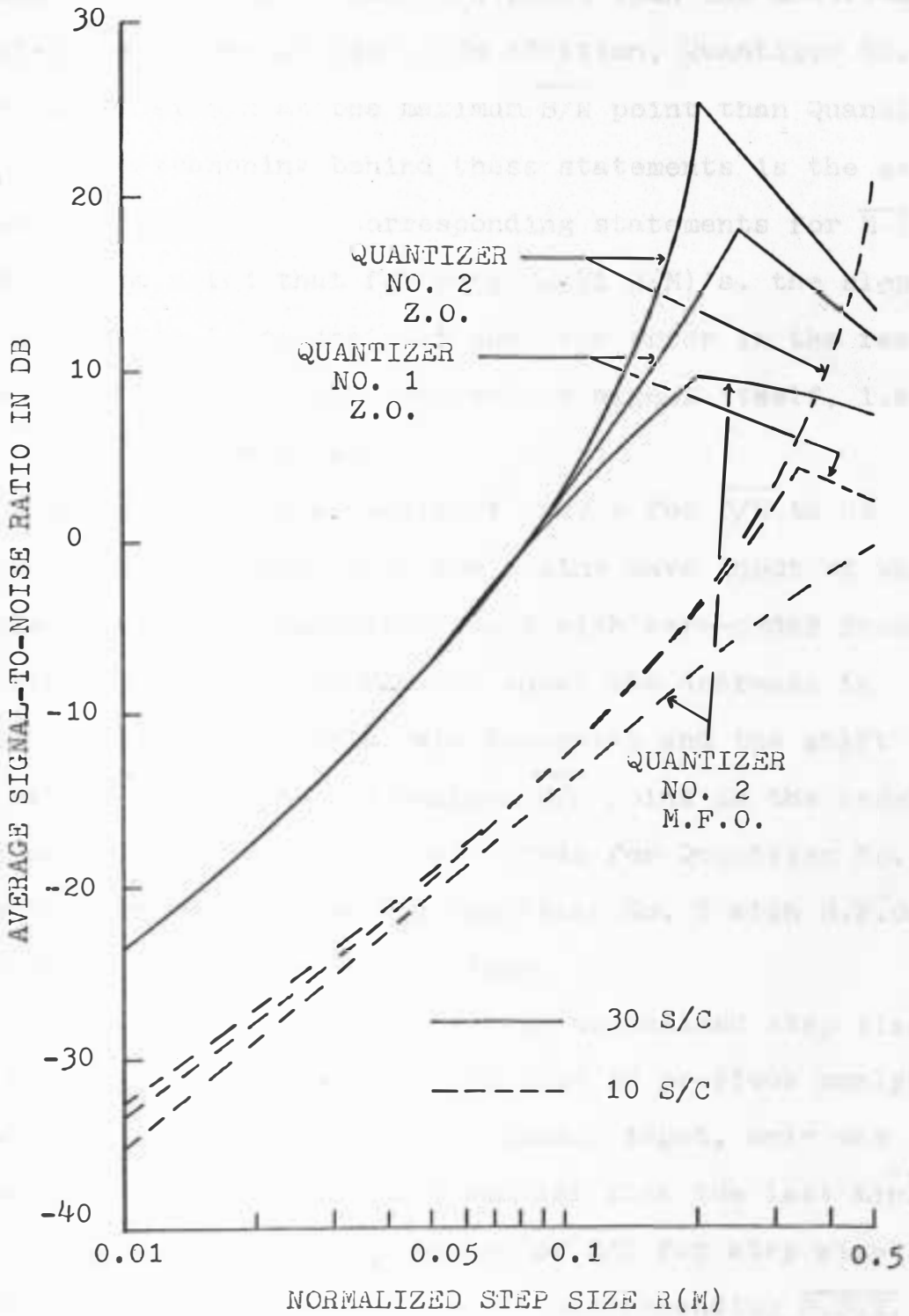

Fig. 46. Average signal-to-noise ratio in db versus normalized step size for a sine wave with sample rates of 30 and 10 S/C.

a higher $\overline{S/N}$ at the maximum $\overline{S/N}$ point than the modified first-order reconstruction. In addition, Quantizer No. 2 gives a higher $\overline{S/N}$ at the maximum $\overline{S/N}$ point than Quantizer No. 1. The reasoning behind these statements is the same as those given for the corresponding statements for $\overline{M.S.E.}$ It should be noted that for very small R(M)'s, the slope overload noise is so dominant that the error in the reconstruction is greater than the output signal itself, i.e., the $\overline{S/N}$ is less than zero.

Figure 47 shows a family of curves for $\overline{S/N}$ in db versus normalized step size for a sine wave input of various sample rates using Quantizer No. 2 with zero-order reconstruction. This figure clearly shows the decrease in maximum $\overline{S/N}$ as the sample rate decreases and the shift to larger step sizes for the maximum $\overline{S/N}$ point as the sample rate decreases. The family of curves for Quantizer No. 1 with Z.O. reconstruction and Quantizer No. 2 with M.F.O. reconstruction are similar in form.

Figure 48 shows the $\overline{S/N}$ versus normalized step size for the filtered random waveform used in previous analysis. As with the $\overline{M.S.E.}$ plot for the random input, only one curve is shown for step sizes smaller than the last minimum $\overline{S/N}$ because of the randomness of $\overline{S/N}$ for step sizes smaller than that point. Like the corresponding $\overline{M.S.E.}$ plot, Quantizer No. 1 with Z.O. reconstruction is better than the M.F.O. reconstruction at the maximum $\overline{S/N}$ point.

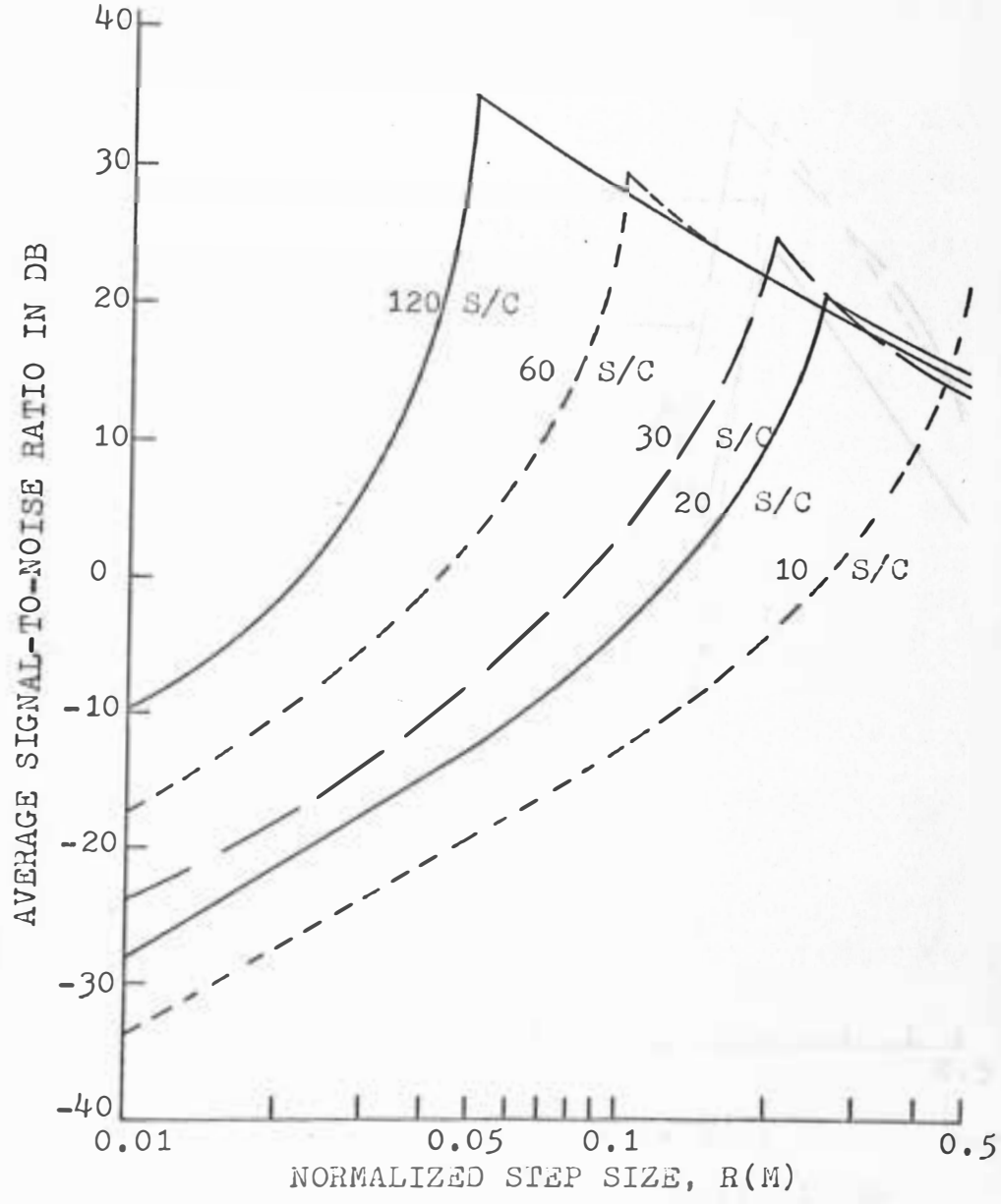

Fig. 47. Average signal-to-noise ratio in db versus normalized step size for a sine wave with sample rates of 120, 60, 30, 20, and 10 S/C using Quantizer No. 2 with zero-order reconstruction.

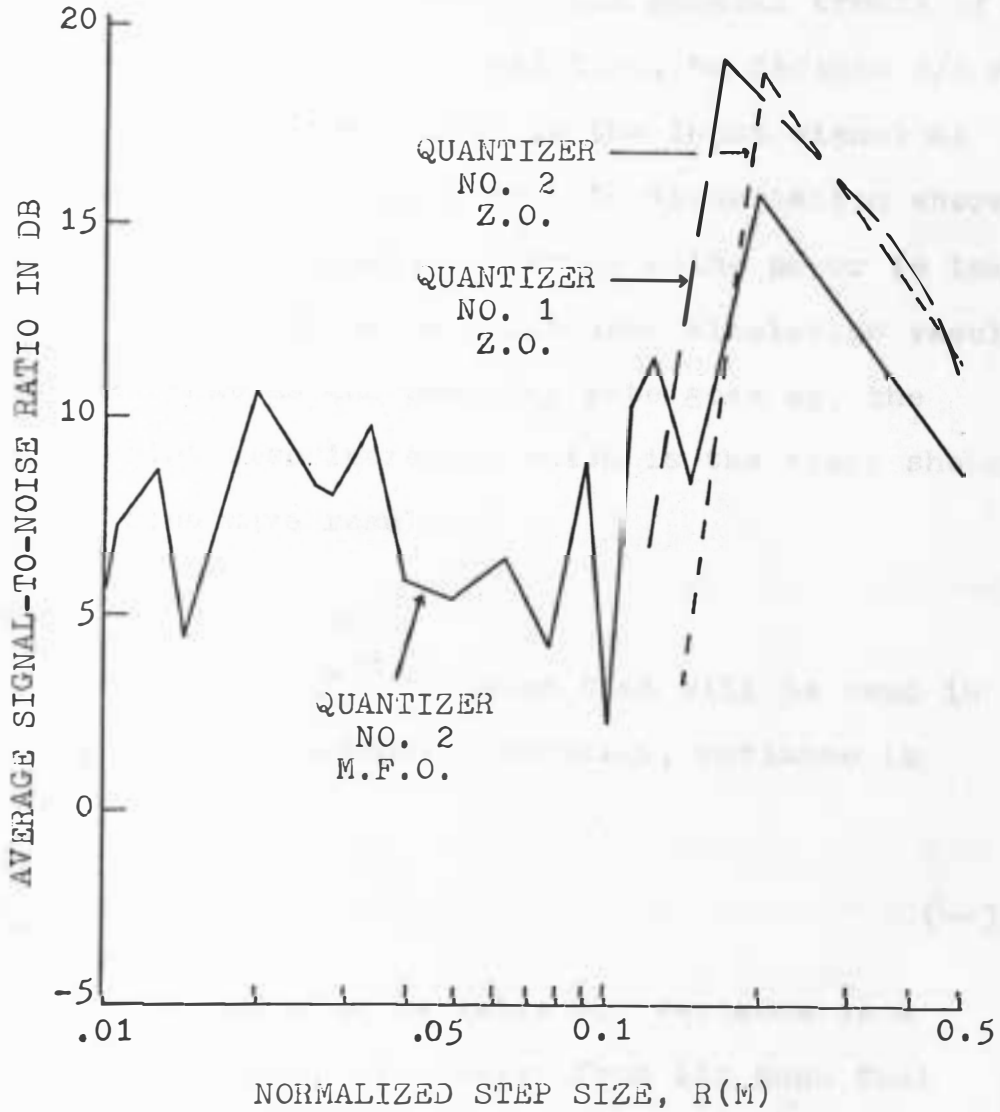

Fig. 48. Average signal-to-noise ratio in db versus normalized step size for a filtered random waveform of 1000 samples.

Comparing the general shapes of the random signal $\overline{S/N}$ curves where granular noise is dominant with those given by O'Neal in (23) show the asymptotes and general trends of the curves to be the same. In addition, he defines S/N as $10 \log_{10}(f(t)^2/n(t)^2)$ where f(t) is the input signal as opposed to the definition used in this dissertation where the ratio of average signal to average noise power is taken. Both the theoretical curves and computer simulation results of O'Neal show that as the sampling rate goes up, the maximum S/N point also increases which is the trend shown in the input sine wave results.

F. Variance of the Error

The main measure of dispersion that will be used in this dissertation is variance. Normally, variance is defined as

$$\sigma_x^2 = \overline{(x-\bar{x})^2} \qquad (4\text{-}32)$$

where $\bar{x}$ = average value of variable x. Variance is a measure of the deviation of a value from its mean that augments the large deviations and diminishes the small ones by the squaring process. In the above cases, the variance of the error is the important parameter of dispersion, where the error is defined as

$$e(t) = f(t) - F(t) \qquad (4\text{-}33)$$

where

$e(t)$ = error at time t

$f(t)$ = input signal at t

$F(t)$ = output signal at t.

Thus the variance of the error is

$$\sigma^2 = \frac{\sum_{i=1}^{N} (e_i - \bar{e})^2}{N} \qquad (4\text{-}34)$$

where

e_i = error for the ith sample

$\bar{e}$ = average error for N samples

N = total number of samples.

Figures 49 and 50 show the variance of the error versus normalized step size for a sine wave input with sampling rates of 120, 60, 30, and 10 samples/cycle. The curves are very similar to those seen in Figs. 37 and 38 for $\overline{M.S.E.}$ In the slope overload region, as R(M) increases, the variance of the error decreases until a minimum variance point is reached. For R(M)'s larger than this point, granular noise dominates and the variance increases. General trends are similar to those for $\overline{M.S.E.}$ That is, the minimum variance values decrease as the sampling rate increase and the minimum variance point moves to smaller R(M)'s as the sampling rate increases. Quantizer No. 2 has the lower variance of the error values at the minimum variance point.

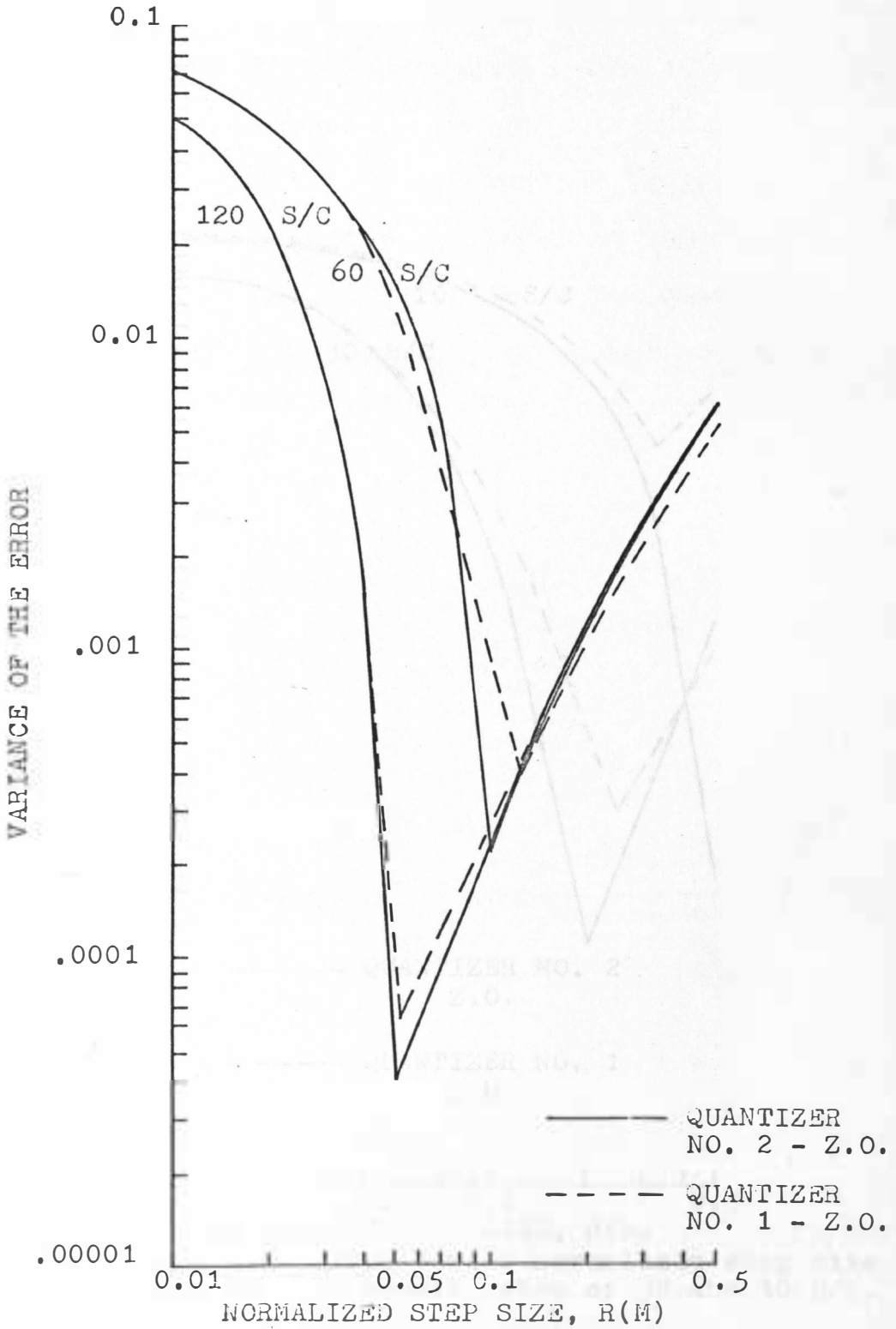

Fig. 49. Variance of the error versus normalized step size for a sine wave of sampling rates 120 and 60 S/C.

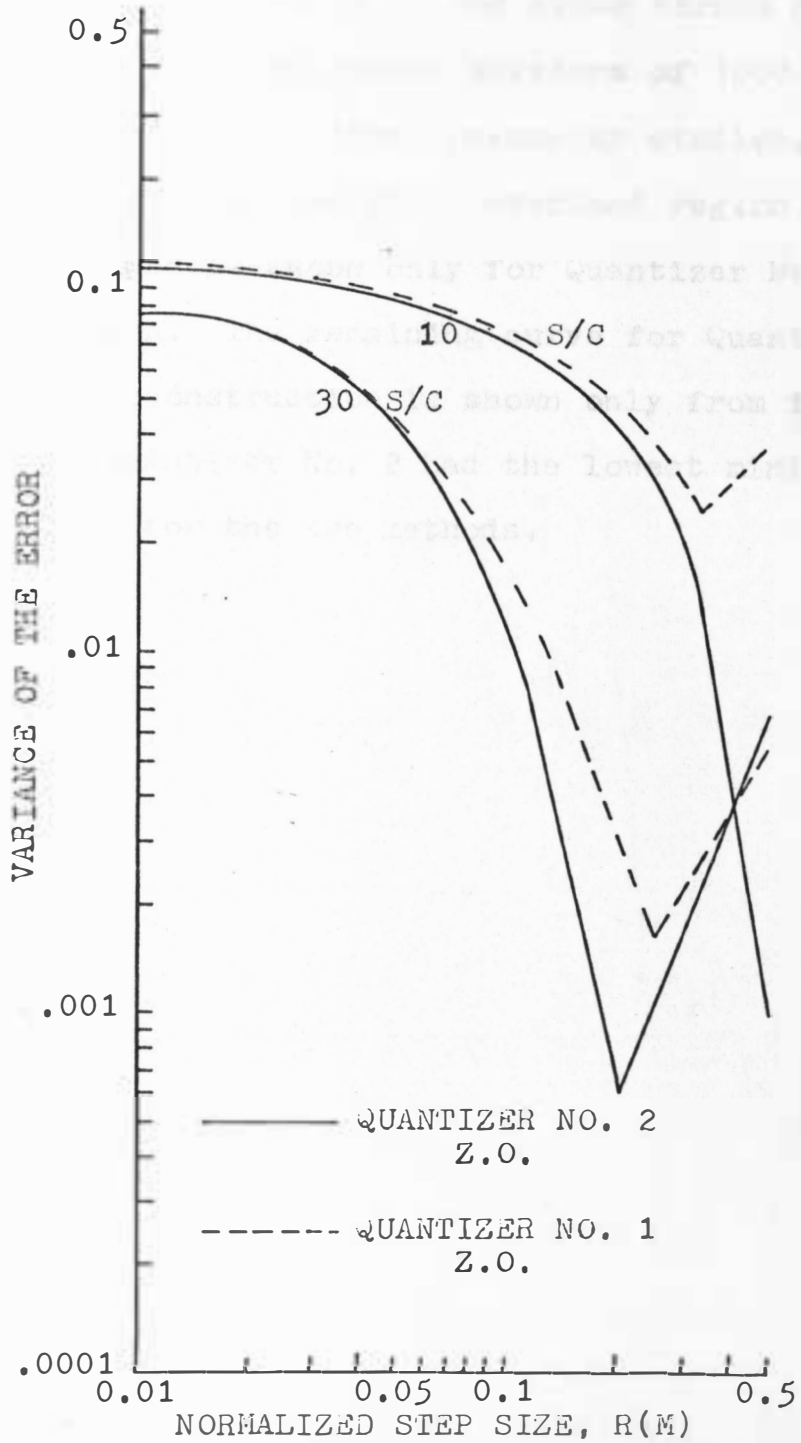

Fig. 50. Variance of the error versus normalized step size for a sine wave of sample rates of 30 and 10 S/C.

Figure 51 shows variance of the error versus normalized step size for the filtered random waveform of 1000 samples. As previously noted in the other parameter studies, the variance of the error in the slope overload region is random in nature and is shown only for Quantizer No. 2 with Z.O. reconstruction. The remaining curve for Quantizer No. 1 with Z.O. reconstruction is shown only from its last positive peak. Quantizer No. 2 had the lowest minimum variance of error for the two methods.

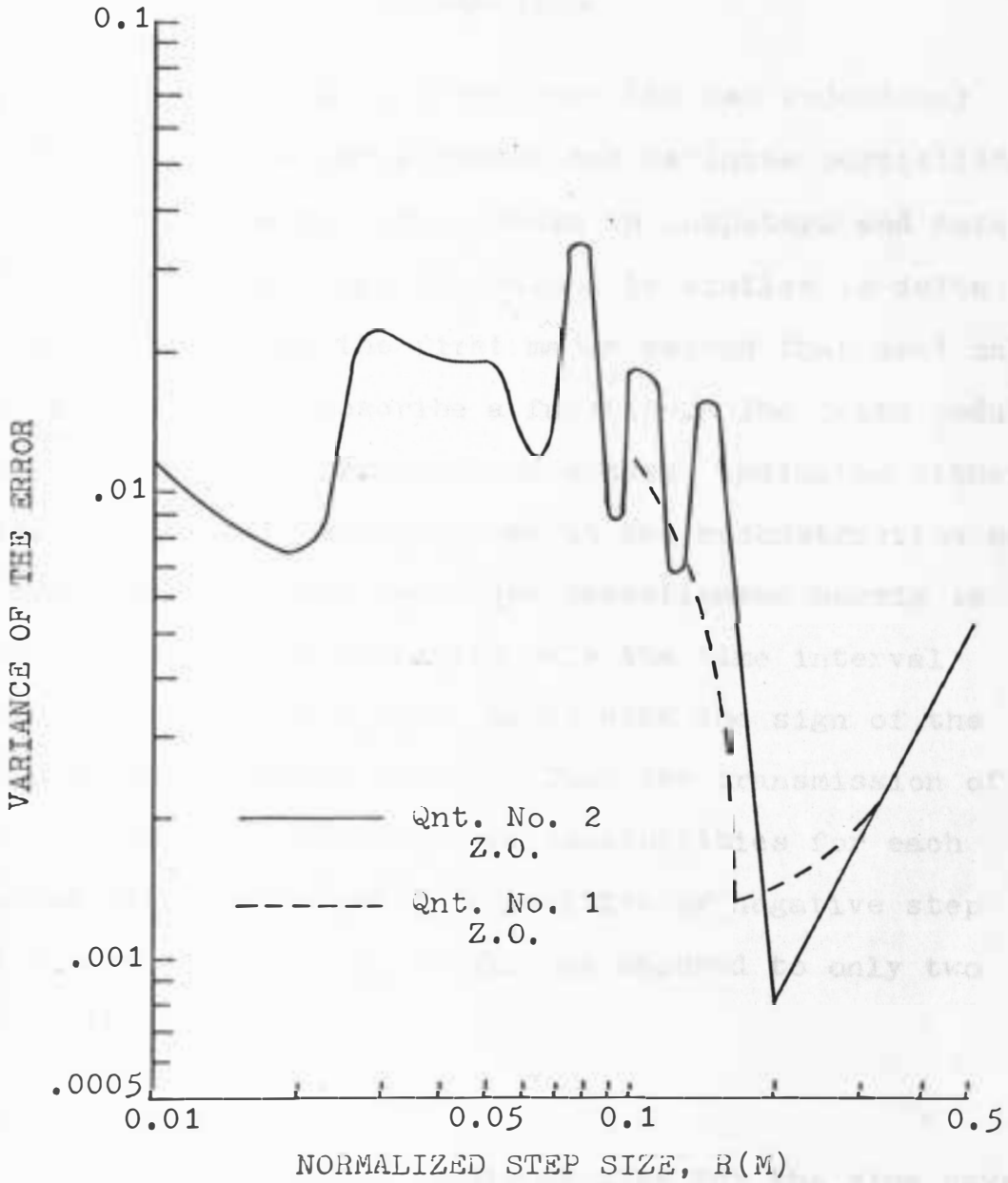

Fig. 51. Variance of the error versus normalized step size for a filtered random input of 1000 samples.

CHAPTER V

CONCLUSIONS

This dissertation shows that the new redundancy reduction technique investigated has definite possibilities for decreasing memory requirements in computers and data storage systems and that the method is similar to delta modulation which was the first major method that used only time information to describe a function. The delta modulation pulse-no pulse transmission scheme, indicates either a positive or negative step change in the reconstruction of the function. The new technique investigated herein is different in that it transmits only the time interval between nonredundant samples along with the sign of the change in quantization levels. Thus the transmission of $\pm\Delta T$ information provides three possibilities for each constant rate sample point, a positive or negative step size change or no change at all, as opposed to only two possibilities for ΔM.

Sine Wave Input

In the compression ratio studies for the sine wave input, Quantizer No. 1 has a larger compression ratio than Quantizer No. 2 above $R(M) = 0.1$. The compression ratio increases as both the step size, $R(M)$, and the sampling rate increase. Average mean-square error has a minimum

point where both the slope overload noise and the granular noise are at a minimum. For step sizes above the size corresponding to the $\overline{\text{M.S.E.}}$, the granular noise is dominant while for smaller step sizes, slope overload noise is dominant. Quantizer No. 2 has a lower $\overline{\text{M.S.E.}}$ minimum point, higher $\overline{\text{S/N}}$ maximum point, and lower σ^2 minimum point than Quantizer No. 1.

Very close correlation is obtained between the $\overline{\text{M.S.E.}}$, $\overline{\text{S/N}}$, and variance of the error curves. That is, as $\overline{\text{M.S.E.}}$ increases, $\overline{\text{S/N}}$ decreases and variance of the error increases, and vise versa. In addition, the inflection points for all three parameter studies are the same for any given sample rate.

Filtered Random Input

In the compression ratio studies for the random input, Quantizer No. 2 gives better compression ratios above R(M) = 0.3 because of the distribution of values as discussed in Chapter IV. The $\overline{\text{M.S.E.}}$, $\overline{\text{S/N}}$, and variance of the error behave in a random nature for those R(M) sizes where slope overload noise is dominant. Where granular noise dominates, the three parameter studies have curves similar to the corresponding sine wave input. Quantizer No. 1 always has a lower $\overline{\text{M.S.E.}}$ minimum point and a higher $\overline{\text{S/N}}$ maximum point. Comparison of data for 500 and 1000 samples indicates convergence of the data at 1000 samples. For both the sine

wave input and the filtered random input, the zero-order reconstruction is better than the first-order or modified first-order reconstruction techniques which substantiates the work of others (12, 15).

A tradeoff is evident between Quantizer No. 1 and Quantizer No. 2. For the two inputs, the quantizer with the better compression ratio has a larger $\overline{M.S.E.}$, smaller $\overline{S/N}$, and larger σ^2. Since the compression ratios for the two quantizers are nearly equal for small R(M) sizes, it can generally be said that the quantizer that has the smaller $\overline{M.S.E.}$, larger $\overline{S/N}$, and smaller σ^2 is the better quantizer for the particular waveform.

For this redundancy reduction technique, a zero-order reconstruction should be used, but the quantizer used will depend on the characteristics of the input signal and whether data reduction or reproduction accuracy is desired. Accuracy requirements will dictate both the sampling rate and the step size, R(M), for a particular quantizer.

Areas which need more investigation before more definite conclusions can be made on this redundancy reduction technique include:

(1) Investigation of the technique with other inputs such as EKG data and statistically described functions.

(2) Investigation of the phase of the output waveforms, especially for the first-order reconstruction.

(3) Investigation of a method to reduce or eliminate slope overload noise.

(4) Mathematical analysis of $\overline{M.S.E.}$ for the granular noise-dominated portion of the curve.

(5) Simulation of the entire adaptive data reduction scheme.

REFERENCES

1. Abate, J. E., "Linear and Adaptive Delta Modulation," Vol. 55, March 1967, pp. 298-307.

2. Andrews, C. A., J. M. Davies, and G. R. Schwartz, "Adaptive Data Compression," Proc. IEEE, Vol. 55, March 1967, pp. 267-277.

3. Balakrishnan, A. V., "On the Problem of Time Jitter in Sampling," IEEE Trans. on Information Theory, Vol. IT-8, April 1962, pp. 226-236.

4. Bello, P. A., R. N. Lincoln, and H. Gish, "Statistical Delta Modulation," Proc. IEEE, Vol. 55, March 1967, pp. 308-309.

5. Black, H. S., Modulation Theory, D. Van Nostrand Company, Inc., 1953, pp. 37-41.

6. Cutler, C. C., "Scanning the Issue," Proc. IEEE, Vol. 55, March 1967, pp. 251-252.

7. Davisson, D. L., Theory of Data Compression, PhD. dissertation, University Microfilms, Inc., 1964.

8. Deming, W. E., Some Theory of Sampling, John Wiley and Sons, Inc., 1950, pp. 53-75.

9. Downing, J. J., "Data Sampling and Pulse Amplitude Modulation," Aerospace Telemetry, Vol. 1, ed. H. L. Stiltz, Prentice-Hall, Inc., 1961, pp. 83-141.

10. Downing, J. J., Modulation Systems and Noise, Prentice-Hall, Inc., 1965, pp. 165-167.

11. Gardenhire, L. W., "Data Redundancy Reduction for Biomedical Telemetry," Biomedical Telemetry, ed. C. A. Caceres, Academic Press, 1965, pp. 255-298.

12. Gardenhire, L. W., "Redundancy Reduction--The Key to Adaptive Telemetry," presented at National Telemetering Conference, Los Angeles, California, June 1964.

13. Gardenhire, L. W., "Selecting Sample Rates," I.S.A. Journal, Vol. II, April 1964, pp. 59-64.

14. Golding, L. S., and P. M. Schultheiss, "Study of an Adaptive Quantizer," Proc. IEEE, Vol. 55, March 1967, pp. 293-297.

15. Hochman, D. and D. R. Weber, "Adaptive Telemetry--Data Compression," Aerospace Telemetry, Vol. 2, ed. H. L. Stiltz, Prentice-Hall, Inc., 1966, pp. 167-201.

16. Inose, H., and others, "New Modulation Technique Simplifies Circuits," Electronics, January 25, 1963, pp. 52-55.

17. Johnson, F. B., "Calculating Delta Modulator Performance," IEEE Trans. on Audio and Electroacoustics, Vol. AU-16, March 1968, pp. 121-129.

18. Kortman, C. M., "Redundancy Reduction--A Practical Method of Data Compression," Proc. IEEE, Vol. 55, March 1967, pp. 253-266.

19. Kuo, B. C., Analysis and Synthesis of Sampled--Data Control Systems, Prentice-Hall, Inc., 1963, pp. 27-28.

20. Liu, B. and T. P. Stanley, "Error Bounds for Jittered Sampling," IEEE Trans. on Automatic Control, Vol. AC-10, October 1965, pp. 449-454.

21. Marsden, M. J., "Design of Filters for Use on Discrete Data," IBM Technical Publication T707.06.061.032, February 28, 1964.

22. Medlin, J. E., "Sampled-Data Prediction for Telemetry Bandwidth Compression," IEEE Trans. on Space Electronics and Telemetry, Vol. SET-11, March 1965, pp. 25-36.

23. O'Neal, J. B., Jr., "Delta Modulation Quantizing Noise Analytical and Computer Simulation Results for Gaussian and Television Input Signals," The Bell System Technical Journal, Vol. XLV, January 1966, pp. 117-141.

24. Sander, D. E., "Adaptive Data Reduction Scheme," private communication, August 1968.

25. Sander, D. E., "Reduction of Memory and Data Storage Requirements by an Adaptive Sampling Technique," private communication, October 1967.

26. Schouten, J. F., F. deJager, and J. A. Greefkes, "Delta Modulation, a New Modulation System for Telecommunication," Phillips Technical Review, Vol. 13, 1952, pp. 237-245.

27. Yamane, T., Elementary Sampling Theory, Prentice-Hall, Inc., 1967, pp. 19-20, pp. 61-63.

28. System/360 Scientific Subroutine Package (360A-CM-03X), Version II, Programmer's Manual, International Business Machines Corporation, 1967, p. 54.

APPENDICES

APPENDIX A

TYPICAL DIGITAL COMPUTER PROGRAM FLOW DIAGRAM

Figure 53(A), (B), and (C) contains a typical computer program flow diagram for the simulation programs of this dissertation. The flow diagram is for the average mean-square error program using Quantizer No. 2 with zero-order reconstruction and sine wave input.

The flow diagram uses standard symbols and format. Variables used in the diagram are defined as:

CYC = number of cycles of the sine wave input

I = sample interval size

M = number of quantization levels in the positive half plane

R(M) = step size of quantizer

FMIDLE(K) = value of the Kth quantization level

XS = argument of the input sin wave in radians

YJ = output of the quantizer

YJL = output of the quantizer previous to YJ

QOUT = output of the comparitor

QRCN = output of the reconstructor

DSFQ = the summation of the squared differences between the input and the reconstructed output waves.

XSIN = value of the input at a sample point

XMSE(M) = average mean-square error for M quantization levels and CYC cycles of sine wave data

XMSEL(M) = average mean-square error for M quantization levels and (CYC-5) cycles.

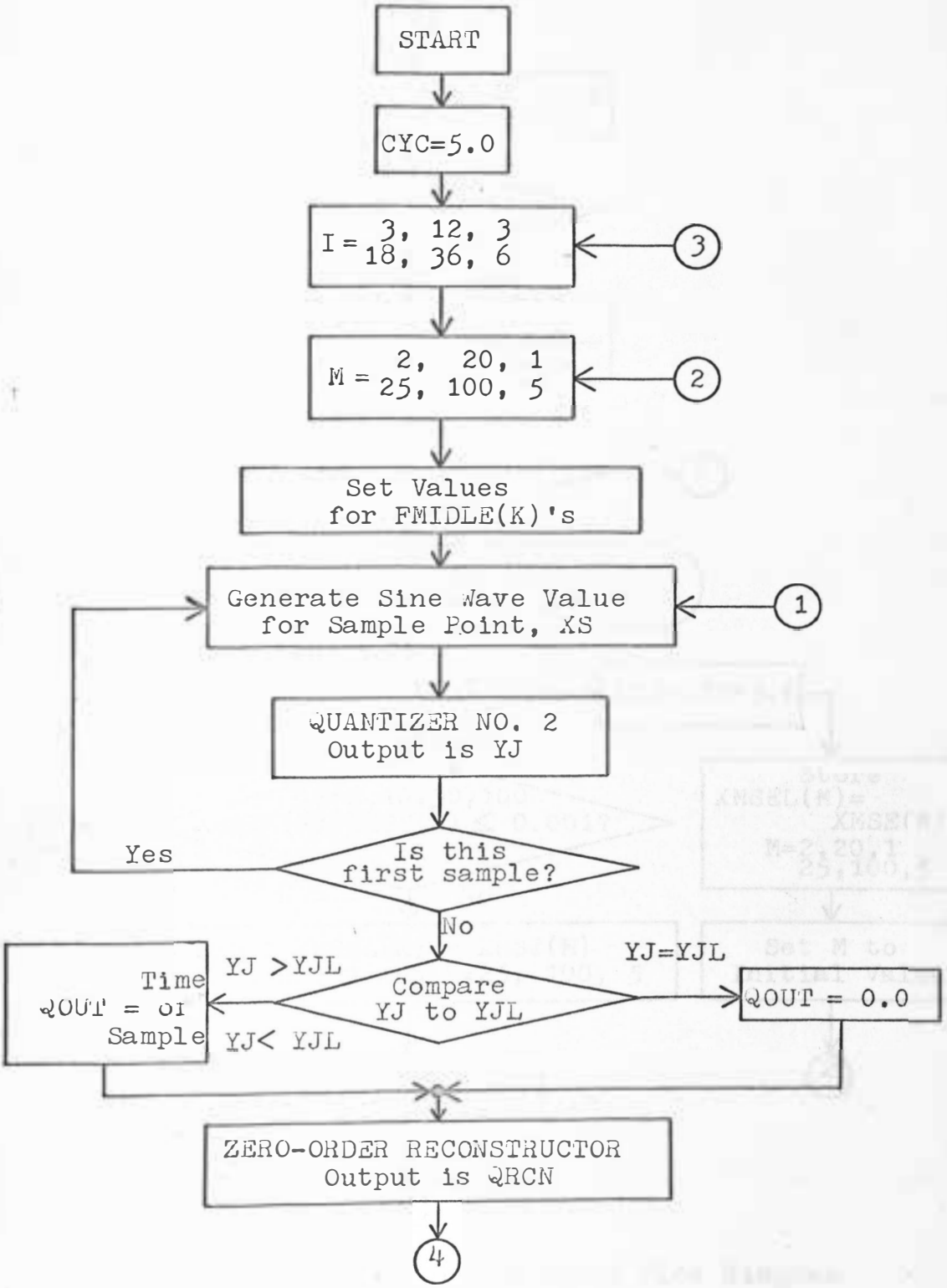

Fig. 52(A). Digital computer program flow diagram.

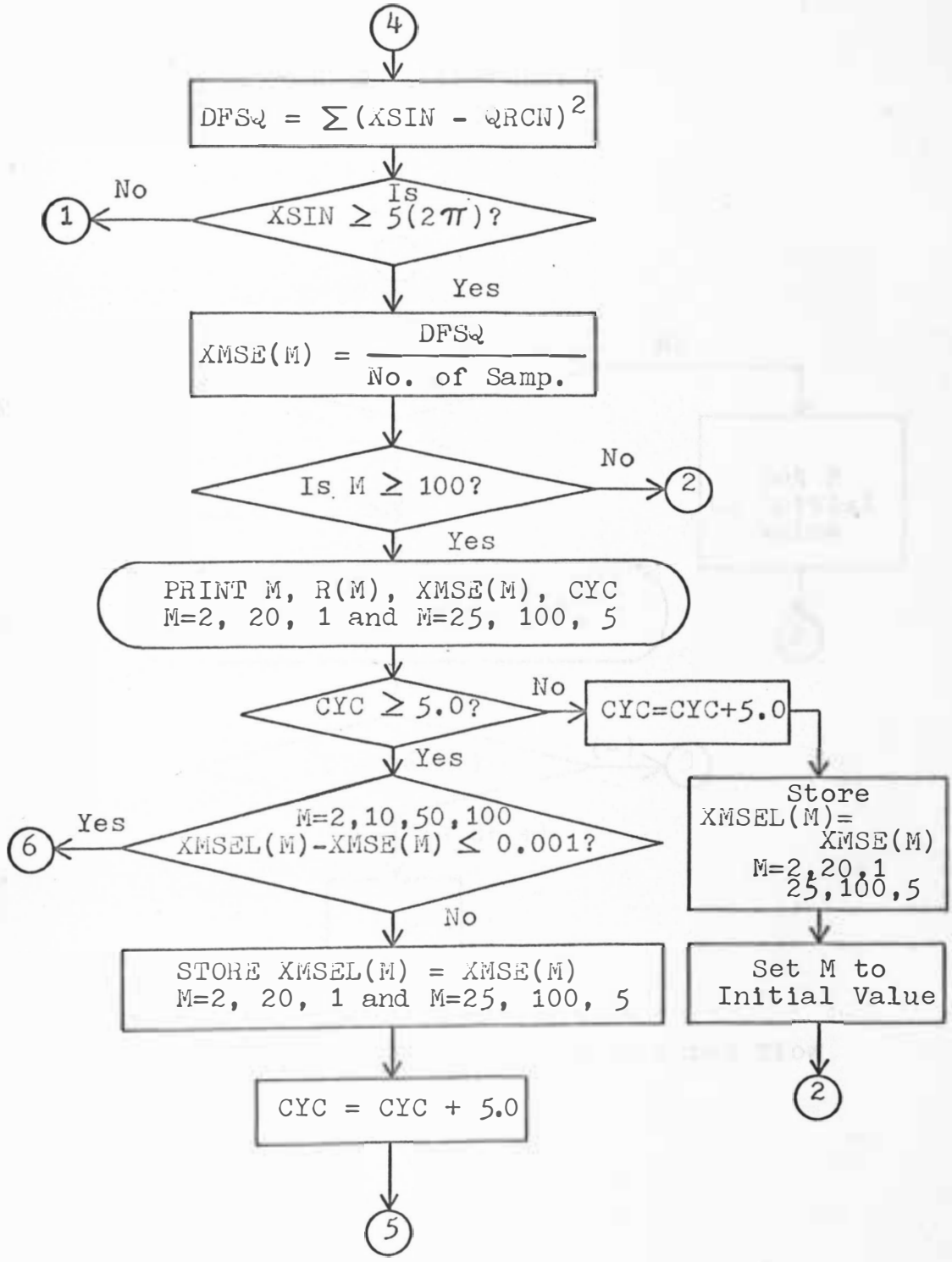

Fig. 52(B). Digital computer program flow diagram

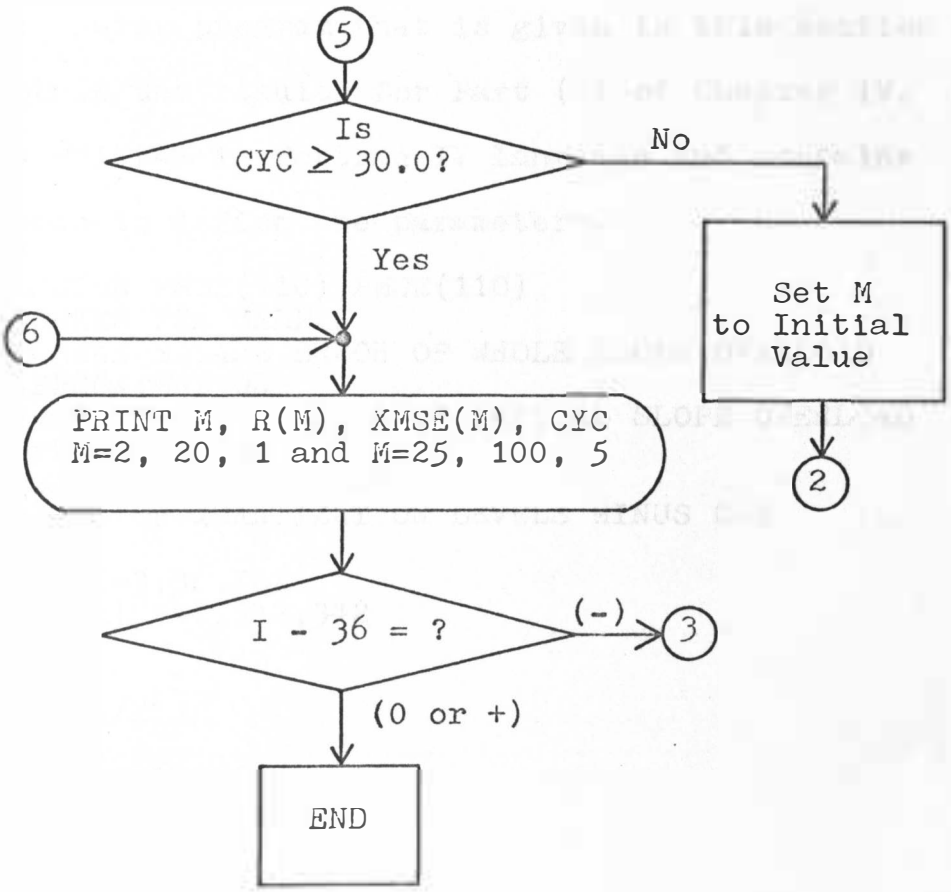

Fig. 52(C). Digital computer program flow diagram.

APPENDIX B

COMPUTER PROGRAMS

A. Mathematical Analysis of Mean-Square Error where Slope-Overload Occurs for a Sine Wave Input.

The computer program that is given in this section was used to obtain the results for Part (D) of Chapter IV. The program is written in Fortran IV language and contains comment cards to define the parameters.

```
      DIMENSION WMSE(110),PMSE(110)
C     I=DEGREES PER SAMPLE
C     WMSE=MEAN SQUARE ERROR OF WHOLE SLOPE OVERLOAD
C        APPROXIMATION
C     PMSE=MEAN SQUARE ERROR OF PARTIAL SLOPE OVERLOAD
C        APPROXIMATION
C     RM=QUANTIZATION INTERVAL
C     M=NUMBER OF QUANTIZATION LEVELS MINUS ONE
      IZZ=3
      DO 500 I=3,36,IZZ
      IF (I-12) 341,342,342
  342 IZZ=6
  341 XI=I
      S=(360.0/XI)
   72 ICH=1
      DO 95 M=2,100,ICH
      IF (M=20) 85,86,86
   86 ICH=5
   85 RI=M
      RM=1/RI
      XK=S/(6.2831853*RI)
      WMSE(M)=0.5-((4.*XK)/3.1415927)+((XK*XK*9.8696044)/12.)
      IF (XK-1.0) 10,10,11
   11 PMSE(M)=0.0
      GO TO 95
   10 RT=SQRT(1.0-XK)
      XK2=XK*XK
      XK3=XK2*XK
      A0=1.5707288
      A1=-0.2121144
      A2=0.0742610
      A3=-0.0187293
```

```
      ASINK=1.5707963-RT*(A0+(XK*A1)+(XK2*A2)+(XK3*A3))
      ACOSK=1.5707963-ASINK
      BS=SIN(ACOSK)-(XK*ACOSK)
      P1=(XK*XK*4.0*ACOSK)/3.1415927
      PS2=SIN(ACOSK)
      P2=(XK*5.0*PS2)/3.1415927
      P3=ACOSK/3.1415927
      P4=BS*BS
      P5=(2.0*BS*BS*ACOSK)/3.1415927
      P6=(XK*XK*2.0*ACOSK*ACOSK*ACOSK)/(3.0*3.1415927)
      PMSE(M)=P1+P6-P2+P3+P4-P5
   95 CONTINUE
  181 WRITE (12,22)
   22 FORMAT(41H1                    MATHEMATICAL ANALYSIS)
      WRITE (12,24)
   24 FORMAT(1H0,11X,1HM,6X,1HI,8X,7HWMSE(M),9X,7HPMSE(M))
      DO 25 M=2,20
   25 WRITE (12,26) M,I,WMSE(M),PMSE(M)
   26 FORMAT(1H ,10X,I3,5X,I2,5X,F11.7,5X,F11.7)
      DO 27 M=25,100,5
   27 WRITE (12,26) M,I,WMSE(M),PMSE(M)
  500 CONTINUE
      END
```

B. Compression Ratio, Average Mean-Square Error, Signal-to-Noise Ratio, and Variance of Error Programs for a Sine Wave.

The four programs presented in this section use Quantizer No. 2 with zero-order reconstruction. The basic program which is used for all four parameter studies is presented first. It contains INSERT statements which when filled with the proper INSERT sections will form a complete program. The INSERT sections for the four programs follow the basic program.

BASIC PROGRAM

```
"INSERT Dimension Section"

C       THIS IS AN EQUAL INCREMENT QUANTIZER
C       IT SIMULATES THE DATA COMPRESSOR WHICH INCLUDES THE
C          SAMPLE AND HOLD UNIT, THE ANOLOG TO DIGITAL
C          CONVERTER, AND THE COMPARATOR.
C       THIS HAS QUANTIZER NO. 2
C       THIS HAS A ZERO ORDER RECONSTRUCTOR
C       DELT=WIDTH OF HORIZONTAL INCREMENT IN RADIANS
C       R(M)=QUANTIZATION INTERVAL
C       M5=MAX NUMBER OF QUANTIZATION LEVELS
C       I=DEGREES PER SAMPLE
C       XSIN=INPUT
C       YJ=OUTPUT BEFORE DATA COMPRESSOR
C       QOUT=OUTPUT OF THE DATA COMPRESSOR
C       J=SAMPLE NUMBER
C       FMIDLE(K)=VALUE OF QUANTIZATION INTERVAL

"INSERT Comment and Initialization Section"

          DO 95 M=2,100,ICH
          IF (M-20) 85,86,86
       86 ICH=5
       85 M3=M
          M2=M
          RINV(M)=M
          R(M)=1.0/RINV(M)
          FMIDLE(1)=0.0
          M5=M3+1
          DO 1 K=2,M5
        1 FMIDLE(K)=FMIDLE(K-1)+R(M)
          XI=I
          DELT=XI*0.0174533
      800 XJ=0.00
       14 J=XJ+1.0
          XS=DELT*XJ
          XSIN=SIN(XS)
C         THIS IS QUANTIZER NO. 2
          NF=0
          XXAB=ABS(XSIN)
          PT=R(M)/2.0
          PINC=0.0
        5 PAT=PT+PINC
          IF (XXAB-PAT) 3,4,4
        4 PINC=PINC+R(M)
          NF=NF+1
          GO TO 5
```

```
      3 NF=NF+1
        M4=M3+1
        IF (NF-M4) 6,6,7
      7 IF (XSIN) 8,9,9
      8 YJ=-FMIDLE(M4)
        GO TO 2
      9 YJ=FMIDLE(M4)
        GO TO 2
      6 IF (XSIN) 10,12,12
     10 YJ=-FMIDLE(NF)
        GO TO 2
     12 YJ=FMIDLE(NF)
      2 IF (J-1) 13,13,15
     13 XJ=XJ+1.0
        XXSIN=XSIN
    900 YJL-YJ
        GO TO 14
C       THIS IS A COMPARISON OF YJ AND YJL
     15 S=J-1
        QOUT=S*DELT
        DIFF=YJ-YJL
        YJL=YJ
        IF (DIFF) 18,19,17
     18 QOUT =-QOUT
        GO TO 17
     19 QOUT=0.0
        GO TO 17
     17 CONTINUE

"INSERT Computation Section"

    500 CONTINUE
        END
```

Compression Ratio INSERT Sections

1. Dimension Section

```
      DIMENSION SAMP(110),RINV(110),R(110),FMIDLE(110)
      DIMENSION CR(110)
```

2. Comment and Initialization Section

```
C       THIS HAS A TEN CYCLE SINE WAVE INPUT AND RUNS ARE
C          MADE FOR 3,6,9,12,15,18,21,24,27,30,33, AND 36
C          DEGREE INTERVALS
C       CR(M)=COMPRESSION RATIO FOR M QUANTIZATION INTERVALS
        DO 500 I=3,36,3
     72 ICH=1
```

3. Computation Section

```
      IF (QOUT) 21,20,21
   21 SAMP(M)=SAMP(M)+1.0
   20 CONTINUE
      NN=(3600/I)+1
      CR(M)=J/SAMP(M)
      IF (J-NN) 32,95,95
   32 XJ=XJ+1.0
      GO TO 14
   95 CONTINUE
      WRITE (12,22)
   22 FORMAT(43H1                    COMPRESSION RATIO DATA)
      WRITE(12,24)
   24 FORMAT(1H0,13X,1HM,9X,4HR(M),7X,3HD/S,6X,3HCSM,
     1 7X,4HUCSM,6X,2HCR)
      DO 25 M=2,20
   25 WRITE (12,26) M,R(M),I,SAMP(M),J,CR(M)
   26 FORMAT(1H ,12X,I3,5X,F10.6,5X,I2,5X,F8.1,5X,I4,5X,F9.4)
      DO 27 M=25,100,5
   27 WRITE (12,26) M,R(M),I,SAMP(M),J,CR(M)
```

In addition, the initial condition statement,

```
      SAMP(M)=1.0
```

is inserted after statement 800 of the Basic Program.

Average Mean-Square Error INSERT Sections

1. Dimension Section

```
      DIMENSION RINV(110),R(110),FMIDLE(110),XMSE(110),
     1 XMSEL(110)
```

2. Comment and Initialization Section

```
C     THIS HAS AN INTEGER NUMBER OF 10 CYCLE SINE WAVE
C        INPUT SEGMENTS AT 3,6,9,12,15,18,21,24,27,30,
C        33, AND 36 DEGREE INTERVALS
C     QRCN=OUTPUT OF THE ADAPTIVE SAMPLER
C     XMSE(M)=MEAN SQUARE ERROR FOR VARIOUS INTERVALS
      DO 500 I=3,36,3
  201 CYC=5.0
   72 ICH=1
```

3. Computation Section

```
C     THIS IS THE ZERO ORDER RECONSTRUCTOR
```

```
      IF (QOUT) 50,51,52
   50 QRCN=QRCN-R(M)
      IF (1.0+QRCN) 111,60,60
  111 QRCN=QRCN+R(M)
      GO TO 60
   51 QRCN=QRCN
      GO TO 60
   52 QRCN=QRCN+R(M)
      IF (1.0-QRCN) 112,60,60
  112 QRCN=QRCN-R(M)
   60 CONTINUE
      IF (J-2) 61,61,62
   61 DFSQ=(XXSIN-QRCN1)*(XXSIN-QRCN1)+DFSQ
   62 DFSQ=(XSIN-QRCN)*(XSIN-QRCN)+DFSQ
   63 XXJ=J
      ENDP=(XXJ-1.0)*XI
      ENDF=ENDP-(360.0*CYC)
      IF (ENDF) 350,351,351
  350 XJ=XJ+1.0
      GO TO 14
  351 XMSE(M)=DFSQ/XXJ
   95 CONTINUE
      WRITE (12,22)
   22 FORMAT(43H1                MEAN SQUARE ERROR DATA)
      WRITE (12,24)
   24 FORMAT(1H0,13X,1HM,10X,4HR(M),12X,6HMSE(M),7X,6HCYCLES)
      DO 25 M=2,20
   25 WRITE (12,26) M, R(M), XMSE(M),CYC
   26 FORMAT(1H ,12X,13,5X,F10.6,7XF11.7,5X,F6.1)
      DO 27 M=25,100,5
   27 WRITE (12,28) M,R(M),XMSE(M),CYC
   28 FORMAT(1H ,12X,13,5X,F10.6,7X,F11.7,5X,F6.1)
      IF(CYC-5.0)70,70,71
   70 CYC=CYC+5.0
      DO 73 M=2,20
   73 XMSEL(M)=XMSE(M)
      DO 74 M=25,100,5
   74 XMSEL(M)=XMSE(M)
      GO TO 72
   71 DIFF2=XMSE(2)-XMSEL(2)
      DIFF2=ABS(DIFF2)
      IF (DIFF2-0.001) 75,75,76
   75 DIFFT=XMSE(10)-XMSEL(10)
      DIFFT=ABS(DIFFT)
      IF (DIFFT-0.001) 77,77,76
   77 DIFFF=XMSE(50)-XMSEL(50)
      DIFFF=ABS(DIFFF)
      IF (DIFFF-0.001) 65,65,76
```

```
   65 DIFFH=XMSE(100)-XMSEL(100)
      DIFFH=ABS(DIFFH)
      IF (DIFFH-0.001) 66,66,76
   76 DO 67 M=2,20
   67 XMSEL(M)=XMSE(M)
      DO 68 M=25,100,5
   68 XMSEL(M)=XMSE(M)
      CYC=CYC+5.0
      IF (CYC-30.0) 131,66,66
  131 GO TO 72
   66 WRITE (12,41)
   41 FORMAT(49H1                FINAL MEAN SQUARE ERROR DATA)
      WRITE (12,42)
   42 FORMAT(1H0,13X,1HM,10X,4HR(M),12X,6HXMSE(M),9X,
     1 6HCYCLES,6X,1HI)
      DO 43 M=2,20
   43 WRITE (12,44) M,R(M),XMSE(M),CYC,I
   44 FORMAT(1H ,12X,I3,5X,F10.6,7X,F11.7,6X,F7.2,5X.I2)
      DO 45 M=25,100,5
   45 WRITE (12,44) M,R(M),XMSE(M),CYC,I
```

In addition, the statement,

```
      DFSQ=0.00
```

is inserted after statement 800 and the statements

```
      QRCN1=YJL
      QRCN=QRCN1
```

are inserted after statement 900 of the Basic Program.

Signal-to-Noise Ratio INSERT Sections

1. Dimension Section

```
      DIMENSION RINV(110),R(110),FMIDLE(110),SNR(110)
```

2. Comment and Initialization Section

```
C     THIS HAS AN INTEGER NUMBER OF 10 CYCLE SINE WAVE
C        INPUT SEGMENTS AT 3,6,9,12,18,24,30, AND 36
C        DEGREE INTERVALS
C     QRCN=OUTPUT OF THE DATA COMPRESSOR AND RECONSTRUCTOR
C     S/N(M)=SIGNAL TO NOISE RATIO IN DB FOR THE VARIOUS
C        STEP SIZES
```

```
      IZZ=3
      DO 500 I=3,36,IZZ
      IF (I-12) 341,342,342
  342 IZZ=6
  341 CYC=10.0
   72 ICH=1
```

3. Computation Section

```
C     THIS IS THE ZERO ORDER RECONSTRUCTOR
      IF (QOUT) 50,51,52
   50 QRCN=QRCN-R(M)
      IF (1.0+QRCN) 111,60,60
  111 QRCN=QRCN+R(M)
      GO TO 60
   51 QRCN=QRCN
      GO TO 60
   52 QRCN=QRCN+R(M)
      IF (1.0-QRCN) 112,60,60
  112 QRCN=QRCN-R(M)
   60 CONTINUE
      IF (J-2) 61,61,62
   61 SUMN=SUMN+(QRCN1*QRCN1)
      SUMD=SUMD+((XXSIN-QRCN1)*(XXSIN-QRCN1))
   62 SUMN=SUMN+(QRCN*ARCN)
      SUMD=SUMD+((XSIN-QRCN)*(XSIN-QRCN))
   63 XXJ=J
      ENDP=(XXJ-1.0)*XI
      ENDF=ENDP-(360.0*CYC)
      IF (ENDF) 350,351,351
  350 XJ=XJ+1.0
      GO TO 14
  351 SUMN=SUMN/XXJ
      SUMD=SUMD/XXJ
      SS=SUMN/SUMD
      SNR(M)=10.0*ALOG10(SS)
   95 CONTINUE
      WRITE (12,22)
   22 FORMAT(47H1                SIGNAL TO NOISE RATIO DATA)
      WRITE (12,24)
   24 FORMAT(1HO,14X,1HM,8X,4HR(M),11X,6HS/N(M),8X,1HI)
      DO 25 M=2,20
   25 WRITE (12,26) M,R(M),SNR(M),I
   26 FORMAT(1H ,12X,I3,5X,F10.6,5X,F11.6,5X,I3)
      DO 27 M=25,100,5
   27 WRITE (12,26) M,R(M),SNR(M),I
```

In addition, the statements,

```
      SUMN=0.0
      SUMD=0.0
```

are inserted after statement 800 and the statements,

```
      QRCN1=YJL
      QRCN=QRCN1
```

are inserted after statement 900 of the Basic Program.

Variance of the Error INSERT Sections

1. Dimension Section

```
      DIMENSION RINV(110),R(110),FMIDLE(110)
      DIMENSION VAR(110),VARL(110),AVGE(110)
```

2. Comment and Initialization Section

```
C     THIS HAS AN INTEGER NUMBER OF 10 CYCLE SINE WAVE
C        INPUT SEGMENTS AT 3,6,9,12,15,18,21,24,27,30,
C        33,AND 36 DEGREE INTERVALS
C     QRCN=OUTPUT OF THE DATA COMPRESSOR AND RECONSTRUCTOR
C     AVGE(M)=AVERAGE ERROR FOR THE QUANTIZATION INTERVAL
C     VAR(M)=VARIANCE OF THE ERROR FOR THE QUANTIZATION
C        INTERVAL
      DO 500 I=3,36,3
  201 CYC=5.0
  720 IJKL=0
      IJK=0
   72 ICH=1
```

3. Computation Section

```
C     THIS IS THE ZERO ORDER RECONSTRUCTOR
      IF (QOUT) 50,51,52
   50 QRCN=QRCN-R(M)
      IF (1.0+QRCN) 111,60,60
  111 QRCN=QRCN+R(M)
      GO TO 60
   51 QRCN=QRCN
      GO TO 60
   52 QRCN=QRCN+R(M)
      IF (1.0-QRCN) 112,60,60
  112 QRCN=QRCN-R(M)
   60 CONTINUE
      IF (IJK) 94,96,94
   96 J2=J-1
      IF(J2-1) 61,61,62
```

```
C       THIS CHECKS THE END POINT OF THE AVG ERROR PART
   61 ERR=ABS(XXSIN-QRCN1)+ERR
   62 ER1=XSIN-QRCN
      ERAB=ABS(ER1)
      ERR=ERR+ERAB
      XXJ=J
      ENDP=(XXJ-1.0)*XI
      ENDF=ENDP-(360.0*CYC)
      IF (ENDF) 350,351,351
  350 XJ=XJ+1.0
      GO TO 14
  351 AVGE(M)=ERR/XXJ
      IF (100-M) 91,92,91
   91 GO TO 95
   92 IJK=1
      GO TO 95
   94 J2=J-1
      IF (J2-1) 171,171,172
C       THIS CHECKS THE END POINT OF THE VARIANCE PART
  171 XXSIN=ABS(XXSIN)
      ERA1=ABS(XXSIN-QRCN1)
      SM=SM+(ERA1-AVGE(M))*(ERA1-AVGE(M))
  172 ERA=ABS(XSIN-QRCN)
      SM=SM+(ERA-AVGE(M))*(ERA-AVGE(M))
      XXJ=J
      ENDP=(XXJ-1.0)*XI
      ENDF=ENDP-(360.0*CYC)
      IF (ENDF) 360,361,361
  360 XJ=XJ+1.0
      GO TO 14
  361 VAR(M)=SM/XXJ
      IJKL=1
   95 CONTINUE
      IF (IJKL) 181,182,181
  182 GO TO 72
  181 WRITE (12,22)
   22 FORMAT(37H1                          VARIANCE DATA)
      WRITE (12,24)
   24 FORMAT(1HO,14X,1HM,10X,4HR(M),12X,6HVAR(M),10X,6HAVG
     1 ER,8X,3HCYC)
      DO 25 M=2,20
   25 WRITE (12,26) M,R(M),VAR(M),AVGE(M),CYC
   26 FORMAT(1H ,12X,I3,5X,F10.6,7X,F11.7,5X,F11.7,5X,F6.1)
      DO 27 M=25,100,5
   27 WRITE (12,26) M,R(M),VAR(M),AVGE(M),CYC
      IF (CYC-5.0) 70,70,71
   70 CYC=CYC+5.0
      DO 73 M=2,20
```

```
   73 VARL(M)=VAR(M)
      DO 74 M=25,100,5
   74 VARL(M)=VAR(M)
      GO TO 720
C     THIS CHECKS CONVERGENCE OF THE VARIANCE
   71 DIFF2=VARL(2)-VAR(2)
      DIFF2=ABS(DIFF2)
      IF (DIFF2-0.001) 75,75,76
   75 DIFFT=VARL(10)-VAR(10)
      DIFFT=ABS(DIFFT)
      IF (DIFFT-0.001) 77,77,76
   77 DIFFF=VARL(50)-VAR(50)
      DIFFF=ABS(DIFFF)
      IF (DIFFF-0.001) 65,65,76
   65 DIFFH=VARL(100)-VAR(100)
      DIFFH=ABS(DIFFH)
      IF (DIFFH-0.001) 66,66,76
   76 DO 67 M=2,20
   67 VARL(M)=VAR(M)
      DO 68 M=25,100,5
   68 VARL(M)=VAR(M)
      CYC=CYC+5.0
      IF (CYC-30.0) 131,66,66
  131 GO TO 720
   66 WRITE (12,41)
   41 FORMAT(43H1                                  FINAL VARIANCE DATA)
      WRITE (12,42)
   42 FORMAT(1HO,13X,4HR(M),11X,6HVAR(M),9X,7HAVG ERR,
     1  9X,3HCYC,9X,1HI)
   43 WRITE (12,44) R(M),VAR(M),AVGE(M),CYC,I
   44 FORMAT(1H ,10X,F10.6,5X,F11.7,5X,F11.7,5X,F6.1,4X,I3)
      DO 45 M=25,100,5
   45 WRITE (12,44) R(M),VAR(M),AVGE(M),CYC,I
```

In addition, the statements,

```
      SM=0.00
      ERR=0.00
```

are inserted after statement 800 and the statements

```
      QRCN1=YJL
      QRCN=QRCN1
```

are inserted after statement 900 of the Basic Program.

These four programs can be converted to use Quantizer No. 1 by inserting the Quantizer No. 1 Section given below.

This section should be inserted between statement 85 and statement 2 of the Basic Program.

Quantizer No. 1 Section

```
      M2=M
      RINV(M)=M
      R(M)=1.0/RINV(M)
      FMIDLE(1)=R(M)/2.0
      DO 1 K=2,M3
    1 FMIDLE(K)=FMIDLE(K-1)+R(M)
      XI=I
      DELT=XI*0.0174533
      XJ=0.00
      SUMN=0.0
      SUMD=0.0
   14 J=XJ+1.0
      XS=DELT*XJ
      SXIN=SIN(XS)
C     THIS IS QUANTIZER NO. 1
      NPOINT=1
      ADJ=1.0
      XXAB=XSIN
      IF (XSIN) 6,3,3
    6 XXAB=ABS(XSIN)
      NPOINT=2
      ADJ=0.0
    3 NY=RINV(M)*XXAB+ADJ
      GO TO (4,5),NPOINT
    4 YJ=FMIDLE(NY)
      IF (NY-M3) 8,8,7
    7 YJ=FMIDLE(M3)
    8 GO TO 2
    5 YJ=-FMIDLE(NY+1)
      IF (NY-M3+1) 10,10,9
    9 YJ=-FMIDLE(M3)
   10 GO TO 2
```

The average mean-square error, signal-to-noise ratio, and variance of error programs can be converted to a modified first-order reconstruction process if the zero-order reconstruction section is replaced by the modified first-order reconstruction section. Listed below is the modified

first-order reconstruction section for the average mean-square error program which replaces the first-order reconstruction program to statement 95.

Modified First-Order Reconstruction Section

```
C     THIS IS THE MODIFIED FIRST ORDER RECONSTRUCTOR
      IF (QOUT) 151,152,151
  152 XJ=XJ+1.0
      YJL=YJ
      GO TO 14
  151 IF (QOUTL) 153,154,153
  154 QIP=YJ1
      J1=1
      GO TO 155
  153 CONTINUE
  155 IF (QOUT) 156,156,157
  156 AQOUT=ABS(QOUT)/XI
      AQOTL=ABS(QOUTL)/XI
      SLP=-R(M)/(AQOUT-AQOTL)
      GO TO 160
  157 AQOUT=ABS(QOUT)/XI
      AQOTL=ABS(QOUTL)/XI
      SLP=R(M)/(AQOUT-AQOTL)
  160 IF (QOUTL) 161,162,161
  162 SLP=SLP/2.0
      GO TO 166
  161 IF (QOUTL) 171,171,172
  171 IF (QOUT) 166,166,164
  172 IF (QOUT) 164,164,166
  164 SLP=0.0
  166 CONTINUE
      DO 165 II=J1,J
      Z=II-1
      QB1=J1-1
      IF (II-3) 167,168,168
  168 Z=II
  167 QRCN=SLP*(Z-QB1)+QIP
      XSS=DELT*Z
      RSIN=SIN(XSS)
      DFSQ=DFSQ+(RSIN-QRCN)*(RSIN-QRCN)
  165 CONTINUE
      XXJ=J
      ENDP=(XXJ-1.0)*XI
      ENDF=ENDP-(360.0*CYC)
```

```
      IF (ENDF) 350,351,351
  350 J1=J+1
      QOUTL=QOUT
      XJ=XJ+1.0
      QIP=QRCN
      YJL=YJ
      GO TO 14
  315 XMSE(M)=DFSQ/XXJ
```

The plot routine results in Chapter IV are obtained by using the proper combination of quantizer-reconstructor sections which are previously given, along with the statement,

```
CALL PLOT (NO,A,N,M,NL,NS)
```

inserted before statement 500. This statement calls a standard subroutine, SUBROUTINE PLOT, which is given in (28). The parameters in the CALL PLOT statement are:

NO = Chart number (3 digits maximum).

A = Matrix of data to be plotted. First column represents base variable and successive columns are the cross-variables (maximum is 9).

N = Number of rows in Matrix A.

M = Number of columns in Matrix A (equal to the total number of variables). Maximum is 10.

NL = Number of lines in the plot. If 0 is specified, 50 lines are used.

NS = Code for sorting the base variable data in ascending order.
- 0 - sorting is not necessary (already in ascending order).
- 1 - sorting is necessary.

C. Compression Ratio, Average Mean-Square Error, Signal-to-Noise Ratio, and Variance of the Error Programs for a Filtered Random Input.

In order to convert the programs in the previous sections, which were for a sine wave input, to programs with a filtered random input, few changes are made. As before, in order to obtain the parameter-quantizer-reconstructor algorithm desired, the proper sections are inserted into the basic program. For the filtered random inputs, symbols ABG and G replace XXAB and XSIN respectively. In addition, the section below replaces the section between statements 85 and 14 of the Basic Program. Statement 100 calls for the random number generator subroutine and statement 87 calls for the filter subroutine. Both subroutines are listed after the filtered random input section.

Filtered Random Input Section

```
      DIMENSION F(19),W(10)
      IJK=0
  101 IX=50469
      DO 100 IB=1,19
  100 F(IB)=RAND(IX)
      W( 1)=0.300
      W( 2)=0.02533
      W( 3)=0.1416
      W( 4)=0.0281
      W( 5)=-0.0354
      W( 6)=-0.0405
      W( 7)=-0.0157
      W( 8)=0.0052
      W( 9)=0.0088
      W(10)=0.0031
      NUU=9
      RINV(M)=M
      R(M)=1.0/RINV(M)
      FMIDLE(1)=0.0
```

```
      M5=M3+1
      DO 1 K=2,M5
    1 FMIDLE(K)=FMIDLE(K-1)+R(M)
      XJ=0.00
      DFSQ=0.00
   87 CALL FILTER (F,W,NUU,F)
      DO 105 L=1,18
  105 F(L)=F(L+1)
      F(19)=RAND(IX)
```

Random Number Generator Subroutine

```
      FUNCTION RAND(IX)
C     THIS MAKES THE RANDOM NUMBERS
      IX=IX*65539
      IF (IX) 5,6,6
    5 IX=IX+2147483647+1
    6 RAND=FLOAT(IX)*0.4654413E-9
      RETURN
      END
```

Filter Subroutine

```
      SUBROUTINE FILTER (F,W,N,G)
C     F IS AN ARRAY OF FUNCTION VALUES TO BE FILTERED
C     F MUST HAVE AN UPPER DIMENSION OF (I*N)+1
C     W IS AN ARRAY OF WEIGHTING FACTORS THERE ARE N+1
C        FACTORS USED
C     N IS THE NUMBER OF POINTS
C     G IS THE VALUE RETURNED
      DIMENSION F(1),W(1)
      NM=N+1
      G=F(NM)*W(1)
      DO 10 I=1,N
      JP=NM+I
      JN=NM-I
   10 G=G+W(I+1)*(F(JP)+F(JN))
      RETURN
      END
```